

Ministry of Transportation  
Provincial Highways Management Division Report  
Highway Infrastructure Innovation Funding Program



# Advanced Vehicle Control Systems (AVCS) Supporting Intelligent Transportation Systems

**Final Report**  
May 2009

HIIFP-064

# Advanced Vehicle Control Systems (AVCS) Supporting Intelligent Transportation Systems

Prepared by  
Lian Zhao and Zaiyi Liao  
Ryerson University  
May 2009

A Report  
presented to MOT  
for the project year 2008 - 2009

350 Victoria Street  
Toronto, Ontario, Canada M5B 2K3  
Tel: (416) 979-5000 ext. 6101; Fax (416) 979-5280

# Executive Summary

With vision obstructed by the neighboring vehicles, the driving performance (i.e. the level of comfort, safety, and efficiency) of individual vehicle in traffic is often far below the optimum, leaving a great room for improvement. One common approach is to use modern wireless communication technology and intelligent instrumentation, referred to as Intelligent Transportation System (ITS), to extend the vision of drivers such that they can “see” beyond what they physically see thus anticipate more effectively and accurately to avoid accidents. This report documents a feasibility study of this approach and discusses future work based on the primary result of this study.

This research is an one-year feasibility study funded by MTO. The objective is to investigate how the vision of individual drivers can be extended beyond his/her physical boundary through the use of inter-vehicle communication technology. The study was organized into two work-packages that took place concurrently, namely (1) investigating inter-vehicle communication (IVC) and (2) modelling of the vehicle dynamics. Through (1) we investigate how the vision of individual driver’s driving vision can be extended and develop a wireless communication protocol suitable for use in harsh traffic environment. The outcome of this work is then used in (2) to study how individual driver should respond to the information passed to him/her through the IVC or how his/her driving condition initiates a message that is to be broadcasted to other surrounding drivers through the IVC.

Through the work-package (1), initial research work on broadcast problems is investigated. Most applications in vehicle ad hoc networks use broadcasting as a main functional block for localization, routing and dissemination of warning messages to other vehicles. Broadcasting in its conventional way may lead to a broadcast storm problem by increasing the nodes contention in using the communication channel and more collisions which may result in a collapse of the communication system. We first investigated the optimal communication range considering traffic density and message generation rate. We proposed an advanced broadcasting scheme, which was verified by simulation to provide reduced time delay of the message to reach the remote vehicles and reduced redundancy for message broadcasting. In addition, advanced ranging and positioning algorithms are investigated. Applying signal processing and filtering techniques, the ranging estimate accuracy can be greatly improved. Simulation has been conducted to verify the proposed algorithms.

Through the work-package (2), the vehicle dynamics is mathematically modelled to address issues related to the important components that influence the handling of road vehicles.

The developed model is used to investigate the performance of conventional Anti-Braking System (ABS). This makes a solid foundation for the development of the advanced ABS that can improve the current technology. In addition, a Virtual Reality module has also been developed to virtually represent the dynamics of vehicle. The purpose of the model is to perform simulation on the effect of the proposed ABS system on the motion and stopping distance on a vehicle.

Overall, three Master students and 1 Ph.D. student have been working on the project and have benefited from the research and development activities. The research output includes four conference papers submitted to IEEE flagship international conferences and one technical report (attached in the Appendix). We have achieved the objectives of this one-year feasibility study and are well positioned to move forward the investigation that aims to achieve the long-term goal of this study: to develop new generation of technology for optimizing the driving performance of motor vehicle in busy traffics. To achieve this, we need set up an inter-vehicle communication platform, which will be used to develop and test the technology. Based on ranging and position techniques studied through this feasibility study and further developed in future projects, an intelligent vehicle trajectory diagnosis technology will be developed and integrated with what is currently known as vehicle black box, resulting in Enhanced Vehicle Black Box that not only provides accurate data for post-accident inspection, but also actively involves in real-time driving for optimal driving performance.

# Contents

<b>1</b>	<b>Project Overview in 2008-2009</b>	<b>1</b>
1.1	Vehicle Dynamic Modelling . . . . .	2
1.2	Inter-vehicle Communication Systems . . . . .	3
<b>2</b>	<b>Modeling of the Vehicle Dynamics</b>	<b>6</b>
2.1	Vehicle Dynamics . . . . .	6
2.2	Model the Dynamics of Ground Vehicle . . . . .	8
2.3	Extend the model to Virtual Reality . . . . .	11
<b>3</b>	<b>Communication Protocols for Efficient IVC</b>	<b>12</b>
3.1	Maximum Communication Range of a Broadcast Message . . . . .	12
3.2	Broadcast Storm Problem . . . . .	15
3.3	Simulation Results . . . . .	20
<b>4</b>	<b>Vehicle Position System</b>	<b>26</b>
4.1	Ranging Smooth Algorithms . . . . .	27
4.2	Constrained Weighted Least Square Optimization . . . . .	29
4.3	Simulation Results . . . . .	30
<b>5</b>	<b>Future Work</b>	<b>35</b>
5.1	Future Research Problems . . . . .	35
5.1.1	Inter-Vehicle Communication (IVC) . . . . .	36
5.1.2	INS Trajectory Diagnosis . . . . .	37

5.1.3	Advanced ABS . . . . .	38
5.1.4	Surveillance and Information Processing . . . . .	38
5.2	Planned Approaches and Methodologies . . . . .	39
5.2.1	Communication Subsystem . . . . .	39
5.2.2	Advanced ABS . . . . .	40
5.2.3	Vehicle Trajectory Diagnosis . . . . .	41
5.2.4	Integration of EVBox . . . . .	41
<b>6</b>	<b>Conclusions</b>	<b>42</b>
<b>A</b>	<b>Abbreviation List</b>	<b>47</b>
<b>B</b>	<b>Papers Submitted</b>	<b>49</b>
<b>C</b>	<b>Modeling of Vehicle Dynamics for Future Integration with Inter-Vehicle Communication Simulation</b>	<b>50</b>

# List of Figures

2.1	Stopping distance as a function of slippage. . . . .	10
3.1	The highway topology setup in ns2 simulator. . . . .	14
3.2	The highway topology setup in ns2 simulator. . . . .	20
3.3	Time delay versus beacon generation rate. . . . .	21
3.4	Percentage of the received redundant messages versus the traffic load. . . . .	22
3.5	Number of vehicles that received the warning message successfully versus the traffic load. . . . .	23
3.6	Tie delay versus the traffic load. . . . .	24
3.7	Percentage of redundant messages received within the relative distance for the flooding and NTPP. . . . .	25
4.1	Unbiased Kalman filter output for LOS and NLOS. . . . .	30
4.2	Unbiased Kalman filter output for LOS in $[0, 0.6]$ s. . . . .	31
4.3	Biased vs unbiased Kalman filter smoothed range data. . . . .	32
4.4	Estimated range data with an abrupt change between LOS and NLOS. . . . .	32
4.5	NLOS mitigation using biased KF. . . . .	33
4.6	NLOS mitigation with CWLS optimization. . . . .	34
5.1	Block diagram of the investigated AVCS. . . . .	37

# Chapter 1

## Project Overview in 2008-2009

Travelling safety is always one of the most important issues in transportation systems. According to WHO (World Health Organization) report, in 2002, an estimated 1.18 million people died from road traffic crashes, which is equivalent to an average of 3242 deaths per day. Road traffic injuries accounted for 2.1% of all global deaths, making them the eleventh leading cause of global deaths. A breakdown of the causes of the traffic accidents shows that about 75% of traffic accidents are caused by driver behavior immediately before the accident.

Advanced Vehicle Control Systems (AVCS) exploit sensor networks on board and inter-vehicle communications, collaboratively use the information collected by individual vehicles to form an enhanced data set to improve vehicle control capabilities and to enhance road driving safety. The proposed research aims to investigate AVCS to improve safety driving and road efficiency. Equipped with AVCS, the driver can receive visual and hearing information about traffic, dangers and all vehicle situations. At the same time, automatic control allows the driver/vehicle to react the dangerous events in a faster and more effective way, like actuate in the braking or acceleration systems. It is foreseeable that by equipping the AVCS on board, safety driving can be greatly improved; the capacity and the productivity of the current highway system can be greatly enhanced.

With the one year support from the Ministry, we have the opportunity to set up a research

team, including two faculty members, 1 Ph.D. student, and 3 Master of Applied Science students. We also hired 1 research assistant (RA) to do some modelling programming. With the successful arrangement of the research team, in the coming project year, we expect to have a smooth transition, a better research progress and a more fruitful research outcome. In the project year 2008-2009, we worked on two aspects of AVCS development: vehicle dynamic modelling and inter-vehicle communication framework development. In the following two subsection, we briefly summarize the research results for vehicle dynamical modelling and inter-vehicle communication respectively.

## 1.1 Vehicle Dynamic Modelling

For vehicle dynamic modelling, we first investigated vehicle dynamics. Then the vehicle dynamics is mathematically modelled to address issues related to the important components that influence the handling of road vehicles. The studied mathematical relationship include coordinate systems, Newton Second Law, tyre characteristics, forces between wheel and road, aerodynamics of road vehicles, vehicle dynamic model, and suspension.

The mathematic model of vehicle dynamics described above is implemented in Matlab and Simulink. The developed model is used to investigate the performance of conventional Anti-Braking System (ABS). We obtained simulated performance of a conventional ABS and observed the problem with the conventional ABS, *i.e.* the ABS tries to maintain the slippage to fluctuate at a set-point of 15%. However, we also simulated that on different road condition, the slippage corresponding to the maximal stopping distance is not fix, but varies with different road surface. Therefore, conventional ABS can be improved using an adaptive ABS control algorithm, which dynamically changes the control set point of the slippage such that the grip coefficient between the wheel and the road is maximized. However, more theoretical study and experimental study need to be conducted in future projects. The developed simulation model serves as a solid foundation for the development of the intelligent electronic control unit for ABS that can improve the current technology.

In addition, a Virtual Reality module has also been developed to virtually represent the dynamics of vehicle. The vehicle dynamic model is implemented in Matlab and Simulink. The simulator is linked with a graphical animation created in Virtual Reality Toolbox. The purpose of the model is to perform simulation on the effect of the new ABS system on the motion and stopping distance on a vehicle. Through the animation toolkit, it is possible to create a graphical representation of the dynamic behavior of the vehicle under different operations. The simulation model ultimately collects input signals from three physical factors to generate its output: the gas and braking pedal, steering wheel, and road surface. By controlling these input signals, the user can control a virtual dynamic model of a vehicle in the 3-dimensional simulation world.

## 1.2 Inter-vehicle Communication Systems

Vehicular ad hoc networks (VANETs) are characterized by their fast changing topology and the high mobility of their nodes (vehicles) which add more challenge in the design of a suitable routing protocol for the vehicular environment. There are many applications and routing protocols that have been developed or under development for VANETs to help the drivers to travel more safely. Most of these applications and routing protocols use broadcasting extensively in finding a route to a destination, sending beacons to neighbors notifying them about their position, acceleration and most importantly to send safety warning messages to neighbors within certain distance to avoid chain collisions. Because vehicles move in a limited area and direction with confined rules, they will be close to each other especially in a jam or high traffic situations. Using broadcast in its flooding way may lead to what is known as the broadcast storm problem when more redundancy, contention and collisions happen at the link layer.

In project year 2008-2009, we first investigated the optimal communication range considering average node density and average message generation rate. We then proposed a broadcasting scheme, referred to as Network Topology p(probability)-Persistence Scheme

(NTPP), which integrates the advantages of the clustering based scheme and the slotted p-persistence scheme. Simulation results verified that the proposed scheme could provide reduced delay for the message to reach the destination vehicles and reduced broadcasting redundancy.

Positioning information is very important for designing efficient communication protocols. Some assisted GPS [1] can achieve an average accuracy of 3m to 10m in open flat areas. Currently, the most promising and widely used positioning techniques are global positioning systems (GPS). However, satellite signals are often disturbed or blocked when the vehicles are travelling through tunnels, under bridges and sky scrapers. Vehicles can also experience sustained GPS outages due to high solar activity, terrestrial interference, multipath fading, and non-line of sight radio propagation. Therefore, GPS alone cannot be applied for vehicular safety applications in order to achieve higher accuracy in position estimates to avoid traffic accidents. The addition of radio-based ranging techniques in the absence of GPS signals can be applied as a promising technique [2].

In the project year 2007-2008, we investigated advanced ranging and positioning algorithms. Biased Kalman filter is applied to mitigate the positive bias introduced by the presence of non-line of sight (NLOS) radio waves. We further investigated the application of the Constrained Weighted Least Square (CWLS) optimization to improve vehicle position tracking. The positioning problem is formulated in a state-space framework and the constraints on system states are considered explicitly. Simulation results show the proposed algorithms for NLOS identification and mitigation with the biased Kalman filter achieve higher accuracy for vehicle positioning and tracking systems. By the application of CWLS optimization algorithm, the estimation can be further improved significantly.

The research output includes one accepted conference paper, which will be presented in the 4th IEEE Conference on Industrial Electronics and Applications, in May 25-27, 2009, in Xi'an, China; three conference papers were submitted to IEEE Globecom 2009, which is a flag conference in communication, and one technical report. These papers are attached in the appendix of this report. We are continuing to conduct the research and to prepare

journal paper submissions.

In the remaining of this report, the progress in vehicle dynamic modelling will be presented in Chapter 2; Chapters 3 and 4 present the research outcome in inter-vehicle communication and ranging/positioning respectively; Chapter 5 summarizes future work proposed in our new proposal; Chapter 6 concludes the report.

## Chapter 2

# Modelling of the Vehicle Dynamics

The long-term goal of this research is to develop an intelligent (Electronic Control Unit) ECU for ABS that can recognize the road condition and accordingly control the slippage that results in the maximum grip thus shortest stopping distance, whilst safe controllability and stability are maintained. The proposed intelligent ECU is based on a dual loop feedback control scheme. In the outer loop, a vehicle motion sensing system will be developed to monitor the dynamics of the vehicle thus the grip between the wheels and the road can be estimated. This estimate is used to determine the most desirable slippage. In the inner loop, the conventional ABS control algorithm will be employed to control the ABS so that the slippage is maintained at the desired level determined by the outer loop. To achieve this goal, a vehicle dynamic simulation platform needs to be developed. The simulator will be used to investigate the dynamics of vehicles during emergency braking and to develop an adaptive ABS control scheme. This chapter describes the main concept and progress in the development of this simulation model. More details can be found in the appendix.

### 2.1 Vehicle Dynamics

The behavior of a road vehicle is the consequence of the dynamic interaction of the various components of the vehicle structure in which the pneumatic tyre plays a major role. In

addition to the aerodynamic forces and the gravity, all the other forces that make a vehicle to accelerate or to decelerate are applied to the vehicle from the ground through the wheels. The primary forces that control a ground vehicle are developed in four patches where the tires contact the ground. Therefore it is essential to understand how the dynamics of ground vehicles is determined by the forces and moments generated by pneumatic tires at the ground. The motions accomplished in acceleration, braking, cornering and ride are the responses to forces imposed. The study of vehicle dynamics involves the principles of how and why the forces are produced. It is understood that the dominant forces acting on a vehicle to control its performance are developed by the tire against the road. Thus the behavior of tires, characterized by the forces and moments generated over the broad range of conditions, is the dominating factor that determines the performance of ground vehicles that is associated with vehicle cornering, turning or directional response.

All modern motor vehicles are equipped with pneumatic tires to support the vehicle (and the payload) and to transfer the driving power. This is obtained through the contact between the wheels and the ground (road). This contact also provides lateral forces to control the trajectory of the vehicle. The rigid structure of the wheel is surrounded by a compliant element that is made by the tire. The tire is a complex structure that consists of a number of layers of rubberized fabric. Structurally, tires can be categorized into two groups: bias tires and radial tires. Presently radial tires have completely substituted the bias tires due to the superior performance. The main function of the tire is to distribute the vertical load in a large area and to insure compliance to absorb the irregularities of the ground.

Generally, understanding on vehicle dynamics can be accomplished at two levels: the empirical and the analytical. Although often leading to failure, the empirical approach has helped develop knowledge on vehicle dynamics. Through trial and error process, empirical understanding is derived on the factors that influence vehicle performance and on how the influence is applied and changed by operating conditions. The analytical approach aims to understand the mechanics of interests based on the proven laws of physics that allows for the establishment of analytical models. In this project, we aimed to develop a mathematical

model of motor vehicle dynamics that will be used to investigate the dynamics of vehicles (*e.g.* braking and acceleration) and that will be integrated with the inter-vehicle communication model for the studies on how the driving safety can be improved through information sharing among vehicles travelling in the same traffic.

## 2.2 Model the Dynamics of Ground Vehicle

The behavior of a road vehicle is the consequence of the dynamic interaction of the various components of the vehicle structure in which the pneumatic tyre plays a major role. The complexity of the structure, behavior of the tyre, and the dynamics of vehicles have attracted enormous research interests in the last fifty years, the period during which the application of mathematics to this field has been established. Vehicle dynamic models have been developed for a broad range of purposes, such as academic study and industrial product design.

The fundamental approach to the modelling of vehicle dynamics is based on the understanding that the dynamic behavior of the vehicle is determined by the forces and moment imposed on the vehicle from the tires, gravity and aerodynamics. In this context, the vehicle dynamics refers to the movement of vehicles on a road surface. The movement of interest include acceleration, braking, ride, and turning.

The vehicle dynamics is mathematically modelled to address issues related to the following important components that influence the handling of road vehicles:

- Tyre characteristics and effective Axle Cornering characteristics;
- Vehicle handling and stability based on non-linear cornering solutions and moment method;
- Tyre Brush model, semi-empirical model and transient tyre models;
- Forces between wheel and road: pneumatic tyres, contact pressure and stiffness, rolling radius, rolling resistance, tractive and braking forces, cornering forces;

- Aerodynamics of road vehicles: aerodynamic drag, lift and pitching moment, side forces and yawing moments;
- Longitudinal dynamics: acceleration, braking;
- Vehicle handling: trajectory control, steering, stability;
- Elastic suspensions: quarter-car models, bounce and pitch motions.

A framework of the model has been implemented in the Matlab with Simulink. The model has been used to investigate conventional ABS. Fig. 2.1 shows the stopping distance of a vehicle with initial speed of 45 km/hr on dry road (top square marked curve) and icy road (bottom curve). The slippage is controlled at different set-point, ranging from 0.05 to 0.5. The result indicates that the shortest stopping distance is achieved by controlling the slippage at 15% while riding on a dry surface. However, while riding on an icy surface, the shortest stopping distance is achieved by controlling the slippage at around 25%. This is because the friction coefficient between the tire and the icy surface peaks at slippage of 25%.

It is accepted by all the designers of Anti-lock Brake System (ABS) that the wheels have the greatest grip on the road when the slippage is between 10% and 15%. Therefore all ABS in use nowadays are designed to control the brake such that the slippage is maintained between 10% and 15%. However, the relationship between slippage and the grip produced between the wheels and the road depends on the surface conditions. The grip may be peaked at a slippage that is significantly different from 10% to 50%. This explains why many experiments have reported that ABS lead to increased stopping distance on the surfaces that a reduced stopping distance is most desirable.

Conventional ABS consists of four major components, including wheel speed sensors on each wheel, electrically controlled hydraulic valves, electric motor powered hydraulic pump, electronic control unit (ECU). This is a typical single loop control system. The ECU estimates the slippage according to the sensor signals and controls the valves so that the slippage is controlled within 10% to 15%. This results in that the grip between the wheels

and the road is not maximized.

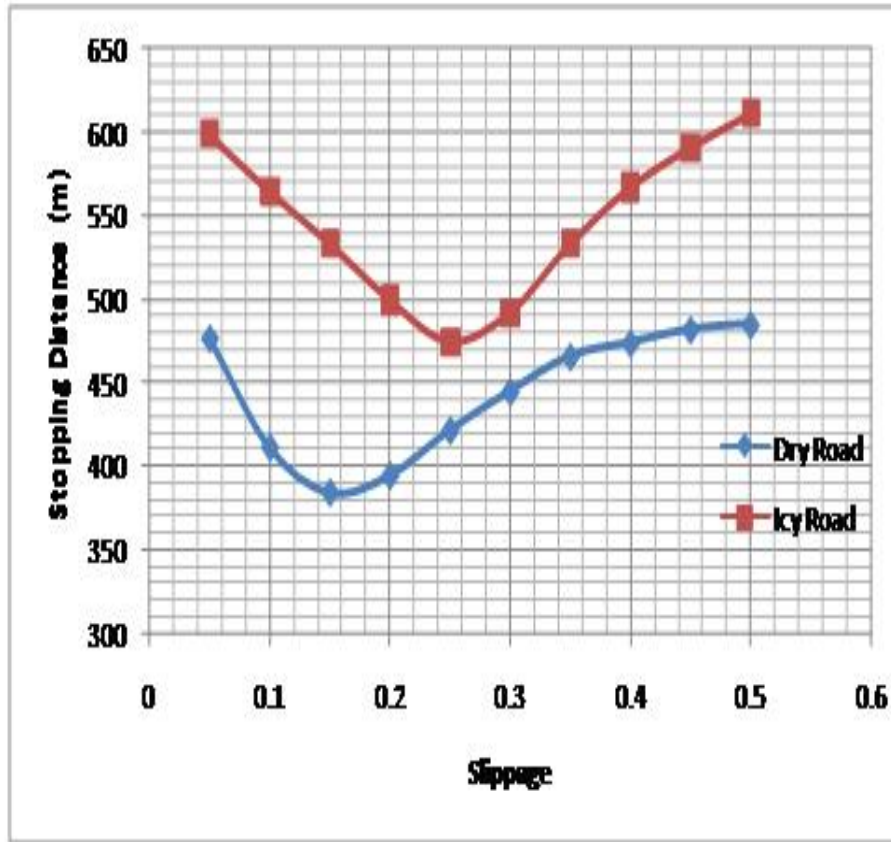


**Figure 2.1:** Stopping distance as a function of slippage.

Further simulation results also show that the vehicles with conventional ABS have up to 20% longer stopping distance on wet, snowy and icy surfaces compared with vehicles without any ABS. Conventional ABS can be improved using an adaptive ABS control algorithm, which dynamically changes the control set point of the slippage such that the grip coefficient between the wheel and the road is maximized. However, more theoretical study and experimental study need to be conducted in future projects.

The long-term goal of this research is to develop an intelligent ECU for ABS that can recognize the road condition and accordingly control the slippage that results in the maximum grip thus shortest stopping distance, whilst safe controllability and stability are maintained.

The proposed intelligent ECU is based on a dual loop feedback control scheme. In the outer loop, a vehicle motion sensing system will be developed to monitor the dynamics of the vehicle thus the grip between the wheels and the road can be estimated. This estimate is used to determine the most desirable slippage. In the inner loop, the conventional ABS control algorithm will be employed to control the ABS so that the slippage is maintained at the desired level determined by the outer loop.

## 2.3 Extend the model to Virtual Reality

The vehicle dynamic model is implemented in Matlab and Simulink. The simulator is linked with a graphical animation created in Virtual Reality Toolbox. The purpose of the model is to perform simulation on the effect of the conventional and the proposed ABS system on the motion and stopping distance on a vehicle. Through the animation toolkit, it is possible to create a graphical representation of the dynamic behavior of the vehicle under different operations. The simulation model ultimately collects input signals from three physical factors to generate its output: the gas and braking pedal, steering wheel, and road surface. By controlling these input signals, the user can control a virtual dynamic model of a vehicle in the 3-dimensional simulation world.

The movement of the vehicle is ultimately based on the force acting on the car. A force balance acting on the vehicle is therefore necessarily to understand and to calculate the acceleration, velocity and displacement of the vehicle. This includes the acceleration and braking torque acting on the wheel, head or trail wind, and friction forces. All these factors contribute to the force acting on the vehicle. The simulation environment is a three-dimensional environment plane. The steering wheel control is the device that accepts turning signals and translates them into the orientation and the turning motion of the vehicle. The engine of the simulation relies heavily on the Random Walk Theory to compute the physical movement of the vehicle. The Random Walk predicts the upcoming movement, or future location, solely based on the present location, regardless of the past movement of the vehicle.

## Chapter 3

# Communication Protocols for Efficient IVC

Vehicles in the near future will be equipped with a Dedicated Short Range Communications (DSRC) [3] wireless device so they can form a mobile ad hoc network on the road. The vehicles will broadcast their status information to each other to help drivers to avoid potential dangers and to extend their awareness to beyond of what they can directly see. IVC (inter-vehicle communication) is expected to be the key technology for cooperative driving systems and a key component to implement AVCS. Broadcast is a major building block for the discovery, routing and localization functions. In this Chapter, the investigations on the broadcast range and broadcast storm problems are reported.

### 3.1 Maximum Communication Range of a Broadcast Message

Broadcast range is one of the critical functions in the success of safety driving. Broadcasting will face a challenge in managing the channel capacity to ensure a good performance in terms of throughput, fairness and broadcast coverage. For example when one of the vehicles has an accident it has to send a warning message to all vehicles behind it to inform them about the traffic situation to avoid a chain collision. This kind of safety information has to be

propagated in a short time (usually less than 0.5 sec) [4]. The communication range is a critical parameter to enable distant drivers to react in a short time. If all vehicles act greedily by maximizing their communication range then the message will reach its destination in a less number of hops. As a consequence more vehicles will content at every point for using the same wireless channel which will collapse due to collisions. On the other hand, a short transmission range will result in more hops and delay but reduces the interfering traffic.

The communication range is a critical parameter for prompt information sharing. If all vehicles act greedily by maximizing their communication range then the message will reach its destination in less number of hops and less delay; as a consequence more vehicles will content the same wireless channel, leading to communication collapse due to the increased collisions. On the other hand, a short transmission range will result in more hops and larger delay but reduces the interfering traffic. By modelling the optimal range as a function of traffic characteristics, such as network density, delay and sending rate, nodes can adjust their transmission range to reduce channel contention between them.

In [5], the authors used the spatial reuse of wireless resources to find the optimal radio range by knowing the sending rate, network density and one hop delay. They built a geometric model that predicted the likelihood of a collision where all nodes had the same broadcasting rate and communication range. They tried to solve this issue by predicting the optimal range from a pre-calculated scenario for a specific network and found that their results are 16% less in range than the simulated ones.

We extend the work in [5] and follow a new approach to solve this important problem. Our result is a closed form formula in contrast to their findings. We claim that nodes within the wireless network can easily calculate their maximum communication range and adjust their transmission power so all nodes within their range will receive the broadcast message successfully.

The geometric model for the highway scenario is shown as in Fig. 3.1, where vehicles are moving in a certain direction and restricted by the traffic laws. The network topology is fast changing and the nodes (vehicles) are moving in a high speed.

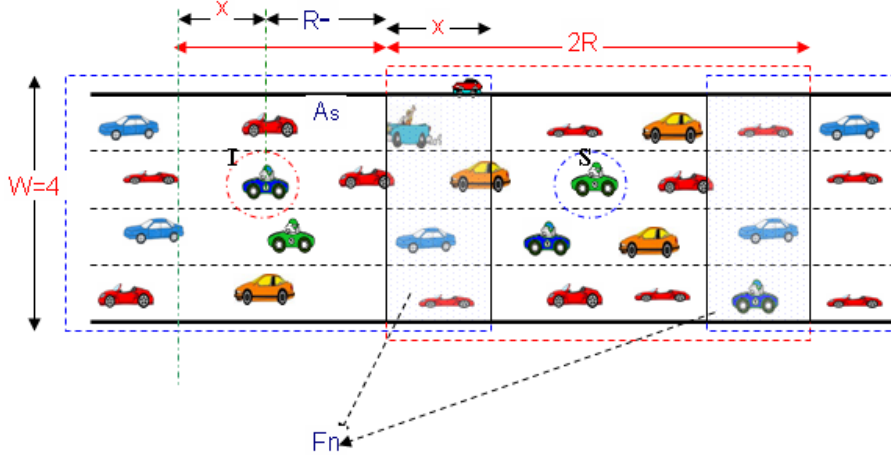


**Figure 3.1:** The highway topology setup in ns2 simulator.

We assume that each node (vehicle) has the same communication range  $R$  and generates packets according to a Poisson process with average sending rate ( $\lambda_p$ ). The packets are of equal size so they need the same time ( $T$  sec) to transmit. The nodes (vehicles) are distributed on the road with an average density ( $\lambda_s$  vehicles/m/lane) and the width of the road is  $W$  lanes.

We can see from the model that if vehicle  $S$  starts broadcasting a warning message then all vehicles within  $R$  distance will hear the transmission and defer from using the channel by carrier sense multiple access (CSMA). Therefore, all vehicles within  $R$  meters will receive the message successfully unless one of the interfering vehicles (vehicle-I), which is located at distance ( $2R - X$ ) from the transmitter, starts transmitting during the current transmission period causing some vehicles in area ( $F$ ) to fail in receiving the message. As a result, the maximum number of nodes that receive the message successfully is that all vehicles within  $R$  meters minus the failed vehicles. Therefore, our goal is to minimize the number of failed nodes.

Since each node (vehicle) is sending packets with independent Poisson process, the probability of a vehicle to send a packet within  $2T$  seconds is given as  $(1 - e^{-\lambda_p 2T})$ . So the expected number of interfering vehicles is:

$$E(I_t) = \lambda_s(2WR)(1 - e^{-\lambda_p 2T})$$

When we set  $E(I_t)$  to be 1, the corresponding  $R_{\max}$  can be derived as

$$R_{\max} = \frac{1}{2W\lambda_s(1 - e^{-\lambda_p 2T})} \quad (3.1)$$

From above equation, we can see that the maximum range is inversely proportional to the vehicle density and the sending rate. Vehicles can adjust their transmission power according to the road density to make sure that all vehicles within its range will receive its message successfully. Roads have different and variable density depending on the time of the day and the traffic situation. Vehicles can sense this density from the beaconing messages exchanged between them or programmed with fixed densities depending on the time of the day and the day of the week. For example, the roads will be in a high density in rush hours (the mornings and afternoons) and in low density at night and weekends.

The proposed optimal communication range is designed as a function of network density, delay and sending rate. More technical details and derivations can be found in our paper [6]. Simulation results, which show higher one hop coverage and less contention will be presented in the later section.

## 3.2 Broadcast Storm Problem

Most applications in Vehicle Ad hoc Networks (VANETs) use broadcasting as a main block for localization, routing and dissemination of warning messages to other vehicles on the road to achieve a safe, reliable and effective transportation system. Broadcasting in its normal way may lead to a broadcast storm problem by increasing the nodes contention in using the communication channel and more collisions which may result in the collapse of the communication system.

When the traffic density is high, where many nodes are moving, the broadcasting faces a challenge in managing the channel capacity to ensure desirable throughput, fairness and broadcast coverage. In this case, using broadcast in its flooding way may lead to what is known as the broadcast storm problem when more redundancy, contention and collisions happen. Those applications will face a challenge in managing the channel capacity to insure a good performance in terms of throughput, fairness and broadcast coverage. For example when one of the cars has an accident it has to send a warning message to all vehicles behind it to inform them to avoid a chain collision. This kind of safety information has to be propagated with minimal delay.

This kind of safety information has to be propagated in a short time (usually less than 0.5 sec) [4]. In most cases not all vehicles within the one hop distance will receive the message due to the hidden terminal problem. Therefore the message has to propagate in a multi hop fashion. If all vehicles within the one hop broadcast try to rebroadcast the same message then there will be more contention for using the channel and the message could be lost due to collisions. Moreover many of the rebroadcasts are redundant since they will cover almost the same area. Prioritization one vehicle over the other to rebroadcast the message is the challenge that we would like to investigate.

The broadcast problem has been studied extensively in the mobile ad hoc networks. The authors in [7] presented five schemes to alleviate the impact of this serious problem by prohibiting some nodes from rebroadcasting and favoring others depending on their location and their knowledge of how many times the message has been broadcasted. The schemes are: (i) probabilistic scheme; (ii) counter-based scheme; (iii) distance-based scheme; (iv) location-based scheme; and (v) cluster-based scheme. In [8] the authors introduced three distributed broadcast suppression techniques to alleviate the impact of the broadcast storm problem in VANETs specifically. Each node will calculate its rebroadcast probability based on its local information about the network. The proposed schemes are: (i) weighted p-Persistence; (ii) slotted scheme; and (iii) a slotted p-Persistence scheme.

In the following, we give a brief analysis of the above schemes. First, discuss the schemes

proposed in [7]:

- Probabilistic scheme: it has a major disadvantage when the traffic is high and there are many vehicles in a small area. If the assigned probability is high then more vehicles will contend to use the channel and this will delay the delivery of crucial messages. Moreover, there will be situations when the message will not propagate to other hops in a light traffic scenario with assigned low probability. Therefore the probability has to be chosen carefully.
- Counter based scheme: the higher the threshold counter is, the more time the node will wait before it decides to transmit or not. This mechanism will introduce more delay. There is also a possibility that the node will receive the same message more than the threshold from far nodes but very close to each other. In this case the node will decide not to transmit while it should since all of the received messages are redundant.
- Distance based scheme: the threshold distance has to be chosen carefully. The higher the threshold is, the less number of vehicles propagate the message. If the traffic is light then there may be no vehicles beyond that threshold and the message will die. On the other hand, if the threshold distance is low and the traffic is high then more vehicles will contend to rebroadcast the message.
- Location based scheme: it is a good choice since it calculates exactly the additional coverage area but it needs a full knowledge of the network topology. The calculation operation is very complicated over many intersecting circles.
- Cluster based scheme: it is also a good choice since it decreases the number of participating nodes in rebroadcasting the message. This scheme is more vulnerable to the hidden terminal problem. If the cluster head broadcasts the message and more than one gateways are in the range of the cluster head but outside the range of each other, then some nodes in the new covered area will fail in receiving the message successfully.

Next, let us analyze the schemes proposed in [8]:

- Weighted p-Persistence scheme: where each node has different probability than the other. This probability depends mainly on the distance. Each node has a fixed time to wait before it rebroadcasts the message. This will add more delay to the message which may not be propagated to the next hop especially in sparse networks.
- Slotted scheme: it introduces more delay especially in sparse networks. The nodes will wait its calculated waiting time even if there are no nodes further than them to rebroadcast the message. The probability and the number of slots have to be chosen very carefully and should depend on the road traffic parameters.
- Slotted p-persistence scheme: it reduces the contention within the one hop broadcast significantly. Furthermore, it introduces the highest delay since the nodes in every slot wait their time before they start contending for the use of the channel. If the network density is low and the probability chosen is also low then the message may not be able to propagate to the next hop.

From the above analysis, we can conclude that the more knowledge the nodes have about the network topology and traffic parameters, the better decision they can make for either to retransmit or not. The rebroadcast decision has to be shared between the data link layer and the above layers especially the application layer in order to decide for how long the message will be alive in the network and how far to be propagated

In the proposed scheme, the first factor we considered is the maximum one hop range that each vehicle can use to reduce the impact of the hidden terminal problem.

Furthermore, we consider the application of the Received Signal Strength (RSS) instead of the inter distance between nodes. Using the distance in calculating the probability may result in wrong decisions especially in a highly mobile environment where the characteristics of the wireless channel are very unstable. Using the received signal strength will take into account all the parameters of the wireless channel. This means that vehicles may have high probability to rebroadcast the message even if they are close to the transmitter if they receive a very low power signal due to obstruction in the channel.

We further consider network density. We believe that the more dense networks are, the less number of nodes needed to participate in rebroadcasting the message to decrease the contention and the number of collisions.

The proposed scheme, called Network Topology p-Persistence scheme (NTPP), is based on the combination of the cluster based scheme in [7] and the slotted p-persistence scheme in [8]. We believe that if each node in the network has information about other nodes in the one hop broadcast range (which can be done through beaconing) then each node can detect the farthest node to itself that can deliver its message to add the maximum possible additional coverage while decreasing the propagation delay.

When the node retransmits the message, we consider to assign probability according to signal strength received and node density. Nodes in low dense networks will have a higher probability to transmit and vice versa. Furthermore, when one node is retransmitting the message, other nodes need to wait for a certain time  $T_W$ . This waiting time has to be proportional to the received signal strength. The higher the signal strength, the larger waiting time should be. Moreover, the node density has also to be included in the waiting time so the nodes have less waiting time in low dense networks to overcome the long delay time problem in sparse networks.

The proposed scheme integrated the advantages of the cluster based scheme [7] and the slotted p-persistence scheme as in [8]. More technical details and algorithms can be found in our paper [9], which is appended in this report.

### 3.3 Simulation Results

The proposed algorithms are verified through simulations by using ns-2.33, which is a well known simulator in both academic and industrial fields. This simulator has been extended to model VANETs by utilizing IEEE 802.11p technology.

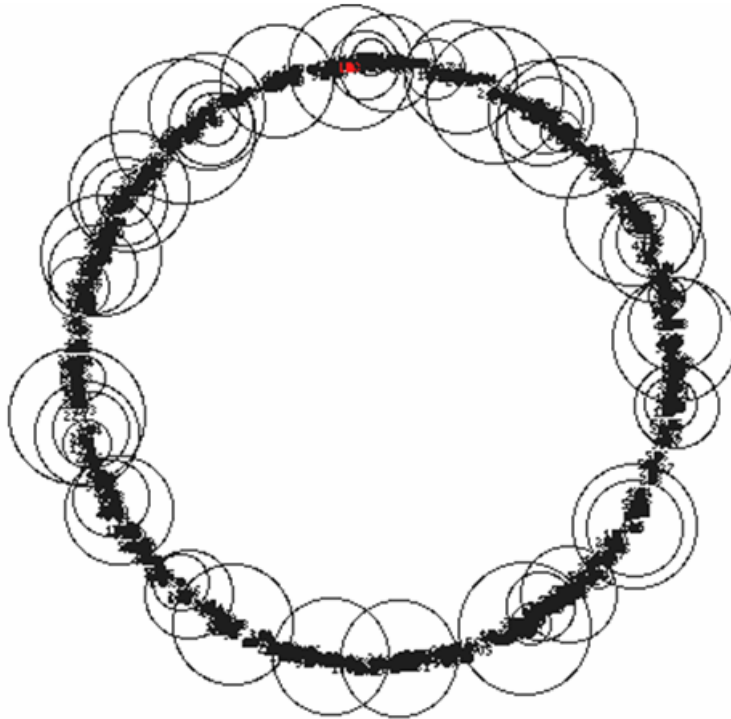


**Figure 3.2:** The highway topology setup in ns2 simulator.

The network models a circular bidirectional highway with a diameter of 2000m (6283m in length) with 4 lanes in each direction. There are 600 vehicles on this highway segment and all of them are equipped with a DSRC technology. We also assume that each vehicle is equipped with a GPS receiver to know its position on the road. The speed of the vehicles is in the range of 40 to 100 Km/h and follow a microscopic mobility model where each vehicle's speed is influenced by the front car and has to change lane if it decides to bypass another car. The topology is shown in Fig. 3.2. All vehicles are moving in the circular highway and transmitting periodically their status messages. The vehicle in the square

is the malfunctioning one and sends the emergency message to all vehicles behind it in a flooding fashion or using the proposed NTPP scheme.

Each vehicle is configured to send 1, 5, 8 and 10 beacons/s of size 500 Bytes. The data rate is 3Mbps. We configure one of the nodes to send an emergency message of size 500 Bytes to all vehicles behind it and up to a distance of 2000m. We are interested in the time the emergency message to reach all the vehicles in the region. We will compare the results for different communication ranges (200m, 400m and 700m) with different traffic loads between the broadcasting in the flooding way and by using the proposed scheme (NTPP).

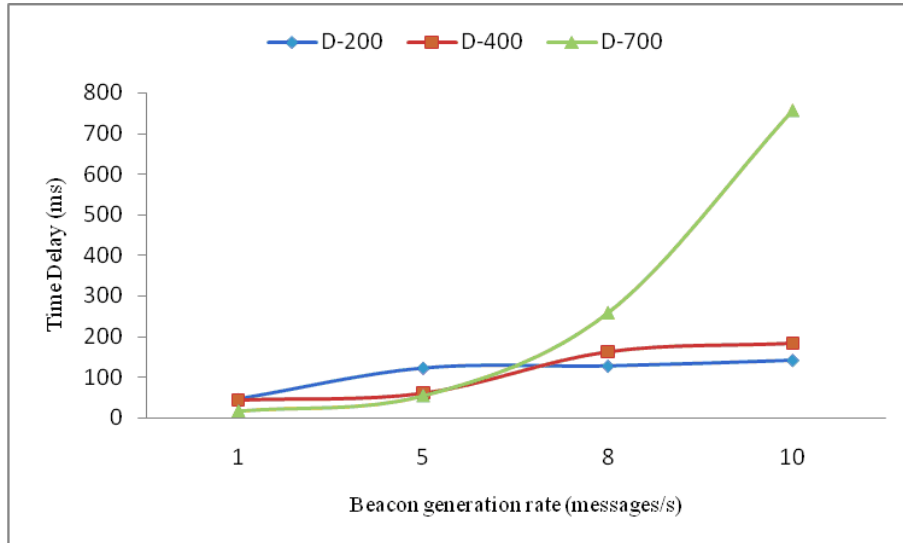


**Figure 3.3:** Time delay versus beacon generation rate.

Fig. 3.3 shows the time the warning message takes to reach all vehicles in the relevant distance (2000m), versus the number of beacon generation rate. It is clear that when the beacon generation rate is low, the higher communication range will perform better than smaller ranges since the message will reach its destination in less number of hops without facing the high contention in using the channel. On the other hand, as the traffic increases, this means more interfering transmissions facing the emergency message propagation to its

destination, using a smaller communication range will perform better than using a higher range. It can be seen from Fig. 3.3, the shorter communication range performs better in high dense networks because the node faces less number of interfering traffic compared with the nodes with high communication range. When the beacons traffic rate is 10 packets/s, the communication range of 200m outperforms the 400 and 700m and this agrees with our theoretical results from where the calculated best range is 198m.

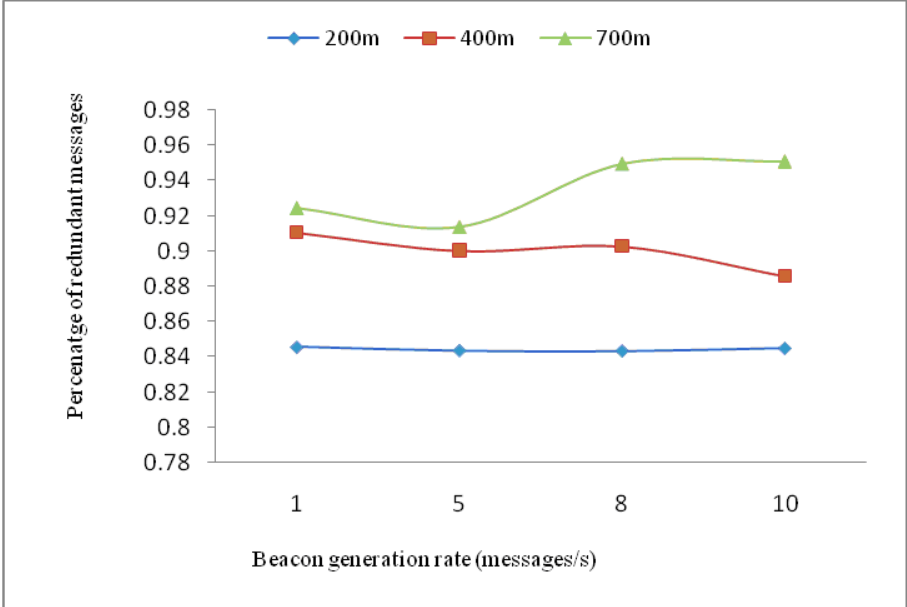


**Figure 3.4:** Percentage of the received redundant messages versus the traffic load.

Figure 3.4 shows the percentage of the redundant messages that have been received by the vehicles within the relative distance (2000m) to all warning messages that have been broadcasted. It is obvious that when vehicles are configured with large communication range, then most of the warning messages are redundant since each vehicle will receive the message more than once. This percentage will increase when the traffic is high since the message propagation speed will be slow due to the high interfering traffic. This explains why the small communication ranges of 200m and 400m have less overhead than the high communication range of 700m.

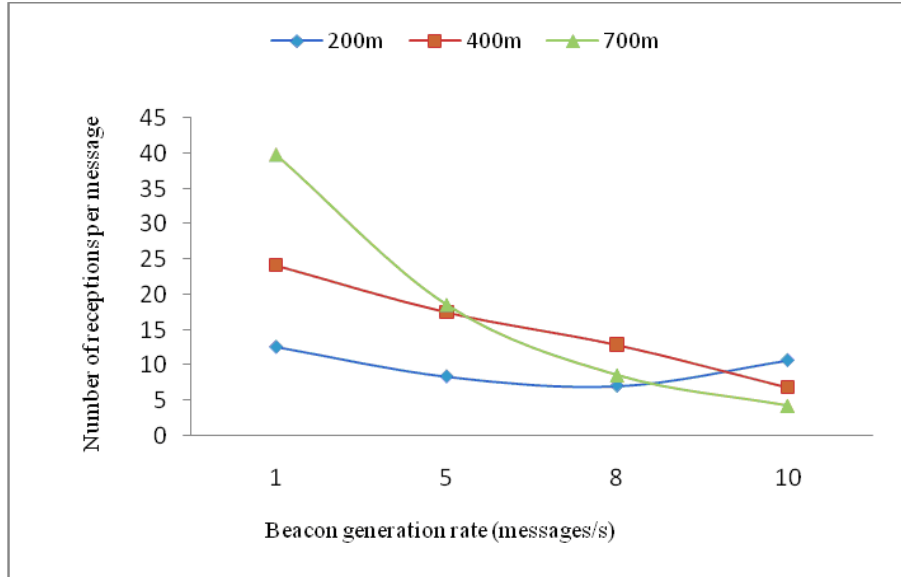


**Figure 3.5:** Number of vehicles that received the warning message successfully versus the traffic load.

Figure 3.5 shows the average number of vehicles that receive the warning message within one hop broadcast range. It is clear that the higher communication range will have better coverage than the lower communication range when the traffic is low. While when the traffic is high, the high communication range (700m) performs worse than that of 200m and 400m in terms of the number of vehicles that receive the warning message successfully. We can see that the communication range of 400m outperforms all others when the traffic is 8 beacons per second and the 200m range outperforms all others when the traffic is 10 beacons per second. This complies with our finding in Eqn. (3.1) which predicts the best communication range that minimizes the contention and collisions between nodes.

Fig. 3.6 shows the time the warning message takes to reach all the vehicles in the relevant distance (2000m), versus the number of beacon message generation rate (traffic load) for the different communication ranges in two scenarios: the first scenario when the broadcast is flooded through the network and the second scenario when the broadcast is

controlled by our algorithm NTPP. It is clear that when the beacon generation rate is low, the flooding approach performs better than our algorithm since there is not much interfering traffic and the nodes will not wait any time before retransmitting the warning message. On the other hand, when the traffic load is high, the rebroadcast in its flooding way will add more contention in using the channel and this will delay the warning message propagation. As we can see from Figure 5, our algorithm NTPP performs better than the flooding way and the message propagates faster to the end of the relative distance.

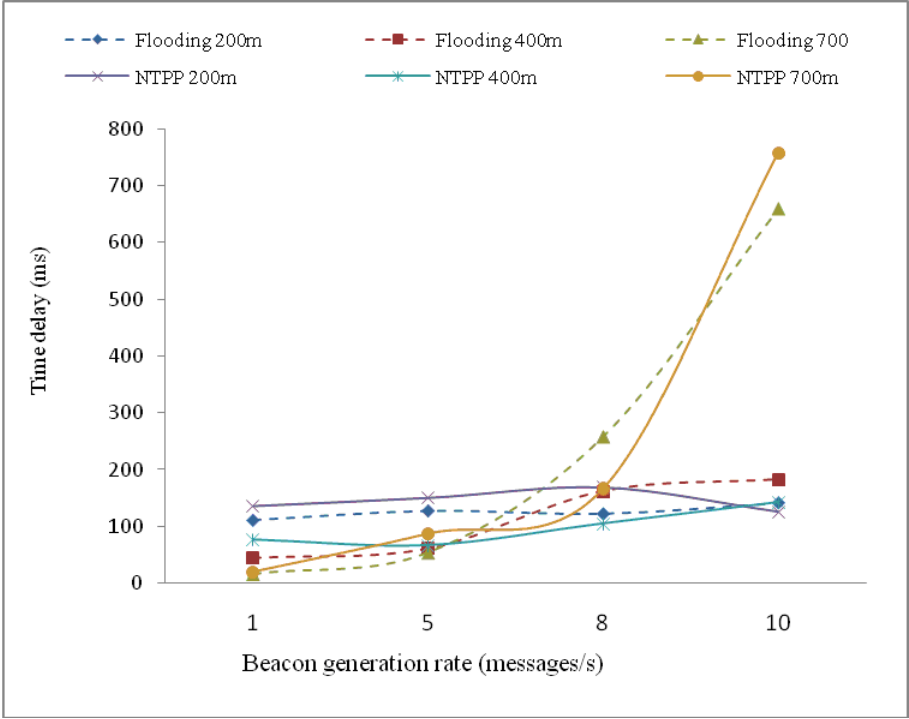


**Figure 3.6:** Tie delay versus the traffic load.

Fig. 3.7 shows the percentage of the redundant messages received in the relative distance for both flooding broadcast and the new scheme NTPP. It is clear that NTPP reduces the redundant traffic significantly compared with the flooding rebroadcast. When the beacons traffic rate is high, the communication range of 700m has high percentage of redundant messages since the propagation speed will be slow and the transmitter will face many collisions

before it succeeds in transmitting the message.

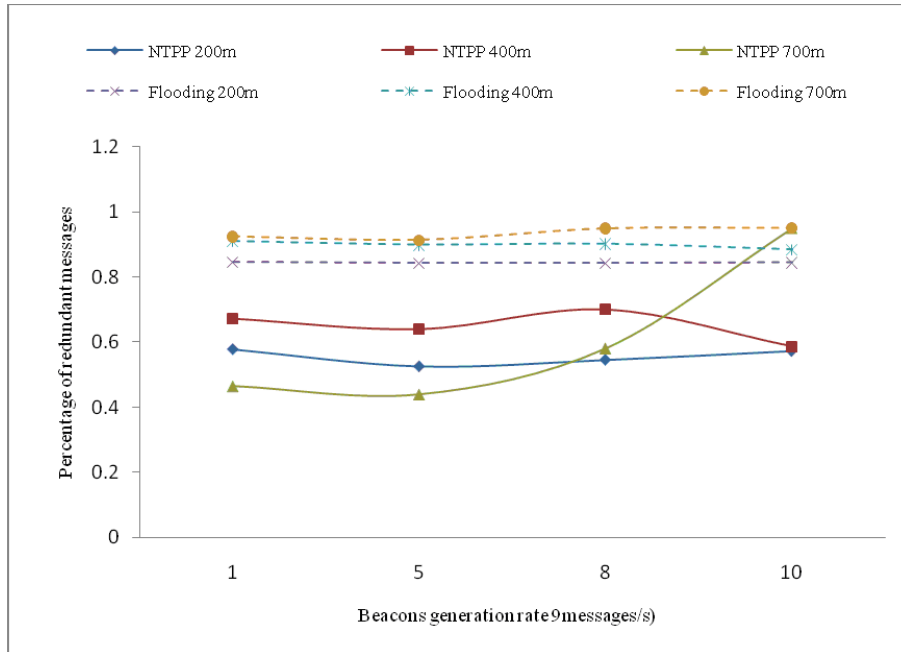


**Figure 3.7:** Percentage of redundant messages received within the relative distance for the flooding and NTPP.

# Chapter 4

## Vehicle Position System

The intelligent cooperative collision warning system is an important class of safety applications that target the prevention of vehicular collisions and provide real-time alerts about hazards and accidents. The cooperative collision warning systems use vehicle-to-vehicle and vehicle-to-infrastructure communications for wireless vehicular networks to improve the level of safety, efficiency, and information availability by the periodic broadcast of short messages bearing status information (*i.e.*, accurate estimations of location, velocity and control settings).

Vehicle position information is important for cooperative collision warning application and other IVC protocols. Currently, the most promising and widely used positioning techniques are global positioning systems (GPS). Some assisted GPS [1] can achieve an average accuracy of 3m to 10m in open flat areas. Besides accuracy concern, in reality, satellite signals are often disturbed or blocked when the vehicles are traveling through tunnels, under bridges and sky scrapers. Vehicles can also experience sustained GPS outages due to high solar activity, terrestrial interference and multipath fading. In persistent GPS outages, vehicles can use dead reckoning systems to obtain position information; however, they are prone to errors. The dead reckoning systems can accurately determine its GPS coordinates with a permissible error of less than 10m for approximately 30s outages if the vehicle is traveling at a speed of 60km/h [2]. Line of sight (LOS) between the object to multiple satellites is

not always possible, therefore, GPS alone cannot be applied for vehicular safety applications in order to achieve higher accuracy in position estimates to avoid traffic accidents. The addition of radio-based ranging techniques in the absence of GPS signals can be applied as a promising technique [2].

## 4.1 Ranging Smooth Algorithms

One of the fundamental steps for positioning is accurate ranging, *i.e.*, an action of estimating the distance between the transmitter and the receiver.

Ranging and positioning accuracy could be limited by the presence of multipath fading, non-line-of-sight (NLOS) conditions, and extra propagation delay, due to the presence of obstacles. In dense urban environment there may not always be a direct path between the vehicles. Due to reflections and diffractions, the range measurements tend to be positively biased, which is known as NLOS error. This problem has been recognized by many researchers as a “killer issue” for accurate ranging and positioning [10]. Therefore, the NLOS problem must be taken into consideration.

There are many positioning approaches established for wireless nodes when LOS exists between the transmitter and the receiver. A method of localizing neighboring vehicles based on inter-vehicle distance measurements using one of the radio-based ranging technique is proposed along with triangulation to determine relative position coordinates of vehicles in [2]. Here position estimation may become very inaccurate since the distance measurements are noisy. Authors in [11] proposed a TDOA error minimizing localization method to estimate the location of group of blind nodes in LOS and NLOS propagations for fixed reference node positions. This is more appropriate for cellular mobile networks where the base stations are at fixed locations but not suitable for inter-vehicle communication where vehicles are moving continually.

To improve the accuracy of ranging and positioning of vehicles, NLOS mitigation techniques must be applied. A polynomial fitting was applied to all available measured range

data to mitigate NLOS effects [10]. This is not accurate due to time delay in total data gathering. A modified Kalman filter algorithm is presented in [12] to estimate NLOS bias for UMTS mobile positioning. The estimation of range bias in the proposed algorithm improves the performance of location tracking in NLOS environments. NLOS mitigation with the biased Kalman filter for the range estimation in Ultra wideband (UWB) systems for wireless sensor networks was proposed in [13], where the mobility of the users had not been considered.

In our work, we implement the biased Kalman filter for vehicular networks where the vehicle mobility complicates the case. Among vehicles, noisy measurements can be misinterpreted as an observed motion and the effects of fading become prevalent for a road topology. Vehicles on the road are not uniformly distributed and the positions of the vehicles are not fixed. We consider the problem of NLOS identification and mitigation for the vehicular communications in the absence of GPS signals to smooth the range data between randomly selected vehicles. A simple hypothesis test, based on the standard deviation of the measured noise, is applied to distinguish between the LOS and NLOS range measurements. If the measurements contain NLOS error, then the NLOS must be mitigated before the position estimation takes place for accurate results. NLOS error correction is possible by applying the biased Kalman filter instead of the unbiased Kalman filter where it can mitigate unexpected high erroneous NLOS data.

To improve the accuracy of ranging and positioning of vehicles, we implemented a biased Kalman filter for NLOS identification and mitigation for vehicular communications to smooth the range data. A simple hypothesis test, based on the standard deviation of the measured noise, is applied to distinguish between LOS and NLOS range measurements. If measurements contain NLOS error, then NLOS must be mitigated before position estimation takes place for accurate results. NLOS error correction is possible by applying the biased Kalman filter instead of the unbiased Kalman filter. The formulation of the problem and the proposed algorithm by using biased Kalman filter can be found in [14] as appended in this report.

## 4.2 Constrained Weighted Least Square Optimization

Further to the research presented in the above section, vehicle position is optimized by applying Constraint Weighted Least Square (CWLS) approach and Lagrange multipliers to minimize the cost function.

In general, the mobile station position is not determined geometrically but is estimated from a set of nonlinear equations constructed from the TOA, RSS, TDOA, or AOA measurements, with the knowledge of the base station geometry. Generally optimization approaches for positioning are Nonlinear Least Square (NLS), Maximum Likelihood (ML), Gaussian ML (GML), Genetic Algorithm Method (GAM) and Constrained Least Square method(CWLS) [15]. Basically, there are two approaches for solving the nonlinear equations. The NLS approach is to solve them directly in a nonlinear least squares (NLS) or CWLS framework. Although optimum estimation performance can be attained, it requires sufficiently precise initial estimates for global convergence because the corresponding cost functions are multi-modal.

The CWLS approach is to reorganize the nonlinear equations into a set of linear equations. In our work, the CWLS approach is adopted and we focus on a unified approach for accurate position algorithms for TDOA measurement. For TDOA-based position systems, it is well known that for noise conditions, the corresponding nonlinear equations can be reorganized into a set of linear equations by introducing an intermediate variable, which is a function of the source position. This technique, is commonly called spherical interpolation (SI) [16]. However, the SI estimator solves the linear equations via standard least squares (LS) without using the known relation between the intermediate variable and the position coordinate. To improve the location accuracy of the SI approach, Chan and Ho have proposed to use a two-stage CWLS to solve the source position in [17], while [18] incorporates the relation explicitly by minimizing a constrained LS function based on the technique of Lagrange multipliers. According to [18], these two modified algorithms are referred to as the quadratic correction least squares and linear correction least squares, respectively. In this work, we developed

a unified approach for mobile location by utilizing TDOA measurement and improving the ranging accuracy with the use of Constrained Weighted Least Square algorithm. Detailed problem formulation and solution can be found in our submitted paper [19] (appended).

### 4.3 Simulation Results

For simulations, LOS and NLOS have been applied to the range measurements and a hypothesis test is used to determine which range measurements have LOS and NLOS. Basically, the true range with the addition of AWGN is known as the LOS condition. The performance metric, root mean square error (RMSE), was applied to determine the range error, which is defined as:

$$\epsilon = \sqrt{\frac{1}{N} \sum_{i=1}^N [\hat{d}_T(i) - d_T(i)]^2} \quad (4.1)$$

where  $d_T(i)$  is the true range of the  $i^{th}$  vehicle and  $\hat{d}_T(i)$  is the estimated range of the  $i^{th}$  vehicle.

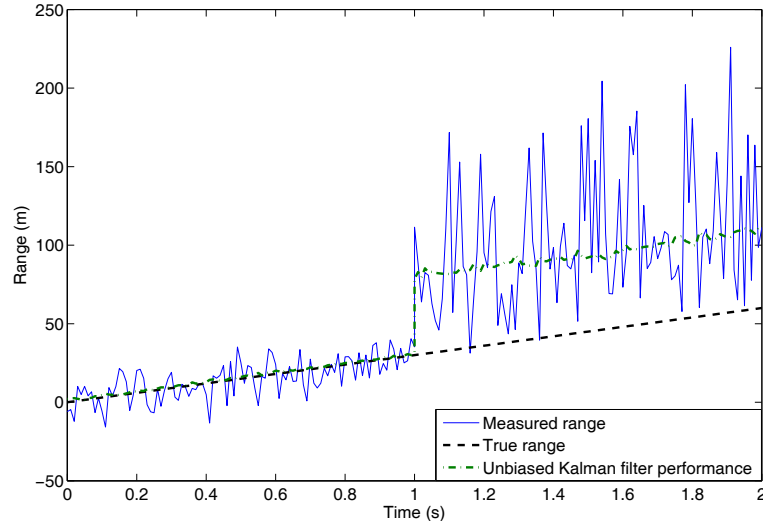


**Figure 4.1:** Unbiased Kalman filter output for LOS and NLOS.

In Fig.4.1, the propagation situation is LOS from the beginning of the simulation to 1 second. Then it changes to NLOS. The straight dashed line is the true range. The curve

with large fluctuation is the measurement results. The dash dotted curve is the results of the unbiased Kalman filter output. It shows that the unbiased Kalman filter can preprocess the range data with a RMSE of 0.05m for the LOS scenario; for the NLOS scenario, the RMSE could be too high to acceptable. Therefore, in the presence of NLOS, unbiased filter is not sufficient to smooth the range measurement. NLOS needs to be filtered out for acceptable estimation.

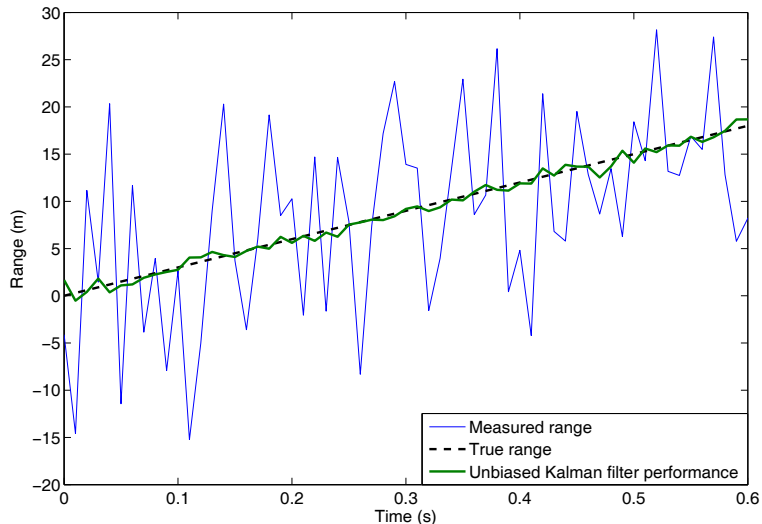


**Figure 4.2:** Unbiased Kalman filter output for LOS in  $[0, 0.6]$ s.

Fig. 4.2 shows a zoomed version of Fig.4.1 from the start to 0.6s. It shows that by using the unbiased Kalman filter, the estimation is almost overlapped with the true range. However, the unbiased Kalman filter cannot eliminate the positively biased NLOS data added for the time period of 1s to 2s.

In Fig. 4.3, we add the results from the biased Kalman filter for the propagation situation changing from LOS to NLOS at time instant of 1s, similar to Fig. 4.1. The inter-vehicle range data smoothed by the unbiased Kalman filter cannot track the sudden changes due to NLOS from time instant of 1s to 2s. However, the NLOS error from the range measurements is mitigated by using the biased Kalman filter with a RMSE value of less than 0.7m.

Fig.4.4 shows the biased Kalman filter smoothed output for a mixed LOS/NLOS condition. From 0s to 1s, LOS is present. It switches to NLOS condition from 1s to 2s, and

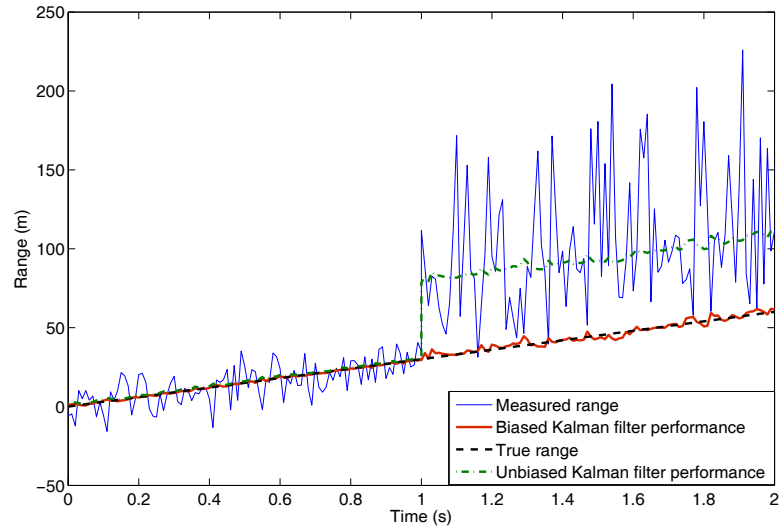


**Figure 4.3:** Biased vs unbiased Kalman filter smoothed range data.

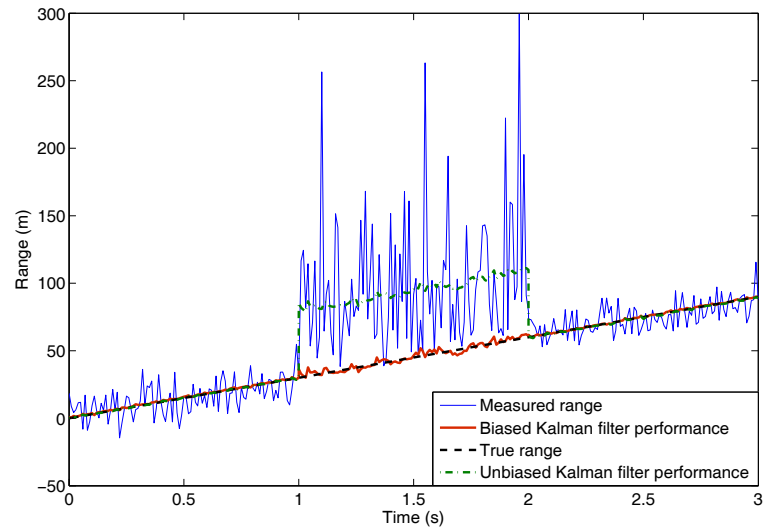


**Figure 4.4:** Estimated range data with an abrupt change between LOS and NLOS.

switches back to LOS condition from 2s to 3s. The dash dotted curve and the solid bold curve denote the results for unbiased Kalman filter and biased Kalman filter respectively. We can observe that the unbiased Kalman filter can give a desirable estimation only in the presence of LOS; while the biased Kalman filter can effectively mitigate the NLOS error even when the vehicle travels with an abrupt switching between the LOS and NLOS conditions.

In the following, we compare the results by using Kalman filter only with the results by applying CWLS optimization approach. Fig. 4.5 illustrates the application of Kalman filter to mitigate the NLOS error, where the solid curve and dished curve denote the true distance and the estimated distance respectively. Fig. 4.6 shows the range measurement which is optimized by applying CWLS optimization technique to improve the estimation. It can be observed that the estimation by applying CWLS technique can greatly improve the estimation accuracy.

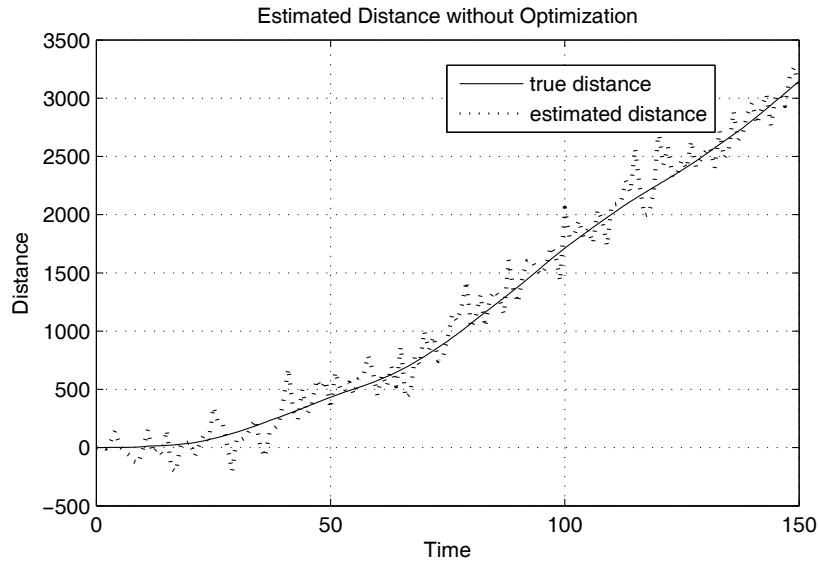


**Figure 4.5:** NLOS mitigation using biased KF.

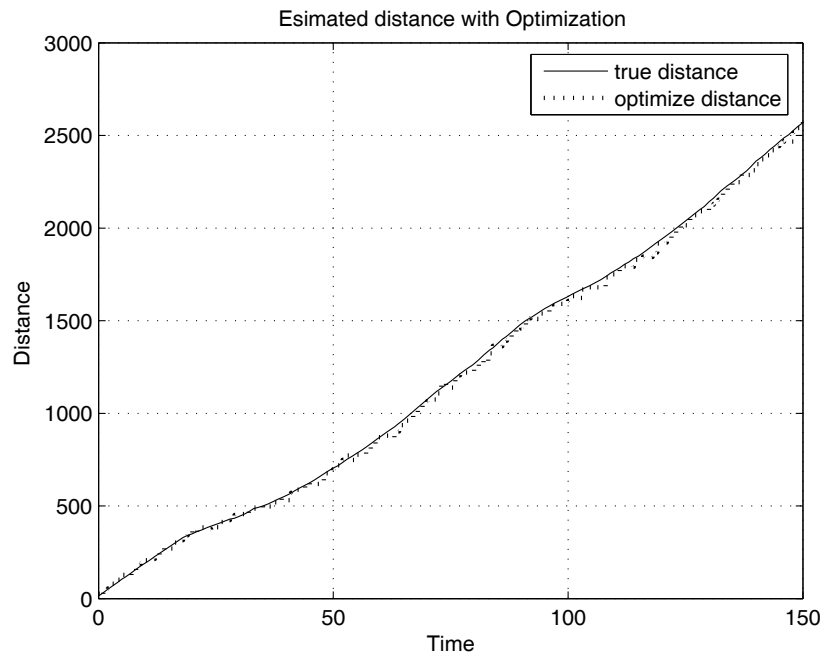


**Figure 4.6:** NLOS mitigation with CWLS optimization.

# Chapter 5

## Future Work

Based on the feasibility study in this first project year, we are determined to continue the research work in developing the AVCS. The output of this study can be integrated with so-called electronic data recorder (EDR) to produce a much enhanced vehicle black box (EVBox), which not only provide accurate data for post-accident inspection, but also actively involves in real-time driving to improve safety.

In the remaining of this Chapter, we analyze the problems in Section 5.1. The proposed approaches are presented in Section 5.2.

### 5.1 Future Research Problems

Due to vision limits, vehicle drivers cannot always maintain adequate awareness of the traffic condition that can quickly influence their safety. This is why all drivers are required by the law to always maintain sufficient gap with the vehicle in front so that they can properly respond to sudden traffic incidents. Unfortunately, most drivers do not always follow the rules and the gap between vehicles is often much shorter than what is needed for a safe stop in case of accident.

Further to our research work in the first project year, we aim to investigate this problem and to develop a technical solution to improve the road safety based on innovative inter-

vehicle communication, MEMS-based inertia navigation, and intelligent data processing for safe driving.

The proposed research aims to develop an Advanced Vehicle Control System (AVCS) to improve the driving safety under the real driving scenario. As shown in Fig 5.1, there are four major components in the proposed AVCS: surveillance, inter-vehicle communication, INS (Inertia Navigation System) based trajectory diagnosis, and information processing for safe driving. The surveillance unit collects relevant information about the vehicle. The vehicle trajectory diagnosis unit computes the trajectory and state of the vehicle to determine whether the movement of the vehicle is normal or not. The inter-vehicle communication unit communicates with the surrounding vehicles to gather information related to traffic safety and to send alert message initialized from the own vehicle. The information processing unit analyzes all these information and determines safety measures to alert the driver. Additionally, the AVCS also logs very accurate trajectory and orientation of the vehicle, which can be used to inspect traffic accidents.

The output of this study can be integrated with so-called electronic data recorder (EDR) to produce a much enhanced vehicle black box (EVBox), which not only provide accurate data for post-accident inspection, but also actively involves in real-time driving to improve safety. To achieve this goal, the following investigation and development will be conducted.

### **5.1.1 Inter-Vehicle Communication (IVC)**

Inter-Vehicle Communication (IVC) is accomplished through the use of radio frequency data transmission. The main purpose of IVC in the context of AVCS is to exchange safety related information between vehicles such that all the drivers can be alerted of any dangers potentially impairing their ability to maintain safe driving. Safety related information include the occurrence and scale of any traffic accident, damaged road infrastructure, abnormal behavior of individual vehicle, special traffic control, *etc.* Once a valid alert is received from the IVC network, the driver can respond accordingly to ensure safe driving. In case any

abnormal behavior of the own vehicle is detected, for example the trajectory indicating the vehicle is out of control, an alert will be sent to the IVC network which can be relayed to a large range of traffic so that all the surrounding drivers become aware of the potential danger.

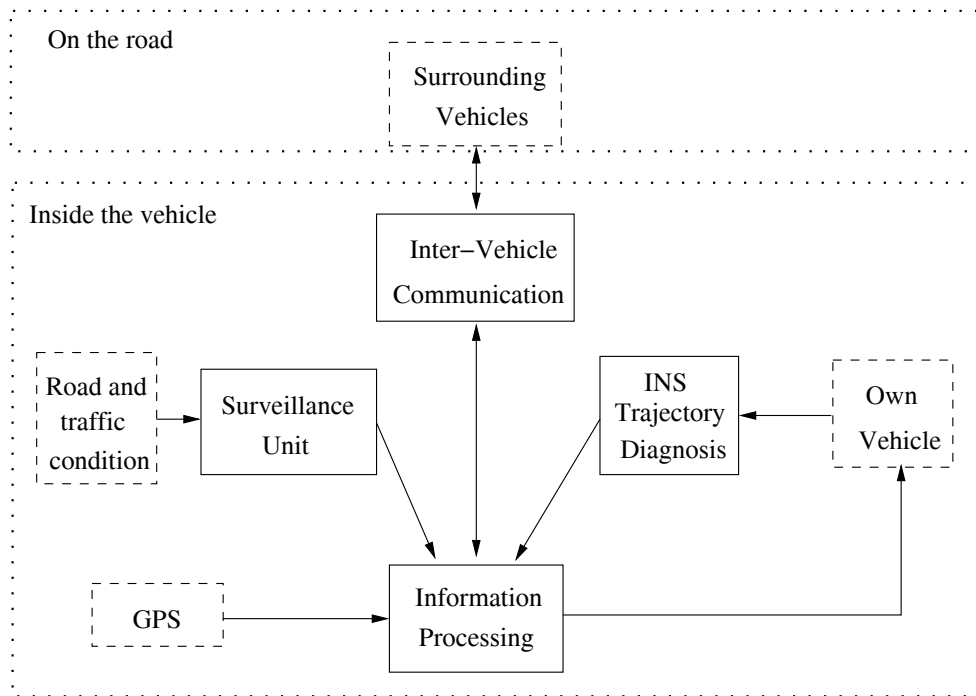


**Figure 5.1:** Block diagram of the investigated AVCS.

### 5.1.2 INS Trajectory Diagnosis

The trajectory and orientation of a moving vehicle provide sufficient data based on which the stability of the vehicle can be mathematically determined. The vehicle condition (vehicle load, mass distribution, suspension, and tires), the road condition (the inclination angle, the road surface and profile, and weather), the driving (the sideslip angle, the camber angle, engine and braking), collectively determine how a vehicle moves. When a vehicle is not handled properly, it may slide sideways, slip due to braced wheels. In this case, the vehicle becomes out of control, imposing danger to the surrounding traffic. Without sufficient alert,

other drivers, especially the drivers without direct line of sight with the vehicle, are likely get into an accident. The trajectory of a vehicle can be detected and diagnosed using an Inertia Navigation System (INS) based on MEMS (Micro Electromechanical System) sensors.

### **5.1.3 Advanced ABS**

Anti-lock Braking System (ABS) has been used in the automobiles for a long time. It is designed to minimize the stopping distance of moving vehicles on all road surfaces. The traditional design of ABS is based on an assumption that the braking force is highest when the slippage between the tire and the road is around 15%. So all traditional ABS control the slippage at 15%. However, this is only true with dry road. For instant, controlling the slippage around 15% on a wet road will result in a reduced tractive or braking force that is much lower than the maximum possible force. Consequently, the stopping distance of a vehicle with ABS on these surfaces may be even longer than those without ABS. This research will investigate the performance of conventional ABS on typical Canadian road profiles using a dynamic vehicle model and design an innovative enhanced ABS based on the principle of close-loop feedback system and adaptive control engineering.

### **5.1.4 Surveillance and Information Processing**

The safety of driving is influenced by a lot of factors, including environmental variables (temperature, humidity, wind speed and direction, rain/snow, visibility, etc), road variables (surface profile and materials, surface condition, terrain), traffic condition (vehicle density, travel speed), inside vehicle environment (temperature, humidity, air movement, air quality), and driver condition (physical, emotional and psychological condition). Theoretically all these variables can be monitored using certain sensors. However in practice, it is neither technically feasible nor economically justifiable to use so many sensors. A suitable surveillance system should be based on limited amount of sensors and be equipped with intelligent data processing capability to infer the critical safety related values based on the informa-

tion provided by the installed sensors. This research will investigate the typical existing surveillance technologies and design the intelligent data processing techniques.

## 5.2 Planned Approaches and Methodologies

The proposed research goal will be achieved through theoretical analysis, simulation study, prototype development and experimental study. Two physical systems are targeted in this study: the vehicle dynamics and the IVC network. Two simulators will be separately developed to simulate the dynamics of vehicles and the performance of IVC and then integrated to allow for overall performance evaluation. Based on the integrated simulation platform, the proposed AVCS technologies, such as advanced ABS, intelligent information processing, IVC, and INS trajectory diagnosis, will be investigated, resulting “soft” version of the proposed technologies. These “soft” technologies will be converted into hardware prototypes that will be tested through experimental study.

The methodologies adapted for the different aspects of this project are briefly summarized in the following subsections. More details are presented in our 2009 new proposal.

### 5.2.1 Communication Subsystem

For communication subsystem, the short-term goal is to develop a reasonable priced on-board Radar system which can implement ranging functions of the neighboring vehicles. Using the on-board Radar system, we can verify the research on ranging smoothing algorithm. Based on this Radar system, we can further develop an ad hoc mobile vehicular network to implement the functions of IVC.

In the same time, we will continue to develop IVC protocols and verify through simulation and experiment study. Vehicular Ad hoc Networks (VANETs) have different characteristics than the regular mobile ad hoc networks such as the high mobility of their nodes, the fast changing of their topology, frequent network fragmentation, constrained mobility pattern with confined rules, difficulties in radio propagation due to obstacles (fast fading, slow fading

and multipath propagation), uneven distribution of vehicles on the road, and the drivers' behavior. We will study the effects of these parameters on the performance of VANETs. Furthermore, the parameters such as the network topology specifications like the number of lanes, mobility and vehicle density, the network setup like message size, data rate and transmission power will be investigated and appropriate recommendations will be provided.

### 5.2.2 Advanced ABS

It is accepted by all the designers of Anti-lock Brake System (ABS) that the wheels have the greatest grip on the road when the slippage is between 10% and 15% [20]. Therefore all ABS in use nowadays are designed to control the brake such that the slippage is maintained between 10% and 15%. However, the relationship between slippage and the grip produced between the wheels and the road depends on the surface conditions. The grip may be peaked at a slippage that is significantly different from 10% to 15%. This explains why many experiments have reported that ABS leads to increased braking distance on some road surfaces although a reduced braking distance is most desirable.

The long-term goal of this research is to develop an intelligent electronic control unit (ECU) for ABS that can recognize the road condition and accordingly control the slippage that results in the maximum grip thus shortest braking distance, whilst safe controllability and stability are maintained. The proposed intelligent ECU is based on a dual loop feedback control scheme. In the outer loop, a vehicle motion sensing system will be developed to monitor the dynamics of the vehicle thus the grip between the wheels and the road can be estimated. This estimate is used to determine the most desirable slippage. In the inner loop, the conventional ABS control algorithm will be employed to control the ABS so that the slippage is maintained at the desired level determined by the outer loop.

To achieve this goal, a vehicle dynamic simulation platform will be developed and validated through this project. The simulator will be used to investigate the dynamics of vehicles during emergency braking and to develop an adaptive ABS control scheme.

### **5.2.3 Vehicle Trajectory Diagnosis**

The vehicle dynamics model will be used for this investigation. For this purpose, the model needs to be able to accurately represent the following aspects of vehicle dynamics: forces between road and wheels (contact pressure and stiffness, rolling radius and resistance, tractive and braking forces, cornering forces), longitudinal dynamics (load distribution, acceleration and deceleration), vehicle handling (trajectory control, kinematic steering, ideal steering, linearized handling).

### **5.2.4 Integration of EVBox**

At the end of second phase of the project, we aim to design an enhanced vehicle black box (EVBox) Prototype by integrating the developed ABS prototype, IVC prototype, and the trajectory diagnosis prototype. The proposed EVBox not only provides accurate data for post-accident inspection, but also actively involves in real-time driving to improve safety. Furthermore, we plan to test the performance of the prototype EVBox under the real driving scenario.

# Chapter 6

## Conclusions

The Intelligent Transportation System (ITS) is referred to the integrated applications of the advanced technologies in computers, communications, logic controls and sensor networks to provide travellers and authorities the important information they need in order to make the transportation system more safe, efficient, effective and reliable. In the project year 2008-2009, we developed our research work in two aspects: vehicle dynamic modelling and inter-vehicle communication for the development of Advanced Vehicle Control Systems (AVCS).

For vehicle modelling, we studied the mathematics governing the dynamics of the vehicles and based on these relations, a dynamic simulator was developed. The developed simulator was used to simulate the performance of the conventional ABS (anti-braking systems). Finding the problem with the conventional ABS technology, we aim to research and develop an advanced ABS which uses an adaptive ABS control algorithm. The control set point of the slippage will be changed dynamically such that the grip coefficient between the wheel and the road is maximized, and leading to the maximal stopping distance. Furthermore, a virtual reality model is developed to create a graphical representation of the dynamic behavior of the vehicle under different operations.

For communication, we mainly investigated the maximal communication range in broadcasting and studied broadcasting storm problem. The broadcast storm problem is a very serious issue in wireless networks and has been studied extensively. We showed how the

increase in the communication range will increase the contention and collisions within the one hop broadcast range and this will result in collapsing of the communication system. While decreasing the communication range will result in less contention but more delay. Determining the optimal communication range is the challenge we investigated. Our result is a closed form formula. We derived the relation between the maximum range that a vehicle can transmit its message and the traffic parameters. We believe that vehicles on the road are more importantly to know the maximum communication range that they can use in order to deliver safety messages in a short time to avoid chain collisions and at the same time decreasing the number of failed nodes.

We introduced a new broadcasting scheme, NTPP, which is based on the nodes knowledge of their neighbors in their range and traffic parameters like the node density and bandwidth. The node has first to determine its maximum range that minimizes the effect of the hidden terminal problem and then decide to rebroadcast or not based on the proposed algorithm. By simulation we showed how the NTPP scheme has fast propagation speed and reduces the redundant traffic compared to the flooding way of rebroadcasting.

Furthermore, we developed strategies to improve ranging and positioning algorithms by using Kalman filter technique and Constrained Weighted Least Square (CWLS) algorithm. Simulation results show the effectiveness of the proposed algorithms. Future plan and target are also outlined in this report.

# Bibliography

- [1] G. M. Djuknic and R. E. Richton, “Geolocation and assisted GPS,” *Computer Communications*, pp. 123–125, Feb. 2001.
- [2] V. Kukshya, H. Krishnan, and C. Kellum, “Design of a system solution for relative positioning of vehicles using vehicle-to-vehicle radio communications during GPS outages,” in *Proceedings of IEEE Vehicular Technology Conference*, pp. 1313–1317, September 2005.
- [3] “IEEE p802.11p/D5.0 draft amendments for wireless access in vehicular environments (WAVE),” Jan. 2009, <https://mentor.ieee.org/802.11/file/08>.
- [4] “Vehicle infrastructure integration (VII),” <http://www.intelldriveusa.org>.
- [5] X. Li, T. D. Nguyen, and R. P. Martin, “An analytic model predicting the optimal range for maximizing 1-hop broadcast coverage in dense wireless networks,” in *Proceedings of the 3rd International Conference on AD-HOC Networks & Wireless Communications*, July 2004.
- [6] K. A. Hafeez, L. Zhao, Z. Liao, and B. Ma, “The optimal range of a broadcast message in vehicular ad-hoc networks,” *Proc. IEEE Globecom Conf.*, 2009, submitted.
- [7] S. Y. Ni, Y. C. Tseng, Y. S. Chen, and J. P. Sheu, “The broadcast storm problem in a mobile ad hoc network,” *Proc. ACM International Conf. Mobile Computing and Networking*, pp. 151–162, 1999.

- [8] N. Wisitpongphan, O. K. Tonguz, J. S. Parikh, P. Mudalige, F. Bai, and V. Sadekar, “Broadcast storm mitigation techniques in vehicular ad hoc wireless networks,” *IEEE Wireless Communications Magazine*, vol. 14, no. 6, Dec. 2007.
- [9] K. A. Hafeez, L. Zhao, Z. Liao, and B. Ma, “The broadcast storm problem in vehicular ad-hoc networks,” *Proc. IEEE Globecom Conf.*, 2009, submitted.
- [10] M. P. Wyelie and J. Holtzmann, “The non-line of sight problem in mobile location estimation,” *IEEE International Conference on Universal Personal Communications*, vol. 2, pp. 827–831, October 1996.
- [11] J. Xu, M. Ma, and C. L. Law, “Position estimation using UWB TDOA measurements,” *IEEE International Conference on Ultra-Wideband*, pp. 605–610, September 2006.
- [12] M. Najjar and J. Vidal, “Kalman tracking for mobile location in NLOS situations,” *The 14th IEEE International Symposium on Personal Indoor and Mobile Radio Communication (PIMRC)*, vol. 3, pp. 2203–2207, September 2003.
- [13] C. D. Wann and C. S. Hsueh, “NLOS mitigation with biased kalman filters for range estimation in UWB systems,” *IEEE Region 10 Conference, TENCN 2007*, pp. 1–4, October 2007.
- [14] M. Shaik, O. Das, L. Zhao, and Z. Liao, “Inter-vehicle range smoothing for NLOS condition in the persistence of GPS outages,” *IEEE Conference on Industrial Electronics and Applications*, May 2009, to appear.
- [15] J. J. Caffery and G. L. Stuber, “Subscriber location in CDMA cellular networks,” *IEEE Transaction on Vehicle transportation*, vol. 47, no. 2, pp. 406–416, 1998.
- [16] J. O. Smith and J. S. Abel, “Closed-form least-squares source location estimation from range-difference measurements,” *IEEE Transactions on Acoustics, Speech and Signal Processing*, vol. 35, no. 12, pp. 1661–1669, 1987.

- [17] Y. T. Chan and K. C. Ho, “A simple and efficient estimator for hyperbolic location,” *IEEE Transactions on Signal Processing*, vol. 35, no. 8, pp. 1905–1915, 1994.
- [18] G. W. Elko, Y. Huang, J. Benesty, and R. M. Mersereati, “Realtime passive source localization: a practical linear-correction least-squares approach,” *IEEE Transactions on Speech and Audio Processing*, vol. 9, no. 8, pp. 943–956, 2001.
- [19] L. Farhi, L. Zhao, and Z. Liao, “Constrained weighted least square optimization for vehicle position tracking,” *Proc. IEEE Globecom Conf.*, 2009, submitted.
- [20] G. F. Mauer, “A fuzzy logic controller for an ABS braking system,” *IEEE Transactions on Fuzzy Systems*, vol. 3, no. 4, pp. 381–388, Nov. 1995.

# Appendix A

## Abbreviation List

For easy reference the abbreviations used throughout the thesis are tabulated below in alphabetical orders.

<u>Symbol</u>	<u>Meaning</u>
ABS	Anti-breaking System
AOA	Angle of Arrival
AWGN	Additive White Gaussian Noise
AVCS	Advanced Vehicle Control Systems
CSMA	Carrier Sense Multiple Access
CWLS	Constrained Weighted Least Square
DSRC	Dedicated Short Range Communications
ECU	Electronic Control Unit
EDR	Electronic Data Recorder
EVBox	Vehicle Black Box
GPS	Global Position System
ITS	Intelligent Transportation System
IVC	inter-Vehicle Communication
LOS	Line of Sight
LS	Least Squares

MEMS	Micro Electromechanical System
NLOS	Non-line of Sight
NLS	Nonlinear Least Square
NTPP	Network Topology P(probability)-Persistence
RMSE	Root Mean Square Error
RSS	Received Signal Strength
SI	spherical interpolation
TDOA	Time Difference of Arrival
TOA	Time of Arrival
UWB	Ultra wideband
VANET	Vehicular ad hoc Networks

# Appendix B

## Papers Submitted

Paper submitted or accepted in project year 2008-2009 as listed below. The full papers are attached here.

- M. Shaik, O. Das, L. Zhao, and Z. Liao, “Inter-vehicle range smoothing for NLOS condition in the persistence of GPS outages,” IEEE Conference on Industrial Electronics and Applications, May 2009, to appear.
- K. A. Hafeez, L. Zhao, Z. Liao, and B. Ma, “The broadcast storm problem in vehicular ad-hoc networks,” Proc. IEEE Globecom Conf., 2009, submitted.
- K. A. Hafeez, L. Zhao, Z. Liao, and B. Ma, “The optimal range of a broadcast message in vehicular ad-hoc networks,” Proc. IEEE Globecom Conf., 2009, submitted.
- L. Farhi, L. Zhao and Z. Liao, “Constrained Weighted Least Square Optimization for Vehicle Position Tracking,” Proc. IEEE Globecom Conf., 2009, submitted.

# Inter-Vehicle Range Smoothing for NLOS Condition in the Persistence of GPS Outages

Meharoon Shaik, Olivia Das, Lian Zhao, and Zaiyi Liao  
Electrical and Computer Engineering Department  
Ryerson University, ON, Canada, M5B 2K3

**Abstract**—Cooperative collision warning, based on vehicle-to-vehicle radio communications and GPS systems, is one of the promising active safety applications that have attracted considerable research interest. In this paper, we address one of the functional key points of the cooperative collision warning application, which is an accurate estimation of the range data of neighboring vehicles during persistent GPS outages under both line-of-sight (LOS) and non-line-of-sight (NLOS) situations. This paper suggests smoothing and mitigating the NLOS for radio-based ranging measurements. Simulation results show that the biased Kalman filter gives accurate range estimations.

**Index Terms**—Vehicular communications, cooperative collision warning, range estimation, NLOS, Kalman filter.

## I. INTRODUCTION

Recently, vehicular active safety applications have attracted considerable research interest in Intelligent Transportation Systems (ITS), due to the potential of saving tens of thousands of lives and hundreds of billions of dollars per year in the US alone [1]. A quarterly review prepared by the Japanese ITS committee [2] shows that 75% of traffic accidents are caused by driver behavior immediately before the accident. In an emergency situation, vehicle drivers rely on the brake lights of the vehicles immediately ahead of them to decide whether or not to apply their own braking system in order to avoid a collision or chain of collisions in a platoon. The typical time for a driver to stop a vehicle safely is around 0.7s to 1.5s [3]. In order to reduce the driver mistakes in traffic accidents, it is therefore necessary to provide prior knowledge about error recognition, alarm and driving assistance functions during the vehicles operation. The intelligent cooperative collision warning system is an important class of safety applications that target the prevention of vehicular collisions and provide real-time alerts about hazards and accidents. The cooperative collision warning systems use vehicle-to-vehicle and vehicle-to-infrastructure communications for wireless vehicular networks to improve the level of safety, efficiency, and information availability by the periodic broadcast of short messages bearing status information (*i.e.*, accurate estimations of location, velocity and control settings).

Currently, the most promising and widely used positioning techniques are global positioning systems (GPS). Some assisted GPS [4] can achieve an average accuracy of 3m to 10m in open flat areas. However, in reality, satellite signals are often disturbed or blocked when the vehicles are traveling through tunnels, under bridges and sky scrapers. Vehicles can also

experience sustained GPS outages due to high solar activity, terrestrial interference and multipath fading. In persistent GPS outages, vehicles can use dead reckoning systems to obtain position information; however, they are prone to errors. The dead reckoning systems can accurately determine its GPS coordinates with a permissible error of less than 10m for approximately 30s outages if the vehicle is traveling at a speed of 60km/h [5]. Line of sight (LOS) between the object to multiple satellites is not always possible, therefore, GPS alone cannot be applied for vehicular safety applications in order to achieve higher accuracy in position estimates to avoid traffic accidents. The addition of radio-based ranging techniques in the absence of GPS signals can be applied as a promising technique [5].

One of the fundamental steps for positioning is accurate ranging, *i.e.*, an action of estimating the distance between the transmitter and the receiver. There are four common radio based ranging techniques applied for position estimation in wireless *ad hoc* networks. These techniques are: Received Signal Strength (RSS), Time Of Arrival (TOA), Time Difference Of Arrival (TDOA) and Angle Of Arrival (AOA).

Among the above techniques, RSS is the least expensive to implement in the cooperative collision warning systems in the vehicular communications as it uses known mathematical channel path loss models. Distance can be extracted by using free-space large scale path loss models between the vehicles for inter-vehicular LOS distances of less than 100m.

TOA and TDOA are time-based ranging techniques. Distance can be extracted from the time of arrival of the signals or time difference of arrival of the signals. These require high-resolution timing measurements, accurate real-time clock synchronization among nodes and LOS propagation conditions. A unique two-way reciprocal time of arrival based ranging technique was proposed in [6]. This technique provides high ranging accuracy of less than 3m even under multipath conditions. According to this technique, vehicles do not need to maintain clock synchronization among the transmitter-receiver vehicle pairs.

In AOA, the angles of the signals received from other vehicles are applied to extract range information. This technique gives errors in the position estimation if the separation between vehicles is large, due to the severe interference between multipath components and the angle measurements. The RSS based ranging technique and two-way reciprocal time of arrival based

ranging technique can be applied in vehicular communications for LOS distances of 100m.

Ranging and positioning accuracy could be limited by the presence of multipath fading, non-line-of-sight (NLOS) conditions, and extra propagation delay, due to the presence of obstacles. In dense urban environment there may not always be a direct path between the vehicles. Due to reflection and diffraction, the range measurements tend to be positively biased, which is known as NLOS error. This problem has been recognized by many researchers as a “killer issue” for accurate ranging and positioning [7]. Therefore, the NLOS problem must be taken into consideration.

There are many positioning approaches established for wireless nodes when LOS exists between the transmitter and the receiver. A method of localizing neighboring vehicles based on inter-vehicle distance measurements using one of the radio-based ranging technique is proposed along with triangulation to determine relative position coordinates of vehicles in [5]. Here position estimation may become very inaccurate since the distance measurements are noisy. Authors in [8] proposed a TDOA error minimizing localization method to estimate the location of group of blind nodes in LOS and NLOS propagations for fixed reference node positions. This is more appropriate for cellular mobile networks where the base stations are at fixed locations but not suitable for inter-vehicle communication where vehicles are moving randomly.

To improve the accuracy of ranging and positioning of vehicles, NLOS mitigation techniques must be applied. A polynomial fitting was applied to all available measured range data to mitigate NLOS effects [7]. This is not accurate due to time delay in total data gathering. A modified Kalman filter algorithm is presented in [9] to estimate NLOS bias for UMTS mobile positioning. The estimation of range bias in the proposed algorithm improves the performance of location tracking in NLOS environments. NLOS mitigation with the biased Kalman filter for the range estimation in Ultra wideband (UWB) systems for wireless sensor networks was proposed in [10], where the mobility of the users had not been considered.

In this paper we implement the biased Kalman filter for vehicular networks where the vehicle mobility complicates the case. Among vehicles, noisy measurements can be misinterpreted as an observed motion and the effects of fading become prevalent for a road topology. Vehicles on the road are not uniformly distributed and the positions of the vehicles are not fixed. We consider the problem of NLOS identification and mitigation for the vehicular communications in the absence of GPS signals to smooth the range data between randomly selected vehicles. A simple hypothesis test, based on the standard deviation of the measured noise, is applied to distinguish between the LOS and NLOS range measurements. If the measurements contain NLOS error, then the NLOS must be mitigated before the position estimation takes place for accurate results. NLOS error correction is possible by applying the biased Kalman filter instead of the unbiased Kalman filter where it can mitigate unexpected high erroneous NLOS data. Based on this height variation it has different effect on the

measurement error. IEEE 802.15.3a UWB model parameters are applied to model LOS and NLOS environments between vehicles for short-range communications [11].

Our simulation results show that the biased Kalman filter can easily track and effectively smooth the positively biased NLOS noise in the measured inter-vehicle range data to mitigate NLOS errors and maintain a high accuracy in the estimated inter-vehicle range data for a high speed vehicular environment.

In the remaining of the paper, an inter-vehicle distance measurement model and approach are formulated in section II. The biased Kalman filter algorithm for NLOS identification and mitigation is discussed in section III. Simulation results are presented in Section IV followed by conclusions in section V.

## II. INTER VEHICLE DISTANCE MEASUREMENT MODEL AND APPROACH

Vehicle range estimation problem can be formulated as follows. In the model, we consider a random number of vehicles at unknown random distinct locations at time  $t_i$ . The range measurement between vehicles is random and can be modeled as:

$$r(t_i) = d_T(t_i) + d_{NLOS}(t_i) + d_{AWGN}(t_i) \quad (1)$$

where  $r(t_i)$  is the total measured range at sampling time  $t_i$ ;  $d_T(t_i)$  is the true range;  $d_{NLOS}(t_i)$  is the range due to multipath, reflection and diffraction;  $d_{AWGN}(t_i)$  is the measurement noise, and modeled as additive white Gaussian random variable with zero mean and variance  $\sigma_v^2$ . In the LOS scenario only the Gaussian measurement noise will be present and the distance error due to NLOS equals to zero. The measurement noise can vary depending on the signal strength. If the received signal is strong then the measurement noise could be lower. The true distance between vehicles can be determined by:

$$d_T(t_i) = |x_n(t_i) + jy_n(t_i) - x_v - jy_v| \quad (2)$$

where  $(x_n(t_i), y_n(t_i))$  are the  $n^{th}$  vehicle coordinates at time  $t_i$  and  $(x_v, y_v)$  are the coordinates of the  $v^{th}$  vehicle, which is a randomly selected vehicle from all the neighboring vehicles.

In general, exponential, uniform, or delta random distributions are applied to model NLOS error in wireless communications. To model excess distance added due to the NLOS component, we used IEEE 802.15.3a UWB model parameters [11]. These parameters are compatible to model the LOS and NLOS noise components in vehicular environments for short-range communications between vehicles [12]. Saleh - Valenzuela (S-V) model was a good fit to define LOS and NLOS scenarios in the vehicular communications. According to S-V model the multipaths arrive in the form of clusters rather than in a continuous form [13]. For a dense multipath environment, the estimation of the arrival time of the first ray of the first path ( $T_0$ ) can be directly related to the range data. Therefore, NLOS component can be modeled as an exponential distribution as following [11]:

$$p(T_0) = \Lambda \exp[-\Lambda(T_0)] \quad (3)$$

where  $\Lambda(1/ns)$  is the cluster arrival rate,  $T_0 \times c$  gives an extra range added due to NLOS where  $c$  is the light velocity.

The raw range data at consecutive time samples are tested to identify the presence of NLOS by applying hypothesis test (*i.e.*, the standard deviation of NLOS measurements is much larger than that of LOS measurements). In the LOS scenario, the unbiased Kalman filter output converges to the true range and the position estimation gives quite accurate results. However, the unbiased Kalman filter cannot track the sudden changes in the variance due to the positively biased NLOS, thus, it can cause severe position error. Our proposed biased Kalman filter can effectively preprocess the inter-vehicle range data for both LOS and NLOS and also effectively track and smooth the measurement noise variations due to signal strength fluctuations when vehicle mobility is high. The processed range data can be applied to the triangulation method of the position finding.

### III. KALMAN FILTER FOR NLOS MITIGATION

In order to smooth the inter-vehicle measured range data, it is preferred to define a dynamic system with a state vector. The state of the system can be estimated for every time step to track the behavior of the system and to compare it with the true state by reducing the variance between the estimated and the true range. This means that the estimated state from the previous time step and the current measurements are needed to compute the estimate for the current state. The Kalman filter is one of the estimation algorithms which satisfy the above criteria and allow a recursive set of operations by processing data from the inter-vehicle distance estimates and incorporates this into a motion model with the addition of additive white Gaussian noise (AWGN) distribution to the measurement model. The model which we have used for distance estimation is defined as in [14]:

$$\mathbf{X}_{k+1} = \mathbf{A}\mathbf{X}_k + \mathbf{B}\mathbf{W}_k \quad (4)$$

where  $\mathbf{X}_k$  is the state vector and defined as:

$$\mathbf{X}_k = [d_n(k) \quad \dot{d}_n(k)]^T \quad (5)$$

where  $d_n(k)$  is the true range;  $\dot{d}_n(k)$  is the first derivative of the true range, which is the speed of the vehicle at time  $k\Delta t$ , with a sampling interval of  $\Delta t$ .  $\mathbf{A} = \begin{bmatrix} 1 & \Delta t \\ 0 & 1 \end{bmatrix}$ ,  $\mathbf{B} = \begin{bmatrix} 0 \\ \Delta t \end{bmatrix}$  and  $\mathbf{W}_k$  is the process noise vector describing the mobility variations. We assumed that  $\mathbf{W}_k$  is an additive white Gaussian random vector, with the following covariance matrix:

$$\mathbf{Q}_k = E\{\mathbf{W}_k \mathbf{W}_k^T\} = \text{diag}(\sigma_n^2) \quad (6)$$

where  $\text{diag}(\cdot)$  denotes a diagonal matrix. The measurement process can be written as:

$$\mathbf{Z}_k = \mathbf{H}\mathbf{X}_k + \mathbf{V}_k \quad (7)$$

where  $\mathbf{H} = [1 \ 0]$  is the observation model which maps the true state space into the observed space and  $\mathbf{V}_k$  is the observation noise, which is a zero mean Gaussian random vector with covariance matrix  $\mathbf{R}_k$ , this covariance matrix describes the noise characteristics of the measurements, given in the following form:

$$\mathbf{R}_k = E\{\mathbf{V}_k \mathbf{V}_k^T\} = \text{diag}(\sigma_x^2) \quad (8)$$

The Kalman filter can be viewed as the following set of recursive relationships:

$$\hat{\mathbf{X}}_{k|k-1} = \mathbf{A}\hat{\mathbf{X}}_{k-1|k-1} \quad (9)$$

$$\mathbf{P}_{k|k-1} = \mathbf{A}\mathbf{P}_{k-1|k-1}\mathbf{A}^T + \mathbf{B}\mathbf{Q}_{k-1}\mathbf{B}^T \quad (10)$$

$$\tilde{\mathbf{Z}}_k = \mathbf{Z}_k - \mathbf{H}\hat{\mathbf{X}}_{k|k-1} \quad (11)$$

$$\mathbf{S}_k = \mathbf{H}\mathbf{P}_{k|k-1}\mathbf{H}^T + \mathbf{R}_k \quad (12)$$

$$\mathbf{K}_k = \mathbf{P}_{k|k-1}\mathbf{H}^T\mathbf{S}_k^{-1} \quad (13)$$

$$\hat{\mathbf{X}}_{k|k} = \hat{\mathbf{X}}_{k|k-1} + \mathbf{K}_k\tilde{\mathbf{Z}}_k \quad (14)$$

$$\mathbf{P}_{k|k} = (\mathbf{I} - \mathbf{K}_k\mathbf{H})\mathbf{P}_{k|k-1} \quad (15)$$

where  $\mathbf{P}_{k|k}$  is the covariance matrix of  $\mathbf{X}_{k|k}$ ,  $\tilde{\mathbf{Z}}_k$  is the innovation matrix,  $\mathbf{S}_k$  is the innovation covariance,  $\mathbf{K}_k$  is the Kalman gain,  $(\cdot)^T$  denotes the matrix transpose and  $(\cdot)^{-1}$  denotes the matrix inverse.

The Kalman filter iterative process can be summarized in two distinct phases: predict and update. Equations (9) and (10) show the predict phase. Here, predict state uses the state estimate from the previous time step to produce an estimate of the state at the current time step. In the update phase from equations (11) to (15), measurement information at the current time step is used to refine this prediction to arrive at a more accurate state estimate, again for the current time step.

For LOS situations, the unbiased Kalman filter procedure, described from equations (9) to (15), can be applied and the filter output converges to the true range and gives accurate range results. However, the unbiased Kalman filter cannot track the sudden changes due to the NLOS component in the measured range data. The biased Kalman filter can be applied for both the LOS and NLOS scenarios. In order to identify the change in channel situation between LOS and NLOS, the hypothesis test is applied as following:

$$H0 : \hat{\sigma}_v < \beta\sigma_v \quad \text{LOS} \quad , \quad H1 : \hat{\sigma}_v \geq \beta\sigma_v \quad \text{NLOS} \quad (16)$$

where  $\beta > 1$  is used to reduce the probability of a false alarm which is chosen experimentally [10];  $\sigma_v$  is the standard deviation of the measurement noise in the LOS environment; and  $\hat{\sigma}_v$  is the standard deviation of the estimated range data and is calculated over a block of  $L$  measured ranges as following:

$$\hat{\sigma}_v = \sqrt{\frac{1}{L} \sum_{i=1}^L [r(t_i) - \hat{d}_T(t_i)]^2} \quad (17)$$

In order to mitigate the NLOS range error, the biased Kalman filter is employed. The positive bias error can be canceled by implementing the following two rules:

- 1) Update the priori error covariance matrix as following when the condition  $\mathbf{Z}_k - \mathbf{H}\mathbf{X}_{k-1} < 0$  is true:

$$\hat{\mathbf{P}}_{k|k-1} = \mathbf{P}_{k|k-1} + \frac{(\mathbf{Z}_k - \mathbf{H}\mathbf{X}_{k|k-1})^2}{\gamma} \quad (18)$$

where  $\gamma$  is the experimentally chosen scaling factor [10].

- 2) Increase the diagonal elements of the measurement noise covariance matrix as follows:

$$\hat{\sigma}_x^2(k) = \sigma_v^2 \quad (19)$$

The unbiased Kalman filter can be modified to the biased Kalman filter, by implementing the above two rules before calculating the Kalman gain, to decrease the dependence on the measurements as a biasing technique. Simulation results will show that the performance of the biased Kalman filter can be improved significantly over the unbiased Kalman filter in the NLOS condition.

#### IV. SIMULATION RESULTS

In order to test the performance of the biased Kalman filter algorithm, we considered a road topology of a length of 4km and a width of 30m with six lanes, each with a width of 5m. There are 3 east-bound and 3 west-bound lanes with vehicles entering from both directions. Vehicles are randomly selected with a minimum threshold distance of 30m between them, which was the minimum requirement in order to avoid collisions in an emergency situation. Vehicle speed limit was set to 30m/s. For simulations we tracked a single vehicle's ability to determine the range estimation with all other vehicles. We assumed each vehicle had 6 neighboring vehicles with 6 inter-vehicle range measurements at any given time as depicted in Fig.1. For simulations  $\beta$  is fixed to 1.1.

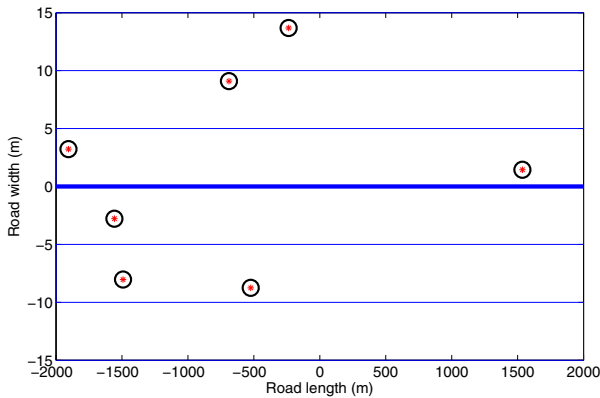


Fig. 1. Road topology for vehicles

UWB channel model parameters have been used to model the NLOS error for simulations [11] with a mean of  $1/\Lambda$  and a variance of  $(1/\Lambda^2)$ . The NLOS error is modeled by equation (3) with  $\Lambda=0.0667(1/\text{ns})$ . The measurement noise  $\mathbf{V}_k$

is assumed to be AWGN with zero mean and variance  $0.25m^2$ . It is also assumed that 1000 data samples are measured with a sampling period of 2ms. The true range is calculated by applying the performance metric  $|x_i + jy_i - x_j - jy_j|$  with initial positions of the vehicles recorded by GPS.

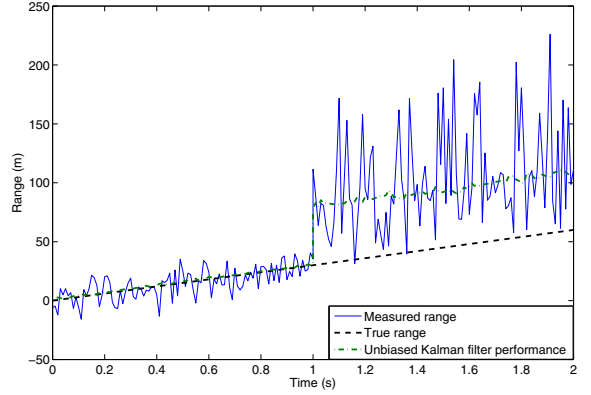


Fig. 2. Unbiased Kalman filter output for LOS and NLOS.

For simulations, LOS and NLOS have been applied randomly to the range measurements and a hypothesis test is used to determine which range measurements have LOS and NLOS. Basically, the true range with the addition of AWGN is known as the LOS condition. The performance metric, root mean square error (RMSE), was applied to determine the range error, which is very sensitive to the distance measurements. RMSE is defined as:

$$\epsilon = \sqrt{\frac{1}{N} \sum_{i=1}^N [\hat{d}_T(i) - d_T(i)]^2} \quad (20)$$

where  $d_T(i)$  is the true range of the  $i^{\text{th}}$  vehicle and  $\hat{d}_T(i)$  is the estimated range of the  $i^{\text{th}}$  vehicle.

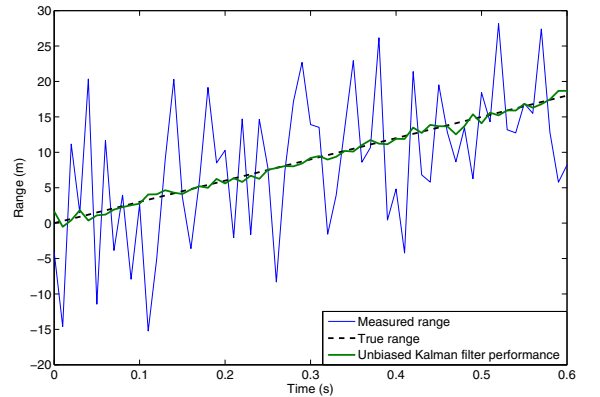


Fig. 3. Unbiased Kalman filter output for LOS in [0, 0.6].

In Fig.2, the propagation situation changes from LOS to NLOS at each time instant of 1s. Simulation results show that the unbiased Kalman filter can preprocess the range data with a RMSE of 0.05m for only the LOS scenario; for the NLOS

scenario, the RMSE could be too high. Therefore, NLOS needs to be filtered out for acceptable measurements.

Fig.3 shows a zoomed version of Fig.2 from the start to 0.6s. It shows that by using the unbiased Kalman filter, the estimation is almost overlapped with the true range. However, the unbiased Kalman filter cannot eliminate the positively biased NLOS data added for the time period of 1s to 2s.

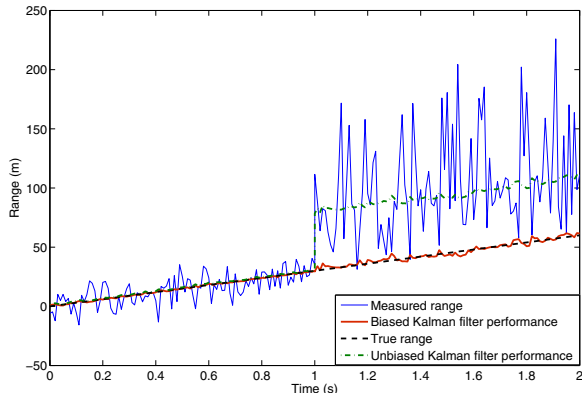


Fig. 4. Biased vs unbiased Kalman filter smoothed range data.

Fig.4 shows the biased versus unbiased smoothed range data for the propagation situation changes from LOS to NLOS at time instant of 1s. The inter-vehicle range data smoothed by the unbiased Kalman filter cannot track the sudden changes due to NLOS from time instant of 1s to 2s. However, the NLOS error from the range measurements is mitigated by using the biased Kalman filter with a RMSE value of less than 0.7m.

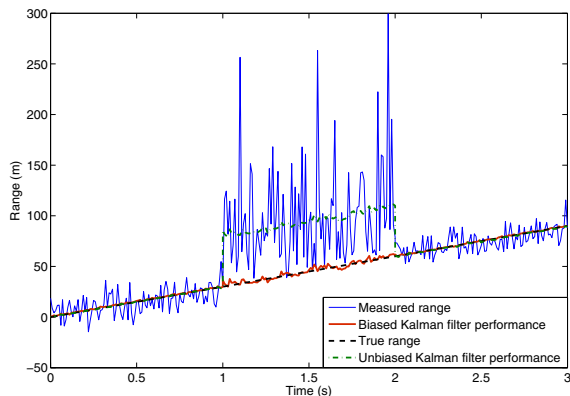


Fig. 5. Estimated range data with an abrupt change between LOS and NLOS.

Fig.5 shows the biased Kalman filter smoothed output for a mixed LOS condition from 0s to 1s, the NLOS condition from 1s to 2s, and again the LOS condition from 2s to 3s. The biased Kalman filter can effectively mitigate the NLOS error even when the vehicle travels with an abrupt change between the LOS and NLOS conditions.

If we assume that the two Gaussian random variables with the standard deviations of 1m and 10m respectively describing the noise characteristics of the distance measurements, then we obtain the results as shown in Fig.6. The curve with higher

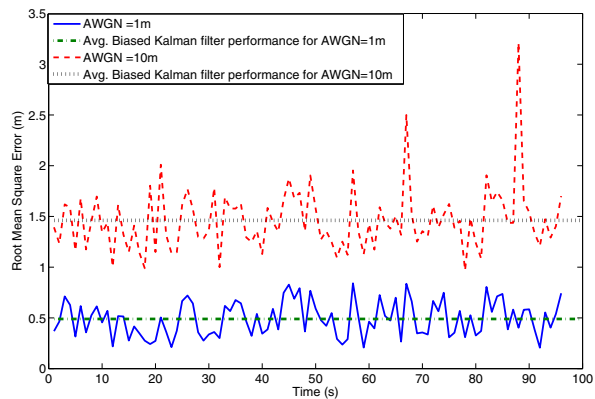


Fig. 6. Biased Kalman filter performance on different AWGN variance.

peaks is the biased Kalman filter performance to smooth the inter-vehicle range data over a time period of 100s. Also, for reference we have included the average performance of the biased Kalman filter (*i.e* the horizontal line with RMSE of approximately 1.5m). The bottom curve with lower peaks shows the biased Kalman filter performance for the measurement noise of 1m. The dashed horizontal line shows the average RMSE of approximately 0.5m. Overall, the biased Kalman filter can effectively smooth range data for various noise levels of strength.

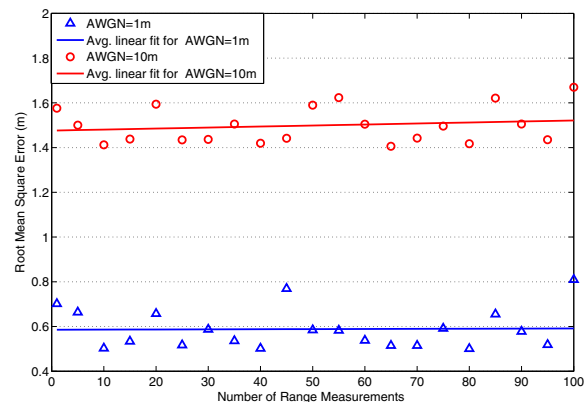


Fig. 7. RMSE vs. number of inter-vehicle range measurements for  $\beta = 1.1$ .

Fig.7 and Fig.8 show the variation of the RMSE with respect to the number of range measurements for two different levels of the measurement AWGN standard deviation (*i.e.*, 1m and 10m respectively at  $\beta = 1.1$  and  $\beta = 1.6$  respectively). A moving linear average fit of the data points is overlaid on each plot. Each data point on the plots represents a single run of the simulation for the inter-vehicle range measurements. The ability of the biased Kalman filter performance goes down as the number of inter-vehicle range measurements increase. Interestingly, the algorithm is most effective with the AWGN standard deviation of 1m at  $\beta = 1.1$ . With higher measurement noise (*i.e.*, AWGN) in the inter-vehicle range data, the algorithm is still effective, but the RMSE could be higher.

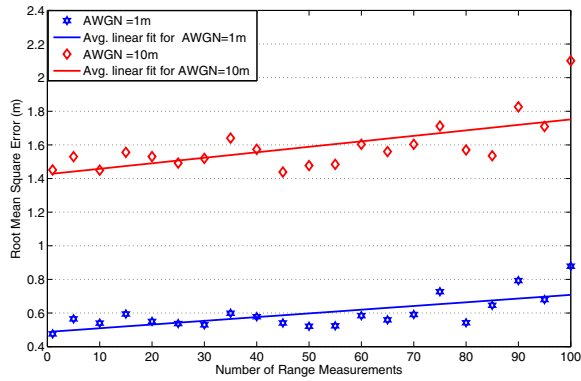


Fig. 8. RMSE vs. number of inter-vehicle range measurements for  $\beta = 1.6$

TABLE I  
RMSE FOR DIFFERENT AWGN MEASUREMENT NOISE

AWGN Standard deviation (m)	Measurement range (<400m)	Measurement range (<1000m)
10m	< 1.0m	< 1.5m
5m	< 0.8m	< 1.3m
1m	< 0.6m	< 1.1m
0.1m	< 0.3m	< 0.7m

The results of RMSE in the measurement range are summarized in Table I by selecting different standard deviation values for the AWGN. Since the Gaussian noise is the measurement noise, if the signal arrives stronger, we can assume the measurement noise to be lower. For different values of AWGN standard deviation, the measurement range of less than 400m and less than 1000m on average is listed. It shows the maximum RMSE in the measured range after smoothing with the biased Kalman filter. The proposed algorithm can achieve an accuracy of less than 0.7m in the inter-vehicle range data when the measured range is less than 1000m and the AWGN standard deviation is less than 0.1m. A maximum inter-vehicle distance of 1000m, based on the dedicated short-range communication (DSRC) standards listed in [1], is compatible for vehicular safety applications.

## V. CONCLUSION

In this paper we presented a range estimation algorithm for typical GPS outages in the presence of NLOS error. We applied the biased Kalman filter to mitigate the positive bias introduced by the NLOS component in the inter-vehicle range measurements. Simulation results show that the proposed algorithm for NLOS identification and mitigation with the biased Kalman filter promises to achieve higher accuracy for vehicle positioning and tracking systems under different received noise levels.

## ACKNOWLEDGMENTS

This work has been supported by the Ministry of Transportation of Ontario (MOT) and Natural Sciences and Engineering Research Council of Canada (NSERC).

Opinions expressed in this report are those of the authors and may not necessarily reflect the views and policies of the Ministry of Transportation of Ontario.

## REFERENCES

- [1] L. J. Blincoe, A. G. Seay, E. Zaloshnja, T. R. Miller, E. O. Romano, S. Luchter, and R. S. Spicer, "The economic impact of motor vehicle crashes 2000," *Posted on National Highway Traffic Safety Administration Website*, pp. 1–86, May 2002.
- [2] K. Takeuchi and S. Maeda, "Outlook on the next steps of intelligent transport systems (ITS) technologies in Japan: for overcoming social and environmental problems brought by automobiles," *Quarterly review*, pp. 25–44, January 2007.
- [3] M. Green, "How long does it take to stop?" methodological analysis of driver perception-brake times," *Transportation Human Factors*, vol. 2, no. 3, pp. 195–216, September 2000.
- [4] G. M. Djuknic and R. E. Richton, "Geolocation and assisted GPS," *Computer Communications*, pp. 123–125, February 2001.
- [5] V. Kukshya, H. Krishnan, and C. Kellum, "Design of a system solution for relative positioning of vehicles using vehicle-to-vehicle radio communications during GPS outages," in *Proceedings of IEEE Vehicular Technology Conference*, pp. 1313–1317, September 2005.
- [6] D. D. McCrady, L. Doyle, H. Forstrom, T. Dempsey, and M. Martorana, "Mobile ranging using low accuracy clocks," *IEEE Transactions on Microwave Theory and Techniques*, vol. 48, no. 6, pp. 951–958, June 2000.
- [7] M. P. Wylie and J. Holtzmann, "The non-line of sight problem in mobile location estimation," *IEEE International Conference on Universal Personal Communications*, vol. 2, pp. 827–831, October 1996.
- [8] J. Xu, M. Ma, and C. L. Law, "Position estimation using UWB TDOA measurements," *IEEE International Conference on Ultra-Wideband*, pp. 605–610, September 2006.
- [9] M. Najar and J. Vidal, "Kalman tracking for mobile location in NLOS situations," *The 14th IEEE International Symposium on Personal Indoor and Mobile Radio Communication (PIMRC)*, vol. 3, pp. 2203–2207, September 2003.
- [10] C. D. Wann and C. S. Hsueh, "NLOS mitigation with biased kalman filters for range estimation in UWB systems," *IEEE Region 10 Conference, TENCON 2007*, pp. 1–4, October 2007.
- [11] A. F. Molisch and J. R. Foers, "Channel modeling for ultrawideband personal area networks," *IEEE Wireless Communications*, vol. 10, no. 6, pp. 14–21, December 2003.
- [12] P. C. Richardson, W. Xiang, and W. Stark, "Modeling of ultrawideband channels within vehicles," *IEEE Journal on Selected Areas in Communications*, vol. 24, no. 4, pp. 906–912, April 2005.
- [13] A. Saleh and R. Valenzuela, "A statistical model for indoor multipath propagation," *IEEE journal on Selected Areas in Communications*, vol. 5, no. 2, pp. 128–137, February 1987.
- [14] H. L. V. Trees, *Detection, Estimation, and Modulation Theory: Part I*, Wiley, New York, 1968.

# The Broadcast Storm Problem in Vehicular Ad-hoc Networks (VANET)

Khalid Abdel Hafeez, Lian Zhao, Zaiyi Liao, Bobby Ngok-Wah Ma  
 Electrical and Computer Engineering Department  
 Ryerson University, ON, Canada, M5B 2K3

**Abstract**—Most applications in VANETs use broadcasting as a main block for localization, routing and dissemination of warning messages to other vehicles on the road to achieve a safe, reliable and effective transportation system. Broadcasting in its normal way may lead to a broadcast storm problem by increasing the nodes contention in using the communication channel and more collisions which may result in collapsing the channel. In this paper we will show how serious this problem in MANETs in general and VANETs in particular. We will discuss and compare between many techniques that have been introduced to alleviate the impact of this problem. We also introduce a new scheme which takes into account the network topology and traffic parameters. At the end we will show performance of our algorithm using the network simulator in ns2 [9].

**Index Terms**— ITS, VANET, DSRC, CSMA, ns-2.33, Two-ray ground model.

## I. INTRODUCTION

Vehicular ad hoc networks are characterized by their fast changing topology and the high mobility of their nodes (vehicles) which add more challenge in the design of a suitable routing protocol for the vehicular environment. There are many applications and routing protocols that have been developed or under development for VANETs to help the drivers to travel more safely. Most of these applications and routing protocols use broadcasting extensively in finding a route to a destination, sending beacons to neighbors notifying them about their position, acceleration and most importantly to send safety warning messages to neighbors within certain distance to avoid chain collisions. Because vehicles move in a limited area and direction with confined rules, they will be close to each other especially in a jam or high traffic situations. Using broadcast in its flooding way may lead to what is known as the broadcast storm problem when more redundancy, contention and collisions will happen at the link layer. Those applications will face a challenge in managing the channel capacity to insure a good performance in terms of throughput, fairness and broadcast coverage. For example if one of the vehicles has an accident, it has to send a warning message to all vehicles behind it to inform them about the traffic situation to avoid a chain collision. This kind of safety information has to be propagated in a short time (usually less than 0.5 sec) [2]. In most cases not all vehicles within the one hop distance will receive the message due to the hidden terminal problem. Therefore the message has to propagate in a multi hop fashion as shown in Figure 1. If all vehicles within

the one hop broadcast try to rebroadcast the same message then there will be more contention for using the channel and the message could be lost due to collisions. Moreover many of the rebroadcasts are redundant since they will cover almost the same area. In [3], the authors found by simulation that after the forth rebroadcast, the expected additional coverage is less than 0.05%.

Prioritization one vehicle over the other to rebroadcast the message is the challenge that we would like to discuss in this paper.

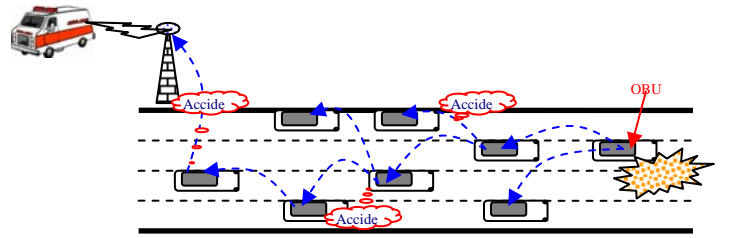


Figure 1: How the emergency information propagated within ITS system.

## II. RELATED WORK

The broadcast storm problem has been studied extensively in the mobile ad hoc networks. The authors in [3] presented five schemes to alleviate the impact of this serious problem by prohibiting some nodes from rebroadcasting and favoring others depending on their location and their knowledge of how many times the message has been broadcasted. The schemes are: Probabilistic scheme, Counter-based scheme, Distance-based scheme, Location-based scheme and Cluster-Based scheme. In [4] the authors introduced three distributed broadcast suppression techniques to alleviate the impact of the broadcast storm problem in VANETs specifically. Each node will calculate its rebroadcast probability based on its local information about the network. The proposed schemes are: weighted p-Persistence, slotted scheme and a slotted p-Persistence scheme.

The probabilistic scheme in [1] has a major disadvantage when the traffic is high and there are many vehicles in a small area, if the assigned probability is high then more vehicles will contend to use the channel and this will delay the delivery of crucial messages. Moreover, there will be situations when the message will not propagate to other hops in a light traffic scenario with assigned low probability. Therefore the probability has to be chosen carefully.

In the counter based scheme in [1], the higher the threshold counter is, the more time the node will wait before it decides to transmit or not. This mechanism will introduce more delay. There is also a possibility that the node will receive the same message more than the threshold from far nodes but very close to each other. In this case the node will decide not transmit

while it should since all of the received messages are redundant.

The threshold distance in the distance based scheme in [1] has to be chosen carefully. The higher the threshold is, the less number of vehicles propagate the message. If the traffic is light then there may be no vehicles beyond that threshold and the message will die. On the other hand, if the threshold distance is low and the traffic is high then more vehicles will contend to rebroadcast the message.

The location based scheme in [1] is a good choice since it calculates exactly the additional coverage area but it needs a full knowledge of the network topology. The calculation operation is very complicated over many intersecting circles.

The cluster based scheme in [1] is also a good choice since it decreases the number of participating nodes in rebroadcasting the message. This scheme is more vulnerable to the hidden terminal problem. If the cluster head broadcasts the message and more than one gateway are in the range of the cluster head but outside the range of each other, then some nodes in the new covered area will fail in receiving the message successfully.

For the weighted p-Persistence scheme in [2], each node has different probability than the others. This probability depends mainly on the distance. Each node has a fixed time to wait before it rebroadcasts the message. This will add more delay to the message which may not be propagated to the next hop especially in sparse networks.

The slotted scheme in [2] introduces more delay especially in sparse networks. The nodes will wait its calculated waiting time even if there are no nodes far than them to rebroadcast the message. The probability and the number of slots have to be chosen very carefully and should depend on the road traffic parameters.

Although the slotted p-persistence scheme in [2] reduces the contention within the one hop broadcast significantly, it introduces the highest delay since the nodes in every slot wait their time before they start contending for the use of the channel. If the network density is low and the probability chosen is also low then the message may not be able to propagate to the next hop.

From the above analysis, we can conclude that the more knowledge the nodes have about the network topology and traffic parameters, the better decision they can make for either to retransmit or not. The rebroadcast decision has to be shared between the data link layer and the above layers especially the application layer in order to decide for how long the message will be alive in the network and how far to be propagated.

### III. THE PROPOSED SCHEME

In order to find the optimal solution for the broadcast storm problem in VANET, we need first to define the maximum one hop range that each vehicle can use to reduce the impact of the hidden terminal problem. In previous work we derived the relation between the maximum range and the traffic parameters like the node density, sending rate and bandwidth. The approach we used is based on a geometric model as shown in Figure 2 to find the aggregate interfering traffic from the interference area during double of the current transmission period (T) and minimizing it. We used double the

transmission period since un-slotted CSMA needs both the current and the previous transmission periods to be quiet for successful reception from the recipient.

We found that the maximum range R should be:

$$R < \frac{1}{2W\lambda_s(1-e^{-\lambda_p 2T})} \quad (1)$$

where  $\lambda_s$  is the node density and  $\lambda_p$  is the average sending rate assuming that nodes are distributed and have packets to send based on a Poisson distribution process.

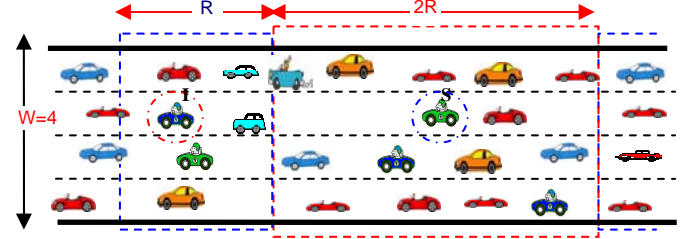


Figure 2: simplified geometric model for VANET scenario.

The second parameter we would like to introduce is the use of the Received Signal Strength (RSS) instead of the inter distance between nodes. Using the distance in calculating the probability may result in wrong decisions especially in a highly mobile environment where the characteristics of the wireless channel are very fluctuating. Using the received signal strength will take into account all the parameters of the wireless channel. This means that vehicles may have high probability to rebroadcast the message even if they are close to the transmitter if they receive a very low power signal due to obstruction on the channel.

The third parameter to introduce is the network density ( $\lambda_s$ ). We believe that the more dense networks are, the less number of nodes needed to participate in rebroadcasting the message to decrease the contention and the number of collisions.

The proposed scheme, called Network Topology p-Persistence scheme (NTPP), is based on the combination of the cluster based scheme in [1] and the slotted p-persistence scheme in [2]. We believe that if each node in the network has information about other nodes in the one hop broadcast range (which can be done through beaconing) then each node can detect the farthest node to itself that can deliver its message to add the maximum possible additional coverage while decreasing the propagation delay.

When the node transmits the message for the first time, it includes the ID of the farthest node possible based on its view of the network topology. The other nodes will calculate their probability to retransmit the message when they receive it. We include the node density in calculating the transmission probability. As a result, nodes in low dense networks will have a higher probability to transmit and visa versa. The transmission probability is calculated as:

$$P_{TR} = \left(1 - \frac{RSS_{T \rightarrow R}}{RSS_{\max\_Range}}\right) \times \left(1 - \frac{\lambda_s}{\lambda_{s\_max}}\right) \quad (2)$$

where  $RSS_{T \rightarrow R}$  is the received signal strength from the transmitter to the receiver,  $RSS_{\max\_Range}$  is the maximum power available to each node to reach the maximum communication range (R) which is given by Eqn. 1 above and  $\lambda_s_{\max}$  is the node density in the jam scenario.

If a node finds its node ID in the received message, the node should start re-transmitting the message immediately, while other nodes have to wait for certain time  $T_w$ . This waiting time has to be proportional to the received signal strength. The higher the signal strength, the larger waiting time should be. Moreover, the node density has also to be included in the waiting time so the nodes have less waiting time in low dense networks to overcome the long delay time problem in sparse networks as follows:

$$T_w = \left( \frac{RSS_{A \rightarrow B}}{RSS_{\max\_Range}} \right) \left( \frac{\lambda_s}{\lambda_s_{\max}} \right) \tau \quad (3)$$

where  $\tau$  is some fixed time plus the propagation time for the message to reach the maximum communication range R. The node will discard the message after it hears it from both directions.

From Eqn. (2), we can see that the probability is inversely proportional with the Received Signal Strength (RSS) from the transmitter and the receiver. The farthest node will have higher probability to retransmit than the adjacent nodes. The same relation with node density can also be seen since the need to suppress the rebroadcast in the high dense scenarios.

From Eqn. (3), we can see that the waiting time for each node is different and proportional to the node density and the inter distance (or RSS) between the transmitter and the receiver.

The state diagram in Figure 3 summarizes the proposed rebroadcast algorithm as follows:

- 1-When the node receives the message it will check first if its ID is included or not. If yes it will start rebroadcast the message immediately. The node then will wait the whole period  $\tau$  before discarding the message to insure that the message is heard from others.
- 2-If the ID is not included, it will calculate its rebroadcast probability ( $P$ ) and it's waiting time ( $T_w < \tau$ ).
- 3-If the node decides to rebroadcast according to it's probability  $P$  and  $T_w$  is expired, it will check if the message was heard from other nodes farther than itself, if yes it will discard the message and if not it will rebroadcast it.
- 4-If the node decided not to rebroadcast, it will wait the whole period  $\tau$  before it discards the message when it hears it from farther nodes. If the node did not hear the message within  $\tau$ , it will rebroadcast it with probability 1 to prevent the message from dying.

This algorithm takes into account the network topology where each node has some information about other nodes in the same hop either from previous communications or beaconing. The node will use this information to reduce the number of rebroadcasts, so only one node which has the most

additive coverage area will rebroadcast the message. If this node is not available any more by exiting from the road or it is out of range due to acceleration, then the farthest node in the same hop will have a higher probability and less waiting time than the others. The message in this algorithm will not die, each node will keep it even if it decides not to transmit based on its calculated probability. If the node did not hear the message from other nodes farther than itself within a certain time it will rebroadcast it with probability 1 otherwise it will discard it.

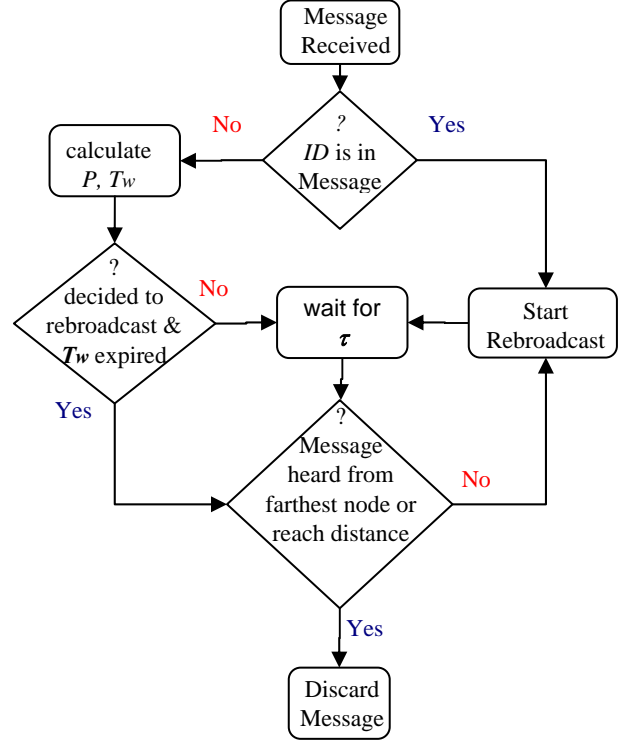


Figure 3: State diagram of NTPP rebroadcast algorithm

We believe that this algorithm is better than the schemes that have been discussed so far since we include the node density and the received signal strength in the calculation of the rebroadcast probability and the waiting time for each node. By including the node density, we reduced the delay especially in a sparse network scenario which is crucial for safety application.

We preferred to use the received signal strength rather than the distance between nodes for many reasons like the inaccuracy of the positioning devices, and the None Line Of Sight (NLOS) scenario. For the NLOS scenario, if we used the inter distance as a measure, then the receiving node may decide not rebroadcast because it is close to the transmitter. While by using the received signal strength (RSS), the same node will have higher probability and less waiting time. This will improve the effectiveness of the proposed algorithm.

#### IV. SIMULATION AND EVALUATION

In this section, we will discuss the simulation results obtained from applying the proposed scheme in a highway scenario. The vehicles are equipped with a DSRC technology and have an access to the GPS system for positioning

requirements and time synchronization. First we begin by the simulation setup, utilized scenarios and evaluation of the results.

### A. Simulation setup

In our simulation we used ns-2.33 [10] which is a well know simulator in both academic and industrial fields. This simulator has been extended to model VANETs by utilizing IEEE 802.11p technology.

The network models a circular bidirectional highway with a diameter of 2000m (6283m length) with 4 lanes in each direction. There are 600 vehicles on this highway segment and all of them equipped with a DSRC technology. We also assume that all vehicles are equipped with a GPS receiver to know their position on the road. The speed of the vehicles range from 40 to 100 Km/h and follow a microscopic mobility model where each vehicle's speed influenced by the front car and has to change lane if it decides to bypass another car. The propagation model used is the Two-Ray ground model [11], [12] with a system loss  $L=1$ . Each vehicle is configured to send 1, 5, 8 and 10 beacons/s of size 500 Bytes. The data rate is 3Mbps. We configure one of the nodes to send an emergency message of size 500 Bytes to all vehicles behind it and up to a distance of 2000m. We are interested in the time the emergency message will reach to all vehicles in the region. We will compare the results for different communication ranges (200m, 400m and 700m) with different traffic loads between the broadcasting in its flooding way and by using the proposed scheme (NTPP).

We calculated the maximum range from Eqn. 1 for the sending rates (1, 5, 8 and 10 messages/s) and found to be equal to 1955m, 393m, 247m and 198m respectively. The range 1955m in the first scenario means that the nodes can send with their maximum rang 1000m. The other ranges mean that the number of communication collisions will be minimized and the network will perform better if all nodes use that range.

We ran the simulation for 3 seconds of real time and each scenario for 10 times to get the average time. All configuration parameters are listed in Table 1.

Parameter	Value
Data rate of IEEE802.11p	3Mbps
Beacons rate	1,5,8 and 10 packets/s
Beacons message size	500Bytes
Warning message size	500Bytes
Communication range	200,400 or 700m
Radio propagation model	Two-ray ground
Highway Specifications	6283m length, 2 directions, 4 lanes/direction
Vehicles speed	40-100km/h
Vehicles density	12 cars/km/lane
Relevant area	2000m

Table 1: Value of parameters used in simulation

### B. Simulation results

Figure 4 shows the network setup in ns2. All vehicles are moving in the circular highway and transmitting periodically

their status messages. The vehicle in the square is the malfunctioning one and sends the emergency message to all vehicles behind it in a flooding fashion or the proposed scheme (NTPP).

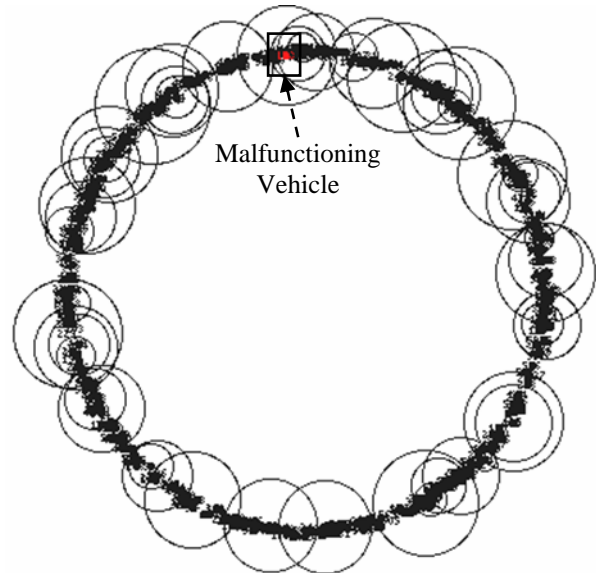


Figure 4: The highway scenario setup in ns2 simulator.

Figure 5 shows the time the warning message takes to reach all vehicles in the relevant distance (2000m), versus the number of beaconing messages rate (traffic load) for the different communication ranges in two scenarios: the first scenario when the broadcast is flooded through the network and the second scenario when the broadcast is controlled by our algorithm NTPP. It is clear that when the beacon generation rate is low, the flooding way performs better than our algorithm since there is no much interfering traffic and the nodes will not wait any time before retransmitting the warning message. On the other hand, when the traffic load is high, the rebroadcast in its flooding way will add more contention in using the channel and this will delay the warning message propagation. As we can see from Figure 5, our algorithm NTPP performs better than the flooding way and the message propagates faster to the end of the relative distance.

Figure 6 shows the percentage of the redundant messages received in the relative distance for both flooding broadcast and the new scheme NTPP. It is clear that NTPP scheme reduces the redundant traffic significantly compared with the flooding rebroadcast. When the beacons traffic rate is high, the communication range of 700m has high percentage of redundant messages since the propagation speed will be slow and the transmitter will face many collisions before it succeeds in transmitting the message.

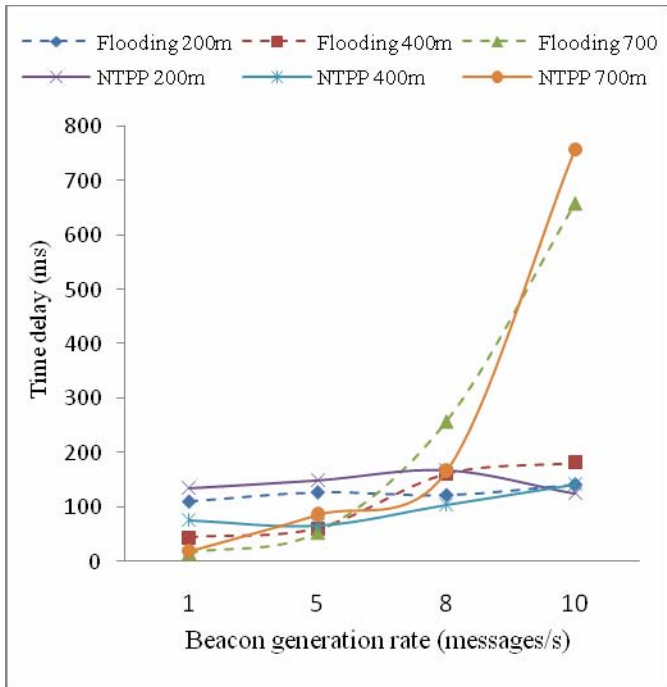


Figure 5: Time delay versus the traffic load.

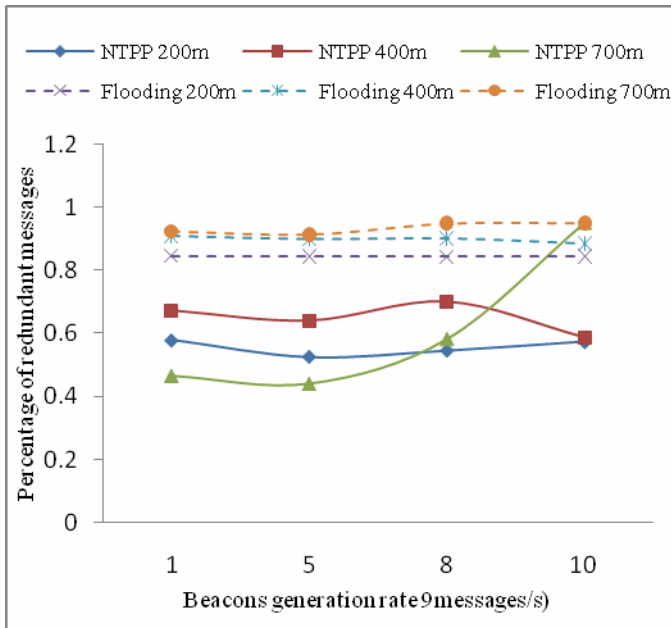


Figure 6: Percentage of redundant messages received within the relative distance for the flooding and NTPP.

## V. CONCLUSION

In this paper we introduced the broadcast storm problem in the MANETs and VANETs. We showed how serious this problem especially in the safety applications where the warning messages have to be propagated to other drivers in order to take a proper action in a very short time. There are many schemes available to alleviate the impact of this problem. From those schemes we found that the more knowledge the nodes have about the network topology and traffic parameters, the better decision they can make to either

rebroadcast or not. We introduced a new scheme NTPP which is based on the nodes knowledge of their neighbors in their range and traffic parameters like the node density and bandwidth. The node has first to determine its maximum range that minimizes the effect of the hidden terminal problem and then decide to rebroadcast or not based on the proposed algorithm. By simulation we showed how the NTPP scheme has fast propagation speed and reduces the redundant traffic compared to the flooding way of rebroadcasting.

## ACKNOWLEDGMENTS

This work has been supported by the Ministry of Transportation of Ontario (MOT). Opinions expressed in this report are those of the authors and may not necessarily reflect the views and policies of the Ministry of Transportation of Ontario.

## REFERENCES

- [1] "IEEE P802.11p/D5.0 Draft Amendments for Wireless Access in Vehicular Environments (WAVE)," January 2009. <https://mentor.ieee.org/802.11/file/08/>
- [2] <http://www.intelidriveusa.org/>
- [3] N. Sze-Yao, T. Yu-Chee, Ch. Yah-Shyan, Sh. Jang-Ping, "The Broadcast Storm Problem in a Mobile Ad Hoc Network," *Proc. ACM Int'l. Conf. Mobile Computing and Networking*, Seattle, WA, 1999, pp. 151–62.
- [4] N. Wisitpongphan, O. K. Tonguz, J. S. Parikh, P. Mudalige, F. Bai, and V. Sadekar, "Broadcast Storm Mitigation Techniques in Vehicular Ad Hoc Wireless Networks," *IEEE Wireless communication Magazine Volume, 14, Issue 6, Dec. 2007*.
- [5] K. Arindam, R.J. Marks II, M.A. El-Sharkawi, P. Arabshahi and A. Gray, "A Cluster-Merge algorithm for solving the minimum power broadcast problem in large scale wireless networks," *Proc. MILCOM*, Boston, MA, Oct. 13-16, 2003.
- [6] L. Stibor, Yunpeng Zang, Reumerman, H.-J., "Evaluation of Communication Distance of Broadcast Messages in a Vehicular Ad-Hoc Network Using IEEE 802.11p" *Wireless Communications and Networking Conference, IEEE 11-15 March 2007*.
- [7] A. Kato, K. Sato, and M. Fujise, "Technologies of Millimeter-Wave Inter-Vehicle Communications Propagation Characters". *Journal of the Communications Research Laboratory*, 2001.
- [8] S. Mangold, S. Choi and N. Esseling "An error model for radio transmissions of wireless LANs at 5GHz". *Proceeding Aachen Symposium 2001*, Aachen, Federal Republic of Germany, Sept. 2001
- [9] The Network Simulator ns2, [www.isi.edu/nsnam/ns/](http://www.isi.edu/nsnam/ns/).
- [10] Theodore S. Rappaport "Wireless Communications Principles and Practice" 2<sup>nd</sup> edition, ISBN-978-81-203-2381-0, Prentice-Hall 2002.
- [11] D. Dhoutaut, A. Régis, and F. Spies, "Impact of radio propagation models in vehicular ad hoc networks simulations". In *Proceedings of the 3rd international Workshop on Vehicular Ad Hoc Networks* (Los Angeles, CA, USA, September 29 - 29, 2006).

# The Maximum Range of a Broadcast Message in Vehicular Ad hoc Networks

Khalid Abdel Hafeez, Lian Zhao, Zaiyi Liao, Bobby Ngok-Wah Ma  
 Electrical and Computer Engineering Department  
 Ryerson University, ON, Canada, M5B 2K3

*Abstract—The research in Vehicular Ad hoc Network (VANET) has attracted great attention from both the academia and the industry to make the transportation system more safe, reliable and efficient. Vehicles in the near future will be equipped with a Dedicated Short Range Communications (DSRC) [1] wireless device so they can form a mobile ad hoc network on the road. The vehicles will broadcast their status information to each other to help drivers to avoid potential dangers and to extend their awareness to beyond of what they can directly see. The broadcast range is one of the critical parameters in the success of safety applications. In this paper we present a geometric model to predict the optimal range for maximizing the one hop broadcast message in a very dense wireless networks while keeping the contention between wireless nodes as minimum as possible. By maximizing the communication range, more nodes will be contending for the wireless channel. Minimizing the range will decrease the contending nodes but will increase the delay by increasing the number of hops the message will travel to reach the destination. Increasing the delay is a challenge for mission critical applications like propagating safety messages on the roads within the Intelligent Transportation System (ITS).*

*Index Terms—ITS, VANET, DSRC, CSMA, ns-2.33, Two-ray ground model.*

## I. INTRODUCTION

In wireless networks, broadcasting is a major building block for the discovery, routing and localization functions. As those wireless networks tend to grow in terms of number of nodes within a certain geographic area like vehicular ad-hoc networks (VANET) where many nodes (vehicles) are moving in a limited area and confined rules, their applications that use broadcasting will face a challenge in managing the channel capacity to insure a good performance in terms of throughput, fairness and broadcast coverage. For example when one of the vehicles has an accident it has to send a warning message to all vehicles behind it to inform them about the traffic situation to avoid a chain collision. This kind of safety information has to be propagated in a short time (usually less than 0.5 sec) [2]. The communication range is a critical parameter to enable distant drivers to react in a short time. If all vehicles act greedily by maximizing their communication range then the message will reach its destination in a less number of hops. As a consequence more vehicles will content at every point for using the same wireless channel which will collapse due to collisions. On the other hand, a short transmission range will result in more hops and delay but reduces the interfering traffic.

By predicting the optimal range as a function of traffic characteristics like network density, delay and sending rate, nodes can adjust their transmission range to reduce channel contention.

In [6], the authors used the spatial reuse of wireless resources to find the optimal radio range by knowing the sending rate, network density and one hop delay. They built a geometric model that predicted the likelihood of a collision where all nodes had the same broadcasting rate and communication range. They tried to solve this issue by predicting the optimal range from a pre-calculated scenario for a specific network and found that their results are 16% less in range than the simulated ones.

In [7], the authors gave a simple model for the per-hop delay in random access networks and computed the optimal transmission range as a function of specified traffic and delay parameters. The model they used to compute the one hop delay is based on the assumption that all nodes in the network have the same transmission policy of optimizing the overall network performance.

We extend the work in [6] and follow a new approach to solve this serious problem. Our result is a closed form formula in contrast to their findings. We claim that nodes within the wireless network can easily calculate their maximum communication range and adjust their transmission power so all nodes within their range will receive the broadcast message successfully.

The rest of the paper is organized as follows: section II discusses the proposed approach in MANETs in general and compare with similar works. Section III extends the same approach to VANETs. In section IV, the results of the simulation study are reported. Finally in section V we conclude our results.

## II. THE PROPOSED APPROACH

In this section we introduce our approach in finding the maximum communication range by building a new geometric model that minimizes the likelihood of a collision given that all nodes are distributed according to a Poisson distribution with an average density of ( $\lambda_s$ ). The nodes uses CSMA protocol and send packets according to a Poisson distribution with average rate ( $\lambda_p$ ) and all packets are of the same length (K Bytes) and need the same time (T sec) to transmit.

We build our model based on a two-ray ground propagation model [4], assuming that all nodes have the same radio range (R meters) and nodes within this transmission range will hear the transmission while nodes outside this range will not. If more than one transmission initiated to a receiver within the

same range then a collision will occur and all packets will be discarded.

Figure 1 show the geometric model behind our approach:

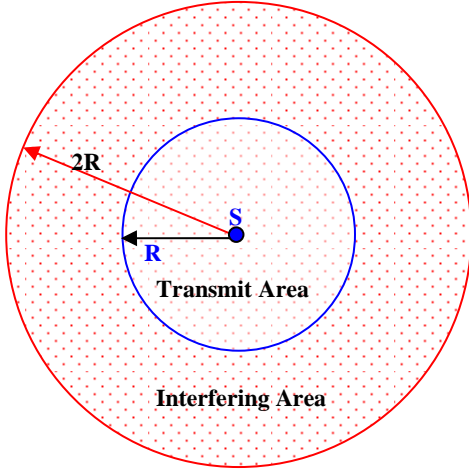


Figure 1: Geometric model used in our derivation

The node (S) has a transmission range of R meters like any other nodes in the network who will defer from transmitting if node S is using the channel. All nodes outside the range R but not far than 2R from the transmitter S will act as a hidden terminal for the current transmission. If one of the hidden terminals starts transmitting during the transmission of S, it will cause some nodes in the range of the source (S) to fail. We call the area within R from the source S as the maximum coverage area, while the dotted area as the interference area. We would like to find the maximum coverage as a function of traffic parameters like node density, sending rate and the bandwidth so we can define the following Definition:

**Definition 1:**

*The maximum coverage area that the source S can reach is the circle with radius R centered at itself given that all nodes in the interference area will not transmit within two times of its current transmission period (T).*

We used double the transmission period since un-slotted CSMA needs both the current and the previous transmission periods to be quiet for successful reception from the recipient.

Proofing Definition 1 can be easily done from the geometric model. If we assume that one of the nodes (node-A) in the interference area which is located at distance (d) from the source S starts transmitting at the same time, then there will be some nodes that lies in the intersection area between the two communication ranges of both S and A will fail to receive the original packet from the source S, and as the distance d decreases, the failed area will increase as shown in Figure 2.

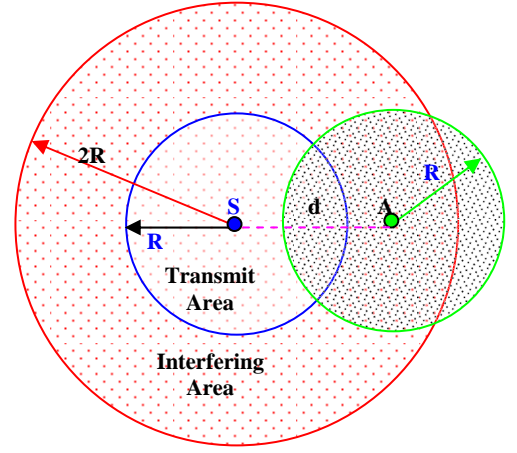


Figure 2: Geometric model to proof Definition 1

Therefore the challenge now is to maximize the communication range R and at the same time to minimize the number of interfering nodes. From the above analysis we can say that the maximum transmission range in a network with average node density ( $\lambda_s$ ) is R when the probability of interfering nodes approaches zero within the transmission period as mentioned in Definition 1. Therefore the problem now is to find the average number of interfering nodes in the interference area and minimize it.

We model each node to have an independent Poisson transmission process with average sending rate ( $\lambda_p$ ), therefore each node will transmit with a probability of  $(1 - e^{-\lambda_p t})$  in the time interval [0,t]. Consequently we can calculate the aggregate interfering transmissions from the interference area as follows:

$$E(I_t) = \lambda_s \pi ((2R)^2 - R^2) (1 - e^{-\lambda_p 2T}) \quad (1)$$

where  $E(I_t)$  is the average number of interfering nodes.

From equation 1, we see that R must be set to zero in order to satisfy Definition 1, which is clearly impractical. To make use of equation 1 to find R, we relax the condition of Definition 1. More specifically, instead of allowing no interfering nodes, we allow one interfering node. In a reasonably dense situation, the number of nodes within R meters of the source is also reasonably large. With the average of one interfering node, there is a high probability that some nodes within R meters of the source will receive the message correctly. By setting  $E(I_t) = 1$ , we have:

$$R_{\max} = \frac{1}{\sqrt{3\pi\lambda_s(1-e^{-\lambda_p 2T})}} \quad (2)$$

Comparing our results in Eqn. (3) with the authors' results in [6], we see that our equation to find the maximum communication range is a closed form formula while their equation allows us to calculate the maximum range based on a known range for a specific network with known traffic parameters.

After finding the maximum range, the nodes in the network can adjust their transmission power to achieve this range so all

nodes within this range will receive the transmitted packet successfully.

### III. MAXIMUM COMMUNICATION RANGE IN VANETS

As we derived before the relation between the maximum range and the traffic parameters for wireless networks, we begin by introducing the geometric model for the highway scenario as in Figure 3, where vehicles are moving in a certain direction and restricted by the traffic laws. The network topology is fast changing and the nodes (vehicles) are moving in a high speed.

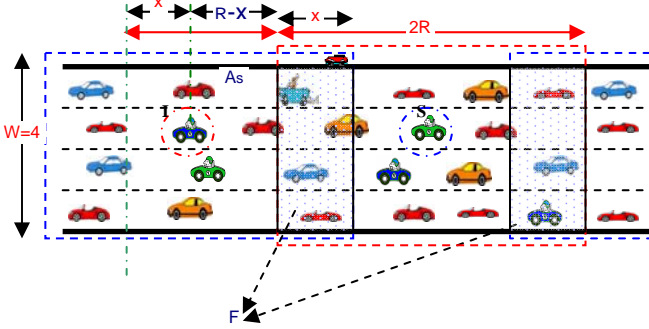


Figure 3: Geometric model for VANET scenario.

We assume that each node (vehicle) has the same communication range  $R$  and generates packets according to a Poisson process with average sending rate ( $\lambda_p$ ). The packets are of equal size so they need the same time ( $T$  sec) to transmit. The nodes (vehicles) are distributed on the road with an average density ( $\lambda_s$  vehicles/m/lane) and the width of the road is ( $W$ ) lanes.

We can see from the model that if vehicle  $S$  starts broadcasting a warning message then all vehicles within  $R$  distance will hear the transmission and defer from using the channel by CSMA. So all vehicles within  $R$  meters will receive the message successfully unless one of the interfering vehicles (vehicle- $I$ ), which is located at distance ( $2R-X$ ) from the transmitter, starts transmitting during the current transmission period causing some vehicles in area ( $F$ ) to fail in receiving the message. As a result, the maximum number of nodes that receive the message successfully is that all vehicles within  $R$  meters minus the failed vehicles. Therefore, our goal is to minimize the number of failed nodes. The new geometric model to solve this issue is shown in Figure 4.

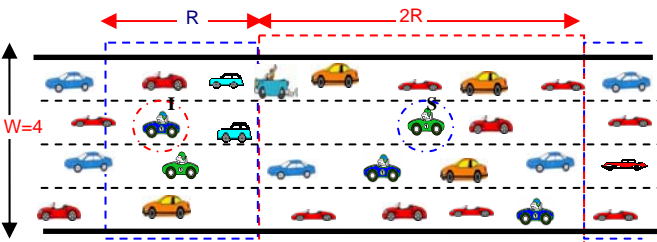


Figure 4: Simplified geometric model for VANET scenario.

As introduced in Definition 1, we can claim that all vehicles within  $R$  meters from the source will receive the broadcast message successfully if and only if the vehicles within  $R$  to  $2R$

distance from both sides of the source will not interfere during the transmission period.

Since each node (vehicle) is sending packets with independent Poisson process, so the probability of a vehicle to send a packet within  $2T$  seconds is derived as before ( $1 - e^{-\lambda_p 2T}$ ). So the expected number of interfering vehicles is:

$$E(I_t) = \lambda_s (2WR) (1 - e^{-\lambda_p 2T}) \quad (3)$$

Similar to the argument made in Section II, we set  $E(I_t)$  to 1 and derived  $R_{\max}$  from Eqn. (3):

$$R_{\max} = \frac{1}{2W\lambda_s(1 - e^{-\lambda_p 2T})} \quad (4)$$

From Eqn. (4), we can see that the maximum range is inversely proportional to the vehicle density and the sending rate. Vehicles can adjust their transmission power according to the road density to make sure that all vehicles within its range will receive its message successfully.

Roads have different and variable density depending on the time of the day and the traffic situation. Vehicles can sense this density from the beaconing messages exchanged between them or programmed with fixed densities depending on the time of the day and the day of the week. For example, the roads will be in a high density in rush hours (the mornings and afternoons) and in low density at night and weekends.

Figure 5 shows the relation between the maximum range  $R$  and the node density  $\lambda_s$ , we can see as the node density decreases, the maximum range  $R$  will increase because there will be less nodes within the range to contend for the use of the communication channel. The same as for the sending rate (traffic load), when the traffic load increases, the nodes have to decrease their communication range to reduce the interfering traffic and as a result the propagation speed will increase. Therefore configuring the nodes with the maximum range derived from Eqn. (4) will result in more nodes that can receive the warning message successfully in a short time as we will show that in the next section.

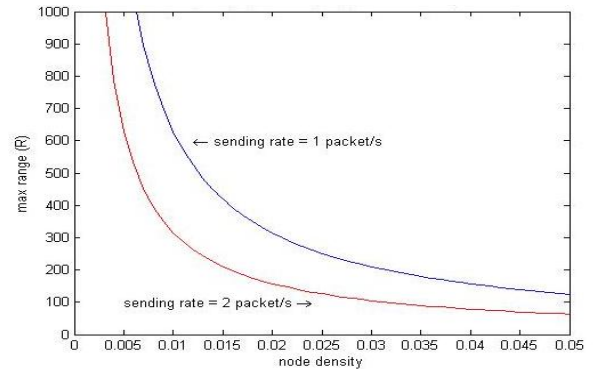


Figure 5: Maximum range ( $R$ ) vs Node density (vehicles/m/lane)

### IV. SIMULATION AND EVALUATION

In this section, we discuss the simulation results obtained

from applying our results in Eqn. (4) to a vehicular network where vehicles are equipped with DSRC devices. We begin with the simulation setup, utilized scenarios and evaluation of the results.

#### A. Simulation setup

In our simulation we used ns-2.33 [10] which is a well know simulator in both academic and industrial fields. This simulator has been extended to model VANETs by utilizing IEEE 802.11p technology.

Our scenario models a circular bidirectional highway with a diameter of 2000m (6283m length) with 4 lanes in each direction. There are 600 vehicles on this highway segment and all of them equipped with a DSRC technology. We also assume that all vehicles are equipped with a GPS receiver so they know their position on the road. The speed of the vehicles range from 40 to 100 Km/h and follow a microscopic mobility model where each vehicle's speed is influenced by the front car and has to change lane if it decides to bypass another car. The propagation model used is the Two-Ray ground model [4],[5] with a system loss  $L=1$ . Each vehicle is configured to send 1, 5, 8 and 10 beacons/s of size 500 Bytes. The data rate is 3Mbps. We configure one of the nodes to send an emergency message of size 500 Bytes to all vehicles behind it and up to a distance of 2000m. We are interested in the time the emergency message will reach to all vehicles in the region and compare the results for the different communication ranges (200m, 400m and 700m).

We calculated the maximum range theoretically from Eqn. (5) for the sending rates (1, 5, 8 and 10 messages/s) and it is equal to 1955m, 393m, 247m and 198m respectively. The range 1955m in the first scenario means that the nodes can send with their maximum rang 1000m while the other ranges mean that the number of communication collisions will be minimum and the network will perform better if all nodes use that range. We ran the simulation for 3 seconds of real time and each scenario for 10 times to get the average time. All configuration parameters are listed in Table1.

Parameter	Value
Data rate of IEEE802.11p	3Mbps
Beacons rate	1,5,8 and 10 packets/s
Beacons message size	500Bytes
Warning message size	500Bytes
Communication range	200,400 or 700m
Radio propagation model	Two-ray ground
Highway Specifications	6283m length, 2 directions, 4 lanes/direction
Vehicles speed	40-100km/h
Vehicles density	12 cars/km/lane
Relevant area	2000m

Table 1: Value of parameters used in simulation

#### B. Simulation results

Figure 6 shows the network setup in ns2. All vehicles are moving in the circular highway and transmitting periodically their status messages. The vehicle in the box is the malfunctioning one and it sends the emergency message to all

vehicles behind it in a flooding fashion.

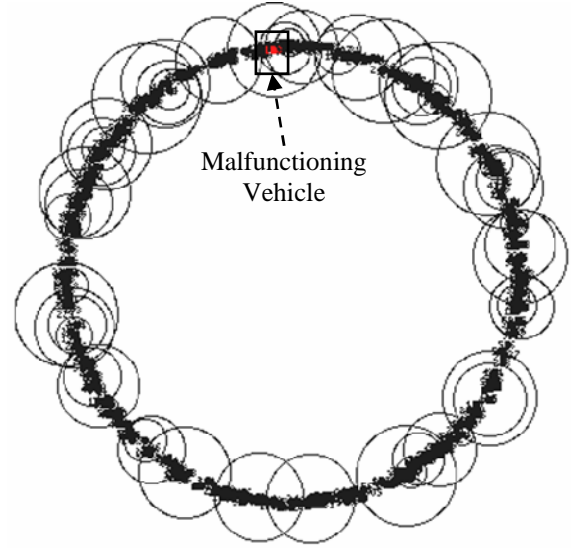


Figure 6: The highway scenario setup in ns2 simulator.

Figure 7 shows the time the warning message takes to reach all vehicles in the relevant distance (2000m), versus the number of beaconing messages rate. It is clear that when the beacon generation rate is low, the higher communication range will perform better than smaller ranges since the message will reach its destination in less number of hops without facing the high contention in using the channel. On the other hand, as the traffic increases, this means more interfering transmissions facing the emergency message propagation to its destination, the small ranges will perform better than the higher range. It can be seen from Figure 7, the shorter communication range performs better in high dense networks because the node will face less number of interfering traffic compared with the nodes with high range. When the beacons traffic rate is 10 packets/s, the communication range of 200m outperforms the 400 and 700m and this agrees with our theoretical results in Eqn. (4) as we calculated the best range to be 198m.

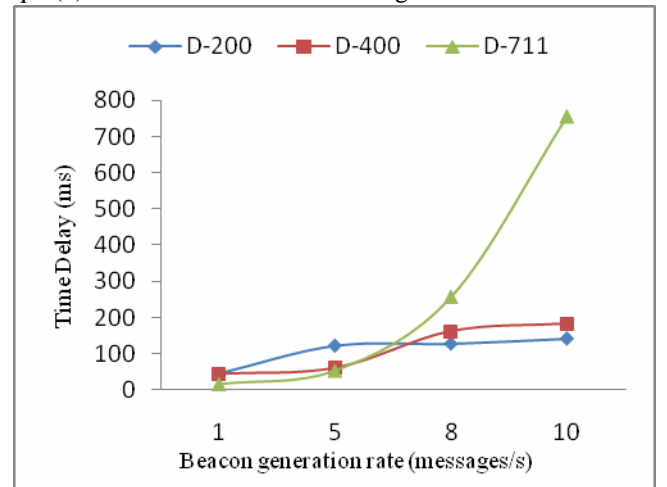


Figure 7: Time delay versus Beacon generation rate.

Figure 8 shows the percentage of the redundant messages that have been received by the vehicles within the relative

distance (2000m) to all warning messages that have been broadcasted. It is obvious that when vehicles are configured with large communication range, then most of the warning messages are redundant since each vehicle will receive the message more than once. This percentage will increase when the traffic is high since the message propagation speed will be slow due to the high interfering traffic. This explains why the small communication ranges of 200m and 400m have less overhead than the high communication range of 700m.

Figure 9 shows the average number of vehicles that receive the warning message within one hop broadcast range. It is clear that the high communication range will have better coverage than the low communication range when the traffic is low. While when the traffic is high, the high communication range (700m) performs worse than the 200m and 400m in terms of the number of vehicles that receive the warning message successfully. We can see that the 400m outperforms all when the traffic is 8 beacons per second and the 200m outperforms all when the traffic is 10 beacons per second. This complies with our finding in Eqn. (4) which predicts the best communication range that minimizes the contention and collisions between nodes.

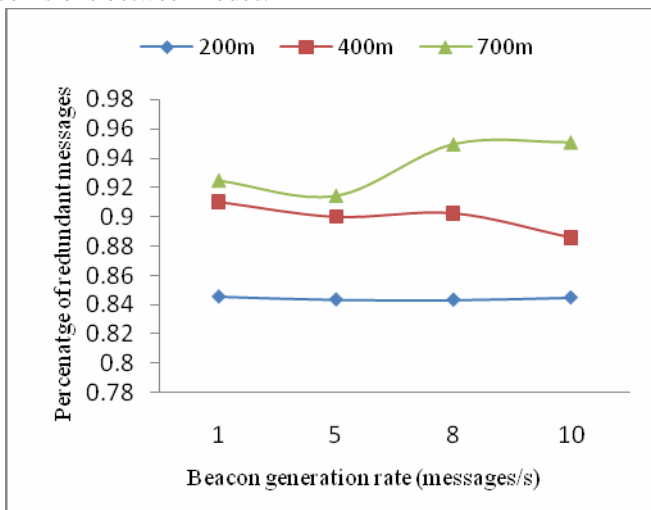


Figure 8: Percentage of the received redundant messages versus the traffic load.

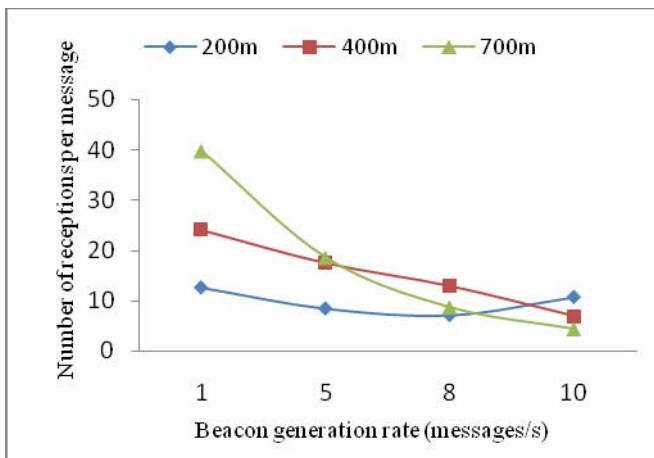


Figure 9: Number of vehicles that received the warning message successfully versus the traffic load.

## V. CONCLUSION

The broadcast storm problem is a very serious issue in wireless networks and has been studied extensively. In this paper we showed how the increase in the communication range will increase the contention and collisions within the one hop broadcast range and this will result in collapsing of the channel communication. While decreasing the communication range will result in less contention but more delay. Predicting the optimal communication range is the challenge that we addressed in this paper. We followed a new approach to solve this serious problem; our result is a closed form formula. We claim that nodes within the wireless network can easily calculate their maximum communication range and adjust their transmission power so all nodes within their range will receive the broadcast message successfully.

We also extended this subject to the Vehicular Ad hoc Networks (VANET) in the scope of Intelligent Transportation System (ITS). We derived the relation between the maximum range that a vehicle can transmit its message and the traffic parameters. We believe that vehicles on the road are more importantly to know the maximum communication range that they can use in order to deliver safety messages in a short time to avoid chain collisions and at the same time decreasing the number of failed nodes. By this we extended the drivers range of awareness to beyond of what they can directly see.

## ACKNOWLEDGMENTS

This work has been supported by the Ministry of Transportation of Ontario (MTO). Opinions expressed in this report are those of the authors and may not necessarily reflect the views and policies of the Ministry of Transportation of Ontario.

## REFERENCES

- [1] IEEE P802.11p/D5.0 Draft Amendments for Wireless Access in Vehicular Environments (WAVE), January 2009. <https://mentor.ieee.org/802.11/file/08/>
- [2] Vehicle Infrastructure Integration (VII), <http://www.intellidriveusa.org/>
- [3] B. Gallagher, H. Akatsuka, H. Suzuki, "Wireless communications for vehicle safety: Radio link performance and wireless connectivity methods", *Vehicular Technology Magazine, IEEE*, vol.1, no.4, pp.4-24, Dec. 2006.
- [4] Theodore S. Rappaport, "Wireless Communications Principles and Practice" 2<sup>nd</sup> edition, ISBN-978-81-203-2381-0, Prentice-Hall 2002.
- [5] D. Dhoutaut, A. Régis, and F. Spies "Impact of radio propagation models in vehicular ad hoc networks simulations. In *Proceedings of the 3rd international Workshop on Vehicular Ad Hoc Networks* (Los Angeles, CA, USA, September 29 - 29, 2006).
- [6] X. Li, T. D. Nguyen, and R. P. Martin, "An Analytic Model Predicting the Optimal Range for Maximizing 1-Hop Broadcast Coverage in Dense Wireless Networks", in *Proceedings of the 3rd International Conference on AD-HOC Networks & Wireless (ADHOC-NOW)*, July 2004.
- [7] L. Kleinrock; G. Akavia, "On a Self-Adjusting Capability of Random Access Networks," *Communications, IEEE Transactions on*, vol.32, no.1, pp. 40-47, Jan 1984.
- [8] H. Takagi; L. Kleinrock, "Optimal Transmission Ranges for Randomly Distributed Packet Radio Terminals,"

*Communications, IEEE Transactions on*, vol.32, no.3, pp. 246-257, Mar 1984.

- [9] L. Stibor; Y. Zang; H.-J. Reumerman, "Evaluation of Communication Distance of Broadcast Messages in a Vehicular Ad-Hoc Network Using IEEE 802.11p," *Wireless Communications and Networking Conference, 2007.WCNC 2007*.
- [10] The Network Simulator ns2, [www.isi.edu/nsnam/ns/](http://www.isi.edu/nsnam/ns/).

# Constrained Weighted Least Square Optimization for Vehicle Position Tracking

Lubna Farhi, Lian Zhao, Zaiyi Liao  
Electrical and Computer Engineering Department  
Ryerson University, ON, Canada, M5B 2K3

**Abstract**—This paper describes an effective method for vehicle positioning estimation for range-based wireless network. The problem of locating a mobile terminal has received significant attention in the field of wireless communications. Time of arrival (TOA), received signal strength (RSS), time difference of arrival (TDOA) and angle-of-arrival (AOA) are commonly used measurements for estimating the position of the vehicles. In this paper, Constrained Weighted Least Squares (CWLS) for vehicle position tracking approach with TDOA technique describes the optimized ranging measurement for the vehicles. Kalman filter is used for smoothing range data and mitigating the NLOS errors. The positioning problem is formulated in a state-space framework and the constraints on system states are considered explicitly. Simulation results show that the proposed tracking algorithm can improve the accuracy significantly.

**Index Terms**—CWLS, Kalman filter, ranging, TDOA.

## I. INTRODUCTION

The time-based methods for locating mobile stations in wireless systems usually involve the usage of location parameters, such as time of arrival (TOA) and time difference of arrival (TDOA). In general, the true range between a transmitter and a receiver in the wireless environment can be correctly calculated only when the direct path of signal propagation is present, which may not always be possible. Among the error sources which may affect the accuracy of wireless location, non-line-of-sight (NLOS) error is considered the major one. Particularly where higher accuracy is required, the effects caused by NLOS error usually cannot be ignored [1].

In this article, we concentrate on the ranging aspect of the vehicle transportation system. In the TOA method, the distance between the Mobile Station (MS) and Base Station (BS) is determined from the measured one-way propagation time of the signal traveling between them. For two-dimensional (2D) positioning, this provides a circle centered at the BS on which the MS lies. By using at least three BSs to resolve ambiguities arising from multiple crossings of the lines of position, the MS location estimate is determined by the intersection of the circles. In the TDOA method, the differences in the arrival times of the MS signal at multiple pairs of BSs are measured. TDOA-based location systems are of more interest because of its potential for high location estimation accuracy. We will

mainly discuss positioning algorithm including fundamental performance in the presence of noise and multi path. Further more we will describe the combination of optimization strategies which will improve the overall accuracy [2].

Accurate positioning of a vehicle is one of the essential features that assist third generation (3G) wireless systems in gaining a wide acceptance and triggering a large number of innovative applications. Although the main driver of location services is the requirement of locating Emergency 911 callers within a specified accuracy, mobile position information will also be useful in designing intelligent transport systems. Global Positioning System (GPS) could be used to provide mobile locations. However, it would be expensive to be adopted in the mobile phone network because additional hardware is required in the MS. Alternatively, utilizing the base stations in the existing network for mobile location is preferable and is more cost effective for the consumer. The basic principle of this software based solution is to use two or more BSs to intercept the MS signal. Each TDOA measurement defines a hyperbolic locus on which the MS must lie and the position estimate is given by the intersection of two or more hyperbola. In general, the MS position is estimated from a set of nonlinear equations constructed from TDOA measurement.

In [3], a method of position location and velocity estimation with signal strength and TOA measurements was suggested. By using a linear recursive model of mobility and by smoothing the position via Kalman filter, an accurate estimated track could be achieved. A Kalman tracking method based on TDOA measurements for UMTS mobile location has been demonstrated in [4]. Using a different way of converting nonlinear equations to linear equations without introducing constrains, Pages-Zamora [5] have developed a simple LS AOA-based location algorithm. However, all these methods ignore the constrains on the movement of mobile users. The goal of this work is vehicle position optimization by constrained weighted least square (WLS) approach [6] and NLOS error identification and mitigation by using biased Kalman filter, as shown in Fig.1. For vehicle position optimization we use WLS and Lagrange multipliers for minimizing the cost function [7].

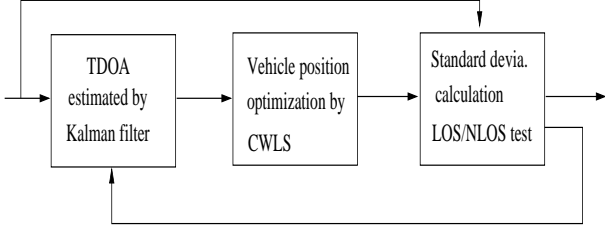


Fig. 1. Vehicle Positioning Architecture.

The rest of the paper is organized as follows. Section II describes the measurement models. Section III presents optimization approaches and formulates CWLS algorithm on which our vehicle positioning algorithm is based. In section IV positioning measurement model and overview of Kalman filter techniques for smoothing, tracking and NLOS mitigation techniques are presented. Section V demonstrates the simulation results. Conclusions are summarized in section VI.

## II. MEASUREMENT MODELS

This section describes the TOA and TDOA measurements. Let  $\mathbf{x} = [x, y]^T$  be the MS position to be determined. The coordinates of the  $i$ th BS is  $\mathbf{x}_i = [x_i, y_i]^T$ ,  $i = 1, 2, \dots, M$ , where the superscript  $T$  denotes the transpose operation and  $M$  is the total number of the receiving BSs. The distance between the MS and the BS, denoted by  $d_i$ , is given by

$$d_i = \sqrt{(x - x_i)^2 + (y - y_i)^2} \quad i = 1, 2, \dots, M \quad (1)$$

The TOA is the one-way propagation time taken for the signal to travel from the MS to a BS. In the absence of disturbance, the TOA measured at the BS, denoted by  $t_i$ , is

$$t_i = \frac{d_i}{c} \quad i = 1, 2, \dots, M \quad (2)$$

where  $c$  is the speed of light. The range measurement based on  $t_i$  in the presence of disturbance, denoted by  $r_{TOA,i}$  is modelled as

$$\begin{aligned} r_{TOA,i} &= d_i + n_{TOA,i} \\ &= \sqrt{(x - x_i)^2 + (y - y_i)^2} + n_{TOA,i} \end{aligned} \quad i = 1, 2, \dots, M \quad (3)$$

where  $n_{TOA,i}$  is the range error in  $r_{TOA,i}$ . Equation (3) can also be expressed in a vector form as

$$\mathbf{r}_{TOA} = \mathbf{f}_{TOA}(\mathbf{x}) + \mathbf{n}_{TOA}, \quad (4)$$

where

$$\mathbf{r}_{TOA} = [r_{TOA,1} \ r_{TOA,2} \ \dots \ r_{TOA,M}]^T, \quad (5)$$

$$\mathbf{n}_{TOA} = [n_{TOA,1} \ n_{TOA,2} \ \dots \ n_{TOA,M}]^T, \quad (6)$$

and

$$\mathbf{f}_{TOA}(\mathbf{x}) = \begin{bmatrix} \sqrt{(x - x_1)^2 + (y - y_1)^2} \\ \vdots \\ \sqrt{(x - x_M)^2 + (y - y_M)^2} \end{bmatrix} \quad (7)$$

### A. TDOA measurement algorithm

The TDOA is the difference in TOAs of the MS signal at a pair of BSs. Assigning the first BS as the reference, it can be easily deduced that the range measurements based on the TDOAs are of the form:

$$\begin{aligned} r_{TDOA,i} &= (d_i - d_1) + n_{TDOA,i} \\ &= \sqrt{(x - x_i)^2 + (y - y_i)^2} - \sqrt{(x - x_1)^2 + (y - y_1)^2} + n_{TDOA,i} \end{aligned} \quad i = 2, 3, \dots, M \quad (8)$$

where  $n_{TDOA,i}$  is the range error in  $r_{TDOA,i}$ . Notice that if the TDOA measurements are directly obtained from the TOA data, then

$$n_{TDOA,i} = n_{TOA,i} - n_{TOA,1}, \quad i = 2, 3, \dots, M.$$

In vector form, (8) becomes

$$\mathbf{r}_{TDOA} = \mathbf{f}_{TDOA}(\mathbf{x}) + \mathbf{n}_{TDOA}, \quad (9)$$

where

$$\mathbf{r}_{TDOA} = [r_{TDOA,2} \ r_{TDOA,3} \ \dots \ r_{TDOA,M}]^T, \quad (10)$$

$$\mathbf{n}_{TDOA} = [n_{TDOA,2} \ n_{TDOA,3} \ \dots \ n_{TDOA,M}]^T, \quad (11)$$

$$\mathbf{f}_{TDOA}(\mathbf{x}) = \begin{bmatrix} d_2 - d_1 \\ d_3 - d_1 \\ \vdots \\ d_M - d_1 \end{bmatrix} \quad (12)$$

## III. OPTIMIZATION APPROACHES

In general, the MS position is not determined geometrically but is estimated from a set of nonlinear equations constructed from the TOA, RSS, TDOA, or AOA measurements, with the knowledge of the BS geometry. Generally optimization approaches for positioning are Nonlinear Least Square (NLS), Maximum Likelihood (ML), Gaussian ML (GML), Genetic Algorithm Method (GAM) and Constrained Least Square method (CWLS) [6]. Basically, there are two approaches for solving the nonlinear equations. The NLS approach is to solve them directly in a nonlinear least squares (NLS) or constrained weighted least squares (CWLS) framework. Although optimum estimation performance can be attained, it requires sufficiently precise initial estimates for global convergence because the corresponding cost functions are multi-modal.

The CWLS approach is to reorganize the nonlinear equations into a set of linear equations. In this paper, the CWLS

approach is adopted and we will focus on a unified development of accurate position algorithms for TDOA measurement. For TDOA-based position systems, it is well known that for noise conditions, the corresponding nonlinear equations can be reorganized into a set of linear equations by introducing an intermediate variable, which is a function of the source position. This technique, is commonly called spherical interpolation (SI) [7]. However, the SI estimator solves the linear equations via standard least squares (LS) without using the known relation between the intermediate variable and the position coordinate. To improve the location accuracy of the SI approach, Chan and Ho have proposed [2] to use a two-stage CWLS to solve the source position, while [6] incorporates the relation explicitly by minimizing a constrained LS function based on the technique of Lagrange multipliers. According to [6], these two modified algorithms are referred to as the quadratic correction least squares (QCLS) and linear correction least squares (LCLS), respectively. In this work, we developed a unified approach for mobile location by utilizing TDOA measurement and improving the ranging accuracy with the use of CWLS [5].

The CWLS mobile positioning approach for the TDOA measurement is: without disturbance, (8) becomes:

$$r_{TDOA,i} = \sqrt{(x - x_i)^2 + (y - y_i)^2} - \sqrt{(x - x_1)^2 + (y - y_1)^2}$$

It can be rewritten as

$$r_{TDOA,i} + \sqrt{(x - x_1)^2 + (y - y_1)^2} = \sqrt{(x - x_i)^2 + (y - y_i)^2} \quad i = 2, 3, \dots, M \quad (13)$$

Squaring both sides of (13) and introducing an intermediate variable,  $R_1$ , which has the form

$$R_1 = d_1 = \sqrt{(x - x_1)^2 + (y - y_1)^2}. \quad (14)$$

We obtain the following set of linear equation

$$\begin{aligned} (x - x_1)(x_i - x_1) + (y - y_1)(y_i - y_1) + r_{TDOA,i}R_1 \\ = \frac{1}{2}[(x_i - x_1)^2 + (y_i - y_1)^2 - r_{TDOA,i}^2] \quad (15) \\ i = 2, 3, \dots, M \end{aligned}$$

Writing (15) in matrix form gives

$$\mathbf{G}\delta = \mathbf{h} \quad (16)$$

where

$$\mathbf{G} = \begin{bmatrix} x_2 - x_1 & y_2 - y_1 & r_{TDOA,2} \\ \vdots & \vdots & \vdots \\ x_M - x_1 & y_M - y_1 & r_{TDOA,M} \end{bmatrix} \quad (17)$$

$$\mathbf{h} = \frac{1}{2} \begin{bmatrix} (x_2 - x_1)^2 + (y_2 - y_1)^2 + r_{TDOA,2}^2 \\ \vdots \\ (x_M - x_1)^2 + (y_M - y_1)^2 + r_{TDOA,M}^2 \end{bmatrix}, \quad (18)$$

and the variable  $\delta = [x - x_1, y - y_1, R_1]^T$ , consists of the MS location as well as  $R_1$  [8].

In the presence of measurement errors, the SI technique determines the MS position by simply solving (16) via standard LS and the location estimate is found from

$$\begin{aligned} \hat{\delta} &= \text{argmin}(\mathbf{G}\hat{\delta} - \mathbf{h})^T(\mathbf{G}\hat{\delta} - \mathbf{h}) \\ &= (\mathbf{G}^T\mathbf{G})^{-1}\mathbf{G}^T\mathbf{h}. \end{aligned} \quad (19)$$

where  $\hat{\delta} = [\hat{x} - x_1, \hat{y} - y_1, \hat{R}_1]^T$  is an optimization variable vector [6].

An improvement to the SI estimator is the linear correction least squares (LCLS) method, which solves the LS cost function in (19) subject to the constraint of  $(\hat{x} - x_1)^2 + (\hat{y} - y_1)^2 = \hat{R}_1^2$ , or equivalently,

$$\hat{\delta}^T \Sigma \hat{\delta} = 0 \quad (20)$$

where  $\Sigma = \text{diag}(1, 1, -1)$ . Optimum estimate of the positioning of the vehicle is computed by minimizing the following CWLS cost function:

$$f = (\mathbf{G}\hat{\delta} - \mathbf{h})^T \mathbf{Q}^{-1} (\mathbf{G}\hat{\delta} - \mathbf{h}) \quad (21)$$

where  $\mathbf{Q}$  is the covariance matrix of TDOA's measure values, which is a function of the estimate of  $R_1$ , denoted by  $\hat{R}_1$  [6].

The idea of CWLS estimator is to combine the key principles in the CWLS and LCLS methods that is, the MS position estimate is determined by minimizing (21) subject to (20). For sufficiently small measurement errors, the inverse of the optimum covariance matrix  $\mathbf{Q}^{-1}$  for the CWLS algorithm is found using the best linear unbiased estimator [2] as

$$\mathbf{Q}^{-1} = \mathbf{S}_1 \mathbf{S}_1^T \odot \mathbf{n}_{TDOA,i} \quad (22)$$

where

$$\mathbf{S}_1 = \begin{bmatrix} d_2 \\ d_3 \\ \vdots \\ d_M \end{bmatrix} = \begin{bmatrix} d_2 - d_1 + R_1 \\ d_3 - d_1 + R_1 \\ \vdots \\ d_M - d_1 + R_1 \end{bmatrix} \quad (23)$$

and  $\odot$  denotes element-by-elements multiplication. Since  $\mathbf{Q}$  contains the unknown  $\{d_i\}$ , we express

$$d_i = d_i - d_1 + R_1$$

and approximate  $(d_i - d_1)$  by  $r_{TDOA,i}$ . Similar to [6], the CWLS problem is solved by using the technique of Lagrange multipliers and the Lagrangian to be minimized is

$$\mathcal{L}_{TDOA}(\hat{\delta}, \eta) = (\mathbf{G}\hat{\delta} - \mathbf{h})^T \mathbf{Q}^{-1} (\mathbf{G}\hat{\delta} - \mathbf{h}) + \eta \hat{\delta}^T \Sigma \hat{\delta} \quad (24)$$

where  $\eta$  is the lagrange multiplier to be determined. The estimate of  $\delta$  is obtained by differentiating (24)  $\mathcal{L}_{TDOA}(\hat{\delta}, \eta)$  with respect to  $\hat{\delta}$  and then equating the results to zero [6] as

$$\frac{\partial \mathcal{L}_{TDOA}(\hat{\delta}, \eta)}{\partial \hat{\delta}} = 2(\mathbf{G}^T \mathbf{Q}^{-1} \mathbf{G} + \eta \Sigma) \hat{\delta} - 2\mathbf{G}^T \mathbf{Q}^{-1} \mathbf{h} = 0.$$

The solution is:

$$\hat{\delta} = (\mathbf{G}^T \mathbf{Q}^{-1} \mathbf{G} + \eta \mathbf{\Sigma})^{-1} \mathbf{G}^T \mathbf{Q}^{-1} \mathbf{h} \quad (25)$$

where  $\eta$  is real value, put the  $\eta$  in (25) and obtain the sub-estimates of  $\hat{\delta}$ . Then choose the solution  $\hat{\delta}$  from those sub-estimates which makes the cost function (21) minimum.

#### IV. POSITION MEASUREMENT MODEL AND NLOS IDENTIFICATION

The range measurement between a mobile station and the  $m$ th base stations corresponding to TOA data can be modeled as:

$$r_m(t_i) = L_m(t_i) + n_m(t_i) + NLOS_m(t_i) \quad (26)$$

where  $r_m(t_i)$  is the measured range at the sampling time  $t_i$ ,  $L_m(t_i)$  is the true range,  $n_m(t_i)$  is the measurement noise and can be modelled as a zero-mean additive Gaussian random variable with variance  $\sigma_m$ ;  $NLOS_m(t_i)$  is the NLOS error component in the received signal. There is no NLOS error if the line-of-sight exists, in which case, the measurement error  $n_m(t_i)$  becomes the only source of range measurement error. To mitigate the NLOS errors, the existence of non-zero NLOS component needs to be identified. To identify the change of channel situation between NLOS and LOS, the standard deviation of the estimated range data  $r_m(t_i)$  can be calculate as

$$\hat{\sigma}_m = \sqrt{\frac{1}{N} \sum_{i=1}^k (r_m(t_i) - \hat{L}_m(t_i))^2} \quad (27)$$

where  $\hat{L}_m(t_i)$  is the estimated range data of the  $m$ th BS at time instant  $t_i$  smoothed by the unbiased Kalman filter. The standard deviation estimated in equation (27) can then be used in the simple hypothesis testing to determine the LOS/NLOS BSs

$$H_0 : \hat{\sigma}_m < \gamma \sigma_m \cdots \text{LOS condition} \quad (28)$$

$$H_1 : \hat{\sigma}_m \geq \gamma \sigma_m \cdots \text{NLOS condition} \quad (29)$$

where  $\gamma$  is a scaling factor, and  $\gamma > 1$  is chosen experimentally for the UWB channels.

##### A. DATA SMOOTHING

A Kalman filter can be used in estimating the state vector of a mobile target from the observed range data and therefore estimating the true range value. The state vector can be represented in [1]

$$\mathbf{X}_{(k+1)} = \mathbf{A}_{(k)} \mathbf{X}_{(k)} + \mathbf{B}_{(k)} \mathbf{W}_{(k)}, \quad (30)$$

where  $\mathbf{X}_{(k)} = [L_m(k) \quad \dot{L}_m(k)]$  is the state vector of the mobile related to the  $m$ th sensor. The  $\mathbf{W}_{(k)}$  is the driving noise vector with covariance matrix  $\mathbf{Q} = \sigma_w^2 \mathbf{I}$ , and

$$\mathbf{A} = \begin{bmatrix} 1 & \Delta t \\ 0 & 1 \end{bmatrix}, \quad \mathbf{B} = \begin{bmatrix} 0 \\ \Delta t \end{bmatrix} \quad (31)$$

The measurement process is

$$\mathbf{y}_{(k+1)} = \mathbf{C}_{(k)} \mathbf{X}_{(k)} + \mathbf{U}_{(k)} \quad (32)$$

where  $\mathbf{y}_{(k+1)}$  is the measured data and

$$\mathbf{C} = \begin{bmatrix} 1 & 0 \end{bmatrix} \quad (33)$$

and  $\mathbf{U}_{(k)}$  is the measurement noise with covariance  $\mathbf{R} = \sigma_u^2 \mathbf{I}$ . The operation of the Kalman filter can be summarized as follows:

- Kalman filter time update equations:

$$\hat{\mathbf{X}}_{(k|k-1)} = \mathbf{A} \hat{\mathbf{X}}_{(k-1|k-1)} \quad (34)$$

$$\mathbf{P}_{(k|k-1)} = \mathbf{A} \mathbf{P}_{(k-1|k-1)} \mathbf{A}^T + \mathbf{B} \mathbf{Q} \mathbf{B}^T \quad (35)$$

- Kalman filter measurement update equations

$$\mathbf{K}_{(k)} = \mathbf{P}_{(k|k-1)} \mathbf{C}^T [\mathbf{C} \mathbf{P}_{(k|k-1)} \mathbf{C}^T + \mathbf{R}_{(k)}]^{-1} \quad (36)$$

$$\hat{\mathbf{X}}_{(k|k)} = \hat{\mathbf{X}}_{(k|k-1)} + \mathbf{K}_{(k)} [\mathbf{y}_{(k)} - \mathbf{C} \hat{\mathbf{X}}_{(k|k-1)}] \quad (37)$$

$$\mathbf{P}_{(k|k)} = \mathbf{P}_{(k|k-1)} - \mathbf{K}_{(k)} \mathbf{C} \mathbf{P}_{(k|k-1)} \quad (38)$$

where  $\mathbf{K}_{(k)}$  is the Kalman gain vector and  $\mathbf{P}_{(k|k)}$  is the covariance matrix of  $\hat{\mathbf{X}}_{(k|k)}$ .

The modified biased Kalman filter is proposed to process the range measurement according to the feedback identification result from the previous processed data. Before computing kalman gain, the measurement noise covariance  $\sigma_u^2$  or the range prediction covariance  $\mathbf{P}_{(k|k-1)}$  is adjusted as follows:

Case 1: if

$$\mathbf{y}_{(k)} - \mathbf{C} \mathbf{X}_{(k|k-1)} > \mathbf{0} \cdots \text{NLOS case} \quad (39)$$

$$\text{then, } \mathbf{X}_{(k+1)} = \mathbf{A} \mathbf{X}_{(k)} + \mathbf{B} \mathbf{W}_{(k)} \quad (40)$$

Case 2: if

$$\mathbf{y}_{(k)} - \mathbf{C} \mathbf{X}_{(k|k-1)} < \mathbf{0} \cdots \text{LOS case} \quad (41)$$

$$\text{then, } \hat{\sigma}_u^2(k) = \sigma_m^2 \quad (42)$$

#### V. SIMULATION RESULTS

Simulation is performed for position estimation by using MATLAB. It is assumed that 200 data samples are measured with the sampling period 3s. The vehicles have a velocity of 4m/s. The range data are created by the true distance from each vehicle position in the trajectory to the known three BSs. The measurement noise is assumed to be AWGN and NLOS noise is added to the true calculated range to get the measured range data. The measurement noise is assumed to be Gaussian distributed with zero mean and a standard deviation  $\sigma_m = 150m$ . The initial value for state vector is  $\mathbf{x} = [0 \quad 0]^T$ .

Fig.2 illustrates the application of Kalman filter to mitigate the NLOS error, where the solid curve and dished curve denote the true distance and the estimated distance respectively. Fig.3

shows the range measurement which is optimized by applying CWLS optimization technique to improve the estimation. It can be observed that the estimation by applying CWLS technique can greatly improve the estimation accuracy.

Fig.4 shows the position estimation error with constrained and unconstrained filters represented by the dashed and the solid curve respectively. It can be seen that the constrained filter results in much more accurate estimates than the unconstrained filter. The unconstrained filter results in average position errors of about 5.8 m, while the constrained filter results in position errors of about 3.3 m.

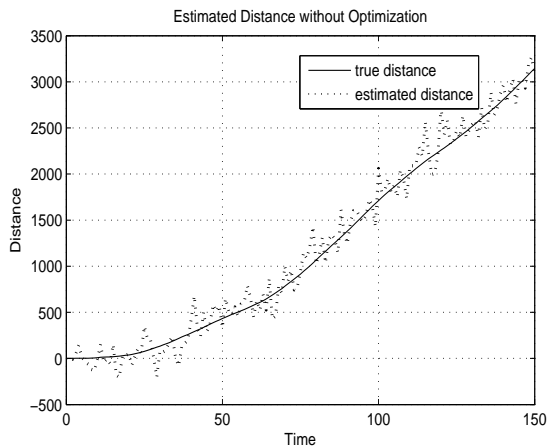


Fig. 2. NLOS mitigation using biased KF.

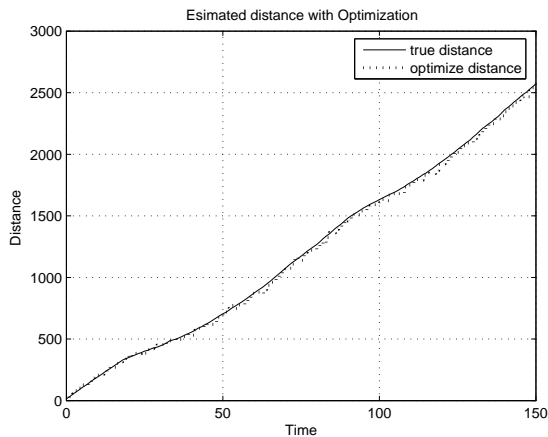


Fig. 3. NLOS mitigation with CWLS optimization.

## VI. CONCLUSION

In this paper, we present a range estimation algorithm with NLOS error mitigation using biased Kalman filter. Simulation results demonstrate the effectiveness of this method. If the state constraints are nonlinear they can be linearized. The proposed

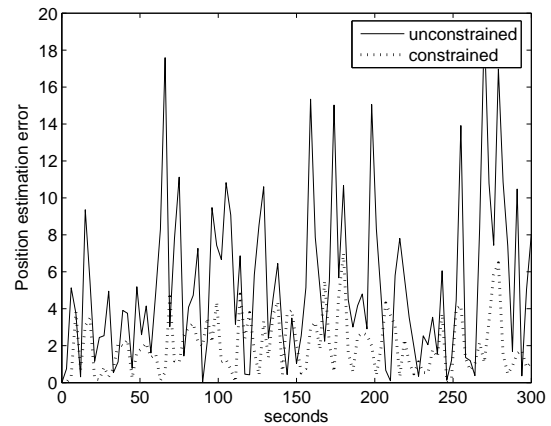


Fig. 4. Position estimation error with the constrained and unconstrained filters.

method gives a real-time constrained least squares estimation algorithm for tracking the position using TDOA measurements. The NLOS errors can be mitigated effectively for achieving higher accuracy in range estimation and wireless location.

## ACKNOWLEDGMENT

This work has been supported by the Ministry of Transportation of Ontario (MTO). Opinions expressed in this report are those of the authors and may not necessarily reflect the views and policies of the Ministry of Transportation of Ontario.

## REFERENCES

- [1] B. L. Le, K. Ahmed, and H. Tsuji, "Mobile location estimator with NLOS mitigation using kalman filtering," *In Proc.IEEE Wireless Communication and Networking*, vol. 3, pp. 16–20, 2003.
- [2] Y. T. Chan and K. C. Ho, "A simple and efficient estimator for hyperbolic location," *IEEE Transactions on Signal Processing*, vol. 35, no. 8, pp. 1905–1915, 1994.
- [3] M. Hellebrandt and R. Mathar, "Location tracking of mobiles in cellular radio networks," *IEEE Transactions on Vehicle Technology*, vol. 48, pp. 1558–1562, 1999.
- [4] M. Najjar and J. Vidal, "Kalman tracking based on tdoa for umts mobile," *IEEE International Symp. Personal, indoor and Mobile Radio Communication*, vol. 1, pp. 45–49, 2001.
- [5] A. Pages-Zamora, J. Vidal, and D. R. Brooks, "Closed-form solution for positioning based on angle of arrival measurements," *13th IEEE International Symposium on Personal, Indoor and Mobile Radio Communications*, vol. 4, pp. 1522–1526, 2002.
- [6] G. W. Elko, Y. Huang, J. Benesty, and R. M. Mersereau, "Realtime passive source localization: a practical linear-correction least-squares approach," *IEEE Transactions on Speech and Audio Processing*, vol. 9, no. 8, pp. 943–956, 2001.
- [7] J. O. Smith and J. S. Abel, "Closed-form least-squares source location estimation from range-difference measurements," *IEEE Transactions on Acoustics, Speech and Signal Processing*, vol. 35, no. 12, pp. 1661–1669, 1987.
- [8] H. C. So and S. P. Hui, "Constrained location algorithm using TDOA measurements," *IEICE Transactions on Fundamentals of Electronics, Communications and Computer Sciences*, vol. E86-A, no. 12, pp. 3291–3293, 2003.

## Appendix C

### Modeling of Vehicle Dynamics for Future Integration with Inter-Vehicle Communication Simulation

The long-term goal of this research is to develop an intelligent ECU for ABS that can recognize the road condition and accordingly control the slippage that results in the maximum grip thus shortest stopping distance, whilst safe controllability and stability are maintained. The proposed intelligent ECU is based on a dual loop feedback control scheme. In the outer loop, a vehicle motion sensing system will be developed to monitor the dynamics of the vehicle thus the grip between the wheels and the road can be estimated. This estimate is used to determine the most desirable slippage. In the inner loop, the conventional ABS control algorithm will be employed to control the ABS so that the slippage is maintained at the desired level determined by the outer loop.

To achieve this goal, a vehicle dynamic simulation platform needs to be developed. The simulator will be used to investigate the dynamics of vehicles during emergency braking and to develop an adaptive ABS control scheme. This chapter describes the development of this simulation model.

#### 1. Introduction to vehicle dynamics

Ground vehicles with mechanical propulsion are perceived as one of the main consequences of the industrial revolution. In order to move a vehicle, including its own structure and the payload, a prime mover is essential. The power (P) needed to move a vehicle and the payload (mass: m) at a speed V on a level surface is as follow:

$$P = mgfV \quad (C.1)$$

where:

- m The mass of the vehicle and the payload (kg)
- g Acceleration of gravity ( $m/s^2$ )
- f Coefficient of friction (sliding or rolling)
- V Velocity of the vehicle (m/s)

Therefore the minimum value of the power/mass ratio of a prime mover above which it can move the vehicle is:

$$\frac{P}{m} = \frac{gfV}{\eta\alpha} \quad (C.2)$$

where:

- $\alpha$  The ratio between the mass of the engine and the total mass of the vehicle
- $\eta$  The total efficiency of the mechanism transferring the power and propelling the vehicle

The behaviour of a road vehicle is the consequence of the dynamic interaction of the various components of the vehicle structure in which the pneumatic tyre plays a major role. In addition to the aerodynamic forces and the gravity, all the other forces that make a vehicle to accelerate or to decelerate are applied to the vehicle from the ground through the wheels. The primary forces that control a ground vehicle are developed in four patches where the tires contact the ground. Therefore it is essential to understand how the dynamics of ground vehicles is determined by the forces and moments generated by pneumatic tires at the ground. The motions accomplished in acceleration, braking, cornering and ride are the responses to forces imposed. The study of vehicle dynamics involves the principles of how and why the forces are produced [Genta, 2006; Rajamani, 2006; Gillespie, 1992]. It is understood that the dominant forces acting on a vehicle to control its performance are developed by the tire against the road [Aleksendriv, etc, 2006; Svendenius, 2006; Miyashita and Kabe, 2005; Imine, etc, 2005]. Thus the behaviour of tires, characterized by the forces and moments generated over the broad range of conditions, is the dominating factor that determines the performance of ground vehicles that is associated with vehicle cornering, turning or directional response.

For a ground vehicle, the cornering, turning and directional response are the properties of the vehicle while the direction is being changed and certain lateral acceleration is sustained in the process. The cornering ability is the level of lateral acceleration being sustained in stable condition [Chumsamutr, etc, 2006; Guo, etc, 2005]. The cornering force is the sideways force produced by a vehicle tyre during cornering. Tyre force is generated by tyre slip. In the case of cornering, tyre force is proportional to slip angle at low slip angles. Slip angle describes the deformation of the tyre contact patch, this deflection of the contact patch deforms tyre in a fashion akin to a spring. The directional response is the time required for lateral acceleration to develop following a steering action. Vehicle handling implies both the vehicle's explicit capability contribution and the combination of the driver and vehicle.

All modern motor vehicles are equipped with pneumatic tires to support the vehicle (and the payload) and to transfer the driving power. This is obtained through the contact between the wheels and the ground (road). This contact also provides lateral forces to control the trajectory of the vehicle [Steenbergen, 2006; Hirschberg, etc, 2002; Li, etc, 2006;]. The rigid structure of the wheel is surrounded by a compliant element that is made by the tire. The tire is a complex structure that consists of a number of layers of rubberized fabric. Structurally, tires can be categorized into two groups: bias tires and radial tires [Genta, 2006]. Presently radial tires have completely substituted the bias tires due to the superior performance. The main function of the tire is to distribute the vertical load in a large area and to insure compliance to absorb the irregularities of the ground.

The force applied to the tire from the ground is assumed to be located at the centre of the contact area. The force is decomposed to the longitudinal force ( $F_x$ ), the lateral force ( $F_y$ ) and the normal force ( $F_z$ ). The moment developed to the tire by the ground in the contact area is similarly decomposed to the overturning moment ( $M_x$ ), the rolling resistance moment ( $M_y$ ) and the aligning torque ( $M_z$ ). The moment applied to the tire from the vehicle about the spin axis is the wheel torque ( $T$ ). These forces and moments, together with the aerodynamic forces and moments, determine the dynamic performance and trajectory of the vehicle.

Generally, understanding on vehicle dynamics can be accomplished at two levels: the empirical and the analytical. Although often leading to failure, the empirical approach has helped develop knowledge on vehicle dynamics. Through trial and error process, empirical understanding is derived on the factors that influence vehicle performance and on how the influence is applied and changed by operating conditions. The analytical approach aims to understand the mechanics of interests based on the proven laws of physics that allows for the establishment of analytical models. In this project, we aimed to develop a mathematical model of motor vehicle dynamics that will be used to investigate the dynamics of vehicles (e.g. braking and acceleration) and that will be integrated with the inter-vehicle communication model for the studies on how the driving safety can be improved through information sharing among vehicles traveling in the same traffic.

## **2. Model the dynamics of ground vehicles**

The behaviour of a road vehicle is the consequence of the dynamic interaction of the various components of the vehicle structure in which the pneumatic tyre plays a major role. The complexity of the structure, behaviour of the tyre, and the dynamics of vehicles have attracted enormous research interests in the last fifty years, the period during which the application of mathematics to this field has been established. Vehicle dynamic models have been developed for a broad range of purposes, such as academic study and industrial product design.

The fundamental approach to the modeling of vehicle dynamics is based on the understanding that the dynamic behaviour of the vehicle is determined by the forces and moment imposed on the vehicle from the tires, gravity and aerodynamics. In this context, the vehicle dynamics refers to the movement of vehicles on a road surface. The movement of interest include acceleration, braking, ride, and turning.

The vehicle dynamics is mathematically modelled to address issues related to the following important components that influence the handling of road vehicles:

- Tyre characteristics and effective Axle Cornering characteristics;
- Vehicle handling and stability based on non-linear cornering solutions and moment method;
- Tyre Brush model, semi-empirical model and transient tyre models;
- Forces between wheel and road: pneumatic tyres, contact pressure and stiffness, rolling radius, rolling resistance, tractive and braking forces, cornering forces;
- Aerodynamics of road vehicles: aerodynamic drag, lift and pitching moment, side forces and yawing moments;
- Longitudinal dynamics: acceleration, braking;

- Vehicle handling: trajectory control, steering, stability;
- Elastic suspensions: quarter-car models, bounce and pitch motions.

A motor vehicle is made up of many components distributed complexly in its exterior envelope. In this study, it is assumed that all the components move together thus the entire mass of the vehicle and the payload is represented as one lumped mass applied at the centre of gravity (CG). For the purpose of targeted research, this approach provides sufficient accuracy. However, it is proposed to develop distributed-mass model in future study. For ride analysis, the wheels are treated as separate masses, referred to as un-sprung masses. In comparison, the lumped mass representing the vehicle body is referred to as sprung mass.

### **Coordinate systems**

The vehicle fixed coordinate system of the modeling is orthogonal originating at the CG of the vehicle and travels with the vehicle [SEA]:

x – Forward and on the longitudinal plane of symmetry

y – Lateral out the right side of the vehicle

z – Downward with respect to the vehicle

p – Roll velocity about the X axis

q – Pitch velocity about the Y axis

r – Yaw velocity about the X axis

The Earth fixed coordinate system is as follow [SEA]:

X – Forward travel

Y – Travel to the right

Z – Vertical travel (positive downward)

$\Psi$  – Heading angle (angle between x and X in the ground plane)

$\nu$  – Course angle (angle between the vehicle's velocity and X)

$\beta$  - Sideslip angle (angle between x and the vehicle velocity)

The relationship of the vehicle fixed coordinate system to the earth fixed coordinate system is defined by Euler angles [Gillespie, 1992].

### **Newtown Second Law**

The vehicle dynamic model is fundamentally based on Newton Second Law that applies to both translational and rotational systems.

In the translational systems, the sum of the external forces applied to a body in a given direction is equal to the product of the mass and the acceleration in that direction:

$$\sum F_x = ma_x \quad (C.3)$$

where:

- $F_x$  Forces in the x-direction
- $m$  Mass of the body
- $a_x$  Acceleration in the x-direction

In the rotational systems, the sum of the torques applied to a body about a given axis is equal to the product of the rotational moment of the inertia and the rotational acceleration about the axis:

$$\sum T_x = I_{xx} a_x \quad (C.4)$$

where:

- $T_x$  Torques about the x-axis
- $I_{xx}$  Moment of inertia about the x-axis
- $a_x$  Acceleration in the x-axis

Applying Newton Second Law, it is possible to determine the axle loadings on a vehicle under all possible conditions. The axle loads in turn determines the tractive forces obtained at each axle that will influence the acceleration, grade-ability, and maximum speed.

### **Tyre characteristics**

The forces applied on a tire are distributed in the contact patch resulting from normal and shear stresses. The pressure distributed on the contact is not uniform and vary in the X and Y directions. Due to the visco-elasticity of the tire, deformation in the leading portion of the contact patch causes the vertical pressure to be shifted forward. The friction between the tire and the road is caused by two major mechanisms: surface adhesion and hysteresis [Gillespie, 1992].

Under acceleration or braking, slip is normally produced by the deformation of the rubber elements in the tire tread that deflect to develop and sustain the friction force. The acceleration and braking forces are generated by the difference between the tire rolling speed and the speed of travel. Slippage ( $\eta$ ) is defined as follows:

$$\eta = \left(1 - \frac{r\omega}{V}\right) \times 100\% \quad (C.5)$$

where:

- r Tire effective rolling radius
- $\omega$  Wheel angular velocity
- V Forward velocity

Under typical braking conditions the longitudinal force ( $F_x$ ) varies with the slippage. Conventional Anti-Lock Braking Systems (ABS) are designed with assumption that the value of  $F_x$  is at the maximum when the slippage is controlled at around 15%. However, the peak of  $F_x$  is heavily affected by the road and tire condition, which may change significantly from vehicle to vehicle or when driving on different roads. Therefore this research aims to investigate the performance of conventional ABS and to develop better algorithm to control ABS such that the slippage can be controlled to maximize the value of  $F_x$  in the presence of all the factors influencing the relationship between the slippage and  $F_x$ .

For a pneumatic tire, the effective rolling radius  $R_e$  is defined as:

$$R_e = \frac{V}{\omega} \quad (C.6)$$

Compared with loaded radius  $R_L$  and unloaded radius  $R$ :

$$R_L < R_e < R \quad (C.7)$$

For radial tires:  $R_e = 0.98R$

$$R_L = 0.92R$$

For bias tires,  $R_e = 0.96R$

$$R_L = 0.94R$$

The value of  $R_e$  and  $R_L$  decreases when the load ( $F_Z$ ) increases or the inflation pressure decreases. When the speed ( $V$ ) increases, tires expands under centrifugal forces, which cause both  $R_e$  and  $R_L$  to increase.

### **Forces between wheel and road**

A variety of methods dealing with the force between the wheels and the road have been researched [Velenis, et al, 2005; Yi, et al, 1999; Oertel, 1997; Dhir and Sankar, 1997; Mastinu, et al, 1997; Pasterkamp and Pacejka, 1997; Lacombe, 2000; Wit and Horowitz, 1999; Germann, et al 1994; Shim and Margolis, 2004]. The forces between the wheels and road are modelled in this project as follows.

The rolling resistance ( $F_r$ ) is related with the normal load ( $F_Z$ ) as follows [Shim and Ghike, 2007]:

$$F_r = -fF_Z \quad (C.8)$$

where:

f Rolling resistance coefficient

The value of f can only be determined through experiments. The rolling resistance coefficient is influenced by a number of factors, including:

- Traveling speed (V)
- Inflation pressure (P)
- The normal force ( $F_z$ )
- Size of the tire and of the contact sone
- The structure and material of the tire
- Working temperature
- Road conditions
- Forces ( $F_x$ ,  $F_y$ ) exerted by the wheel

Two empirical equations (C.9 and C.10) are used to calculate the value of f:

$$f = \sum_{i=1}^n f_i V^i \quad (C.9)$$

Which is commonly used in two-term form as:  $f = f_0 + kV^2$

$f_0 = 0.008 \sim 0.010$  for very good concrete road, 0.25 for snow surface of 50mm deep, 0.37 for snow surface of 100mm deep, 0.15~0.30 for sand surfaces.

Or according to inflation pressure (P) and forward speed (V):

$$f = \frac{K'}{1000} \times \left( 5.1 + \frac{5.5 \times 10^5 + 90F_z}{P} + \frac{1100 + 0.0388F_z}{P} \times V^2 \right) \quad (C.10)$$

where:

$K'$  Constant (1 for conventional tires, 0.8 for radial tires)

The effect of the sideslip angle ( $\alpha$ ) on the rolling resistance is as follows:

$$F_r = F_x \cos(\alpha) + F_y \sin(\alpha) \quad (C.11)$$

The effect of the camber angle ( $\gamma$ ) on the rolling resistance is as follows:

$$F_r = \frac{-F_z \times \Delta X \times \cos(\gamma) - M_z \sin(\gamma) + M_f}{\quad} \quad (C.12)$$

where:

$\Delta X$  The offset of  $F_Z$  and the centre of the wheel

$M_f$  Drag moment

$M_Z$  Aligning torque

The impact of the camber angle on the rolling resistances is normally very small so ignored.

The tractive and braking forces are related to the load ( $F_Z$ ) as follows:

$$F_x = F_z \cdot \mu_x \quad (C.13)$$

where  $\mu$  is the longitudinal force coefficient, approximated as:

$$\mu_x = A(1 - e^{-B\sigma}) + C\eta^2 - D\eta \quad (C.14)$$

$$B = \left( \frac{K}{\alpha + d} \right)^{1/n} \quad (C.15)$$

where:

$\eta$  Greater than -1 and less than 1

Constants A, C, D, K, d and n must be obtained experimentally.

The longitudinal force  $F_X$  can also be expressed a function of slippage by that is so-called the Magic Formula as follows:

$$F_x = D \sin(C \arctan\{B(1 - E)(\eta + S_h) + E \arctan[B(\eta + S_h)]\}) + S_v \quad (C.16)$$

where B, C, D, E,  $S_v$ , and  $S_h$  are coefficients that depends on the load ( $F_Z$ ) and the camber angle ( $\gamma$ ). These coefficients can only be obtained experimentally.

The cornering force ( $F_Y$ ) is a function of the sideslip of the tire ( $\alpha$ ):

$$F_y = D \sin(C \arctan\{B(1 - E)(\alpha + S_h) + E \arctan[B(\alpha + S_h)]\}) + S_v \quad (C.17)$$

where:

$$C = a_0$$

$$D = \mu_y F_z$$

$$E = a_6 F_z + a_7$$

$$BCD = a_3 \sin\left[2 \arctan\left(\frac{F_z}{a_4}\right)\right] (1 - a_5 |\gamma|)$$

$$S_h = a_8 \gamma + a_9 F_z + a_{10}$$

$$S_v = a_{11} \gamma F_z + a_{12} F_z + a_{13}$$

The aligning torque is a function of the sideslip of the tire ( $\alpha$ ):

$$M_Z = D \sin(C \arctan\{B(1-E)(\alpha + S_h) + E \arctan[B(\alpha + S_h)]\}) + S_v \quad (C.18)$$

where:

$$C = c_0$$

$$D = c_1 F_Z^2 + c_2 F_Z$$

$$E = (c_7 F_Z^2 + c_8 F_Z + c_9)(1 - c_{10} |\gamma|)$$

$$BCD = (c_3 F_Z^2 + c_4 F_Z)(1 - c_6 |\gamma|) e^{-c_5 F_Z}$$

$$S_h = c_{11} \gamma + c_{12} F_Z + c_{13}$$

$$S_v = (c_{14} F_Z^2 + c_{15} F_Z) \gamma + c_{16} F_Z + c_{17}$$

### **Aerodynamics of road vehicles**

The aerodynamic drag on a vehicle depends on the vehicle drag factors and the speed (V). The drag is proportional to the square of the speed ( $V^2$ ). At low speed, it is negligible. However, at normal highway speed, it may cause a force equivalent to about 0.03g. Generally, the equivalent aerodynamic drag force on a vehicle is represented as follows:

$$F_{aero} = \frac{1}{2} \rho C_D S (V + V_{wind})^2 \quad (C.19)$$

where:

$\rho$  Density of air

$C_d$  The aerodynamic drag coefficient

S The frontal area of the vehicle

$V_{wind}$  Wind velocity (positive for a headwind and negative for a tailwind)

### **Vehicle dynamic model**

For a vehicle moving at a constant speed on a level and straight road, the forces to be overcome to maintain the speed are aerodynamic drag and rolling resistance. If the road is not level, the components of weight may act in a direction parallel to the velocity V thus as a resistance to motion. Therefore the total resistance to motion is expressed as follows [Genta, 2006]:

$$R = [mg \cos(\alpha) - \frac{1}{2} \rho V^2 S C_z] (f_0 + kV^2) + \frac{1}{2} \rho V^2 S C_x + mg \sin(\alpha) \quad (C.20)$$

This can be converted into:

$$R = A + BV^2 + CV^4$$

where:

$$A = mg[f_0 \cos(\alpha) + \sin(\alpha)]$$

$$B = mgK \cos(\alpha) + \frac{1}{2} \rho S [C_x - C_{zf_0}]$$

$$C = -\frac{1}{2} \rho SK C_z$$

For road with small grade angle ( $\alpha$ ),  $\cos(\alpha)$  is approximated as 1 and  $\sin(\alpha)$ ,  $\tan(\alpha)$  are both approximated as the grade of the road ( $i$ ). In this case,

$$A = mg(f_0 + i)$$

Therefore the power needed to move the vehicle at constant speed  $V$  is:

$$P_r = RV = AV + BV^3 + CV^5 \quad (C.21)$$

The braking force  $F_X$  is expressed as follows:

$$F_X = \sum_{\forall i} \mu_x(i) F_x(i) \quad (C.22)$$

The longitudinal equation of motion in vehicle braking is therefore calculated as:

$$\frac{dV}{d\tau} = \frac{\sum_{\forall i} \mu_x(i) F_x(i) - \frac{1}{2} \rho V^2 S C_x - f \sum_{\forall i} F_z(i) - mg \sin(\alpha)}{m} \quad (C.23)$$

Where  $m$  is the mass of the vehicle and  $\alpha$  is positive for uphill grade.

In case of ideal braking, all force coefficients ( $\mu_x(i)$ ) are equal, the acceleration becomes:

$$\frac{dV}{d\tau} = \mu_x [g \cos(\alpha) - \frac{1}{2m} \rho V^2 S C_z] - \rho \sin(\alpha) \quad (C.24)$$

If the road is level,

$$\frac{dV}{d\tau} = \mu_x \left( g - \frac{1}{2m} \rho V^2 SC_z \right) \quad (\text{C.25})$$

### Suspension

An automotive suspension supports the vehicle body on the axles. The vehicle body is the “sprung mass” and the mass due to the axles and tires is the “unsprung mass”. The suspension system are springs and dampers between the sprung mass and the unsprung mass. The automotive suspension typically has the following major functions:

- To isolate a car body from road disturbances to provide good ride.
- To keep good grip on road
- To provide good handling
- To support the vehicle static weight

There are two types of suspension systems: dependent and independent suspensions. In dependent suspensions, the vertical motions of one wheel of an axle are directly linked to that of the other wheel of the axle. In this case, the axle cannot be represented by two independent unsprung masses. In independent suspensions, the vertical motions of the two wheels of one axle are not directly linked to each other.

The equations of motion of a two-degree-of-freedom (2 DOF) quarter-car suspension are as follows:

$$m_s \ddot{Z}_s + b_s (\dot{Z}_s - \dot{Z}_u) + k_s (Z_s - Z_u) = F_a \quad (\text{C.26})$$

$$m_u \ddot{Z}_u + b_t (\dot{Z}_u - \dot{Z}_r) + k_t (Z_u - Z_r) - b_s (\dot{Z}_s - \dot{Z}_u) - k_s (Z_s - Z_u) = -F_a \quad (\text{C.27})$$

where:

- m    Mass
- Z    Vertical position (height from the ground)
- k    Spring factor
- b    Damper factor
- F<sub>a</sub>    Active force actuator
- Subscript s: refer to Sprung mass
- Subscript u: refer to Unsprung mass
- Subscript t: refer to tire

### 3. Implementation of the model

The mathematic model of vehicle dynamics described above is implemented in Matlab + Simulink. Figure C-1 shows a black-box presentation of the implementation.

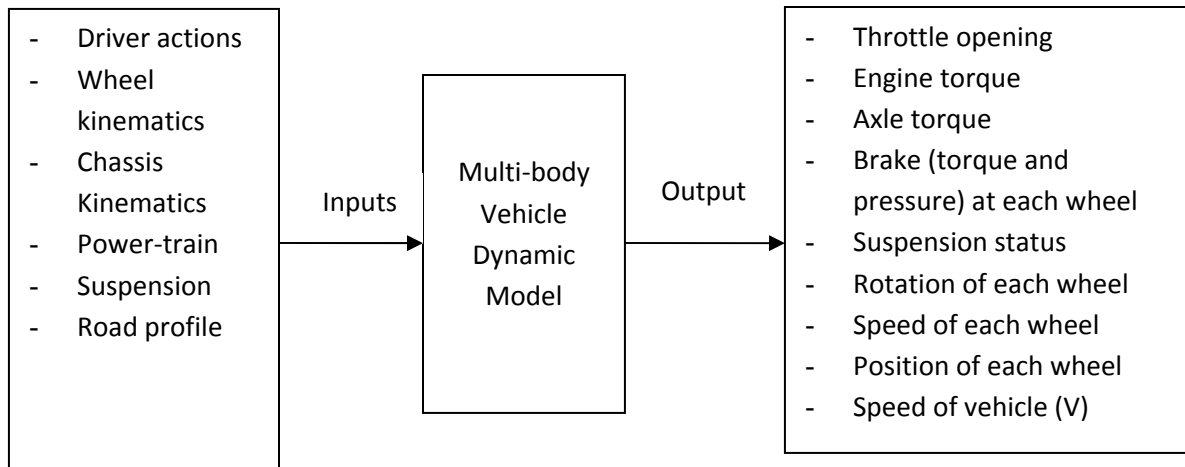


*Figure C-1 The black-box presentation of the implemented vehicle dynamic model*

Figure C-2 shows the modular structure of the multi-body vehicle dynamic model.

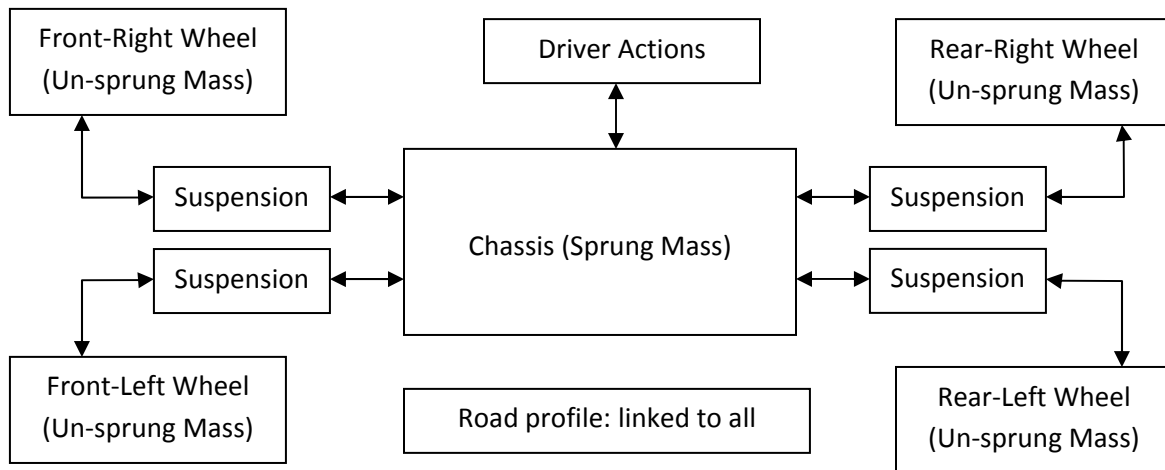


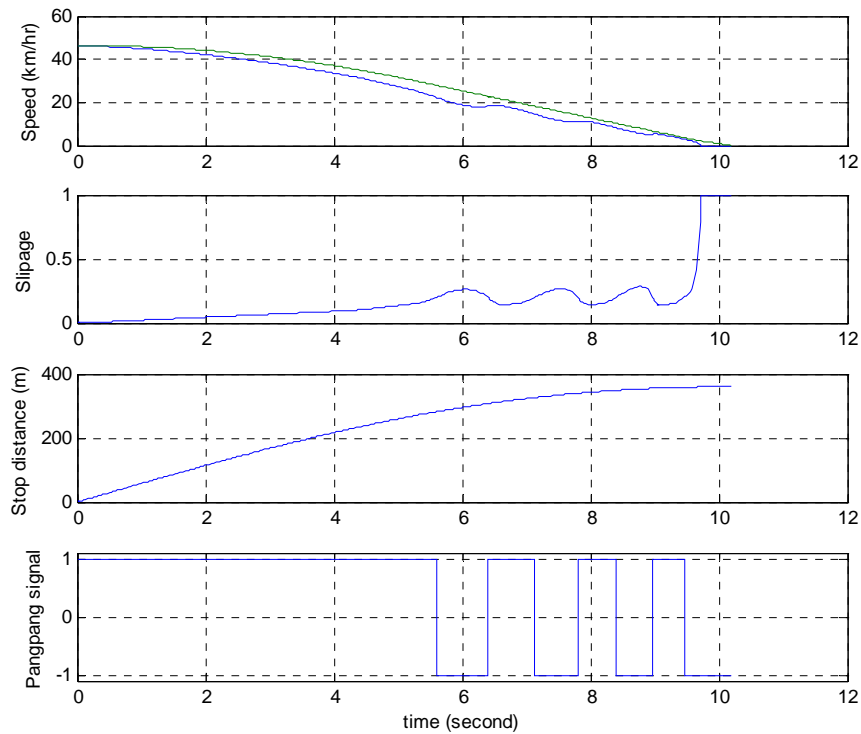
*Figure C-2 Structure of the Simulink implementation of the vehicle dynamic model*

#### 4. Using the model to investigate the performance of conventional ABS

The Simulink implemented vehicle dynamic model has been used to investigate conventional ABS. The vehicle parameters used in the investigation are as follows:

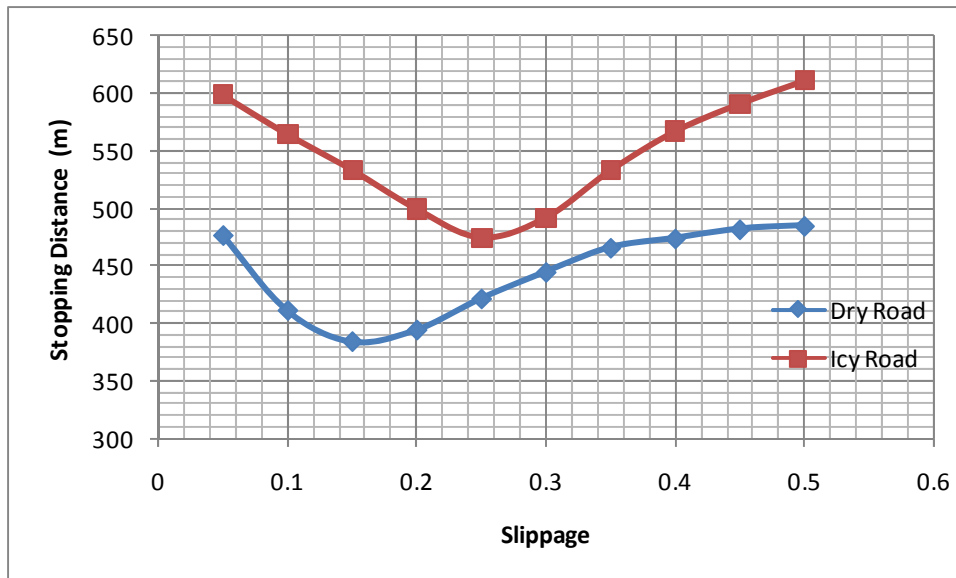
- Sprung mass: 1400 kg
- Front/rear unsprung mass: 85 kg
  
- Sprung mass roll inertia: 950 kgm<sup>2</sup>
- Sprung mass yaw inertia: 2100 kgm<sup>2</sup>
- Sprung mass pitch inertia: 2100 kgm<sup>2</sup>
- Tire/wheel roll inertia: 1 kgm<sup>2</sup>
  
- Distance of sprung mass CG from front axle: 1.100m
- Distance of sprung mass CG from rear axle: 1.600m
- Sprung mass CG height: 0.70m
- Front/rear track width: 1.5m
- Front roll center distance below sprung mass CG: 0.65m
- Rear roll center distance below sprung mass CG: 0.6m
- Nominal tire radius: 0.284m
  
- Front/rear tire stiffness: 210,000N/m
- Front suspension stiffness: 35,000N/m
- Front suspension damping coefficient: 2600 Ns/m
- Rear suspension stiffness: 30,000N/m
- Rear suspension damping coefficient: 2100 Ns/m

Figure 2-3 shows the simulated performance of a conventional ABS. The top figure shows how the speed  $V$  and ideal speed  $V_0$  vary against time when the ABS is operated. The second top figure shows the slippage, calculated from the data shown in the top figure. The third figure shows the stop distance from the position where the ABS starts to operate. The bottom figure shows the action of the ABS. In this simulation, the ABS tries to maintain the slippage to fluctuate at a set-point of 15%.



**Figure C-3 Performance of a conventional ABS**

Figure C-4 shows the stopping distance of a vehicle with initial speed of 45 km/hr. The slippage is controlled at different set-point, ranging from 0.05 to 0.5. The result indicates that the shortest stopping distance is achieved by controlling the slippage at 15% while riding on a dry surface. However, while riding on an icy surface, the shortest stopping distance is achieved by controlling the slippage at around 25%. This is because the friction coefficient between the tire and the icy surface peaks at slippage of 25%.



***Figure C-4 Stopping distance vs slippage (initial speed: 45 km/hr)***

It is accepted by all the designers of Anti-lock Brake System (ABS) that the wheels have the greatest grip on the road when the slippage is between 10% and 15% [Baslamisli, et al, 2007; Kim, et al, 2006;]. Therefore all ABS in use nowadays are designed to control the brake such that the slippage is maintained between 10% and 15%. However, the relationship between slippage and the grip produced between the wheels and the road depends on the surface conditions. The grip may be peaked at a slippage that is significantly different from 10% to 50%. This explains why many experiments have reported that ABS lead to increased stopping distance on the surfaces that a reduced stopping distance is most desirable.

An ABS consists of four major components, including wheel speed sensors on each wheel, electrically controlled hydraulic valves, electric motor powered hydraulic pump, electronic control unit (ECU). This is a typical single loop control system. The ECU estimates the slippage according to the sensor signals and controls the valves so that the slippage is controlled within 10% to 15%. This results in that the grip between the wheels and the road is not maximized.

Further simulation results also show that the vehicles with conventional ABS have up to 20% longer stopping distance on wet, snowy and icy surfaces compared with vehicles without any ABS. Conventional ABS can be improved using an adaptive ABS control algorithm, which dynamically changes the control set point of the slippage such that the grip coefficient between the wheel and the road is maximized. However, more theoretical study and experimental study need to be conducted in future projects.

The long-term goal of this research is to develop an intelligent ECU for ABS that can recognize the road condition and accordingly control the slippage that results in the maximum grip thus shortest stopping distance, whilst safe controllability and stability are maintained. The proposed intelligent ECU is based on a dual loop feedback control scheme. In the outer loop, a vehicle motion sensing system will be developed to monitor the dynamics of the vehicle thus the grip between the wheels and the road can be estimated. This estimate is used to determine the most

desirable slippage. In the inner loop, the conventional ABS control algorithm will be employed to control the ABS so that the slippage is maintained at the desired level determined by the outer loop.

Potentially, the simulator can be further developed for other investigations, such as passenger comfort [Pennestri, et al, 2005], car handling [Arnold, et al, 2003], software-in-loop control design [Russo, et al, 2007], steering control [Chen and Ulsoy, 2007], electronic stability control [W Pan and Y E Papelis, 2005], yaw moment control [Boada, et al, 2005], advanced driver assistance [Gietelink, et al, 2006], advanced ABS [Pasillas-Lepine, 2006], mechatronics [Kortum and Vaculin, 2003 ], non-linear dynamics and stability [Shen, et al, 2007].

## **5. Extend the model to Virtual Reality**

The vehicle dynamic model is implemented in Matlab + Simulink. The simulator is linked with a graphical animation created in Virtual Reality Toolbox. The purpose of the model is to perform simulation on the effect of the new ABS system on the motion and stopping distance on a vehicle. Through the animation toolkit, it is possible to create a graphical representation of the dynamic behaviour of the vehicle under different operations. The simulation model ultimately collects input signals from 3 physical factors to generate its output: the gas and braking pedal, steering wheel, and road surface. By controlling these input signals, the user can control a virtual dynamic model of a vehicle in the 3-dimensional simulation world.

The movement of the vehicle is ultimately based on the force acting on the car. A force balance acting on the vehicle is therefore necessarily to understand and to calculate the acceleration, velocity and displacement of the vehicle. This includes the acceleration and braking torque acting on the wheel, head or trail wind, and friction forces. All these factors contribute to the force acting on the vehicle. The simulation environment is a three-dimensional environment plane. The steering wheel control is the device that accepts turning signals and translates them into the orientation and the turning motion of the vehicle.

The engine of the simulation relies heavily on the Random Walk Theory to compute the physical movement of the vehicle. The Random Walk predicts the upcoming movement, or future location, solely based on the present location, regardless of the past movement of the vehicle. The theory of random walk is applied to calculate the instantaneous upcoming motion of the vehicle over an incremental unit of time based on the current input, location, and motion. This theory is required for computation with instantaneous input to provide a smooth motion of the vehicle in a graphical form. The following table summarize all the variables that are used to control a vehicle in the Virtual Reality.

Table C-1 Variables controlling a vehicle in Virtual Reality

Variables	Description	Number of Dimension
Vehicle_pos_Car1.rotation	Controls the absolute rotation of the vehicle. This variable receives absolute signal so abrupt fluctuation of the signal will cause the graphical display to “flash”	4
Vehicle_pos_Car1.translation	Controls the displacement of the vehicle. The rate of change of this variable represents the speed of the vehicle. This variable receives absolute signal so abrupt fluctuation of the signal will cause the graphical display to “flash”	3
SteeringWheelAngle1_Car1.rotation	Controls the steering wheel of the vehicle. This is displayed at the top of the vehicle.	4
WheelFL_Car1.rotation	Controls the turning action of front left tire of the vehicle. The angle is relative to the Vehicle_pos_Car1.rotation	4
WheelFR_Car1.rotation	Controls the turning action of front right tire of the vehicle. The angle is relative to the Vehicle_pos_Car1.rotation	4
WheelSpinFL_Car1.rotation	Controls the spinning action of the front left tire of the vehicle as the vehicle moves forward.	4
WheelSpinFR_Car1.rotation	Controls the spinning action of the front right tire of the vehicle as the vehicle moves forward.	4
WheelSpinRL_Car1.rotation	Controls the spinning action of the rear left tire of the vehicle as the vehicle moves forward.	4
WheelSpinRR_Car1.rotation	Controls the spinning action of the rear right tire of the vehicle as the vehicle moves forward.	4
Brake_switch_Car1.whichChoice	Controls the brake light at the rear of the vehicle. The light will glow red when the vehicle slows down and stop.	1

## 6. Future work

An ABS consists of four major components, including wheel speed sensors on each wheel, electrically controlled hydraulic valves, electric motor powered hydraulic pump, electronic control unit (ECU). This is a typical single loop control system. The ECU estimates the slippage according to the sensor signals and controls the valves so that the slippage is controlled within 10% to 15%. This results in that the grip between the wheels and the road is not maximized.

The long-term goal of this research is to develop an intelligent ECU for ABS that can recognize the road condition and accordingly control the slippage that results in the maximum grip thus shortest braking distance, whilst safe controllability and stability are maintained.

The proposed intelligent ECU is based on a dual loop feedback control scheme. In the outer loop, a vehicle motion sensing system will be developed to monitor the dynamics of the vehicle thus the grip between the wheels and the road can be estimated. This estimate is used to determine the most desirable slippage. In the inner loop, the conventional ABS control algorithm will be employed to control the ABS so that the slippage is maintained at the desired level determined by the outer loop.

To achieve this goal, the vehicle dynamic model will be fully developed and rigorously validated using experimental data to be obtained from different sources. The simulator will be used to investigate the dynamics of vehicles during emergency braking and to develop an adaptive ABS control scheme.

Specifically, the following researches are recommended:

- To investigate existing vehicle dynamic models. A number of models developed for different purposes will be investigated for the development of the proposed model.
- To develop a vehicle model suitable for analyzing the stability of vehicles during emergency braking and for developing the dual loop self-adaptive ABS control algorithm.

Two different models need to be investigated: multi-body model and single rigid lumped mass model. In the multi-body model, a vehicle is divided into a number of sections that each is modelled as being rigid lumped mass at the relevant gravity center with 6 DOF (degree of freedom). In the single rigid lumped mass model, the entire vehicle mass is modelled as a rigid lumped mass at the center of gravity with 6 DOF. In both models, each of the four wheels will be modelled with 2 DOF.

More representative road profile needs to be modelled as an important input to the model. The adhesive coefficients between tires and road surfaces, including dry, wet and icy, should be modelled.

- To implement and validate the simulator

The mathematical model needs to be developed to more accurately represent the dynamics of vehicles and to be implemented as a general simulator. The implemented simulator needs to be validated using the experimental data obtained from other researchers.

- To develop more detailed vehicle presentation in Virtual Reality environment

- To develop algorithm for Vehicle Trajectory Diagnosis

Two principal function of all types of vehicles are propulsion and trajectory control. With piloted vehicles, the trajectory is determined by a guidance system that is controlled by a human pilot or by a device. The guidance system acts by exerting forces on the vehicle that are able to change its trajectory. In the case of road vehicles, the driver operates the steering wheel causing certain wheels to work with a sideslip and to generate lateral forces, which change the attitude of the vehicle thus a sideslip of all wheels. The resulting forces bend the trajectory. If the tractive force between the wheels and ground is not sufficient, the vehicle will be out of control and slide away its normal trajectory, a dangerous driving situation.

It is recommended to investigate the steering stability of road vehicles based on non-linear vehicle handling model. Under normal driving conditions, the sideslip angles of wheels and of the vehicles are very small, in which case the non-linear model can be linearised to simplify the calculation. Both static and dynamic stability will be included in the diagnosis.

The vehicle dynamics model will be used for this investigation. For this purpose, the model need be able to accurately represent the following aspects of vehicle dynamics: forces between road and wheels (contact pressure and stiffness, rolling radius and resistance, tractive and braking forces, cornering forces), longitudinal dynamics (load distribution, acceleration and deceleration), vehicle handling (trajectory control, kinematic steering, ideal steering, linearised handling).

## References

- D Aleksendriv, C Duboka, P F Gotowicki, G V Mariotti and V Nigrelli, Braking procedure analysis of a pego-wing ventilated disk brake rotor, *Int. J. Vehicle Systems Modelling and Testing*, Vol. 1, No. 4, pp 233-52 (2006)
- M Arnold, A Carrarini, A Heckmann, and G Hippmann, Simulation techniques for multidisciplinary problems in vehicle system dynamics, *Vehicle System Dynamics Supplement* 40 (2003), p17-36
- S Baslamisli, I E Kose and G Anlas, Robust control of anti-lock brake system, *Vehicle System Dynamics*, Vol.45, No. 3, p217-232 (2007)
- B L Boada, M J L Boada and V Diaz, Fuzzy-logic applied to yaw moment control for vehicle stability, *Vehicle System Dynamics*, Vol. 43, No, 10, p753-770, (2005)
- L K Chen and A G Ulsoy, Experimental evaluation of a vehicle steering assist controller using a driving simulator, *Vehicle System Dynamics*, Vol. 44, No. 3, p223-245 (2006)
- R Chumsamutr, T Fujioka and M Abe, Sensitivity analysis of side-slip angle observer based on a tire model, *Vehicle System Dynamics*, Vol 44, No. 7, p513-527, (2006)
- A. Dhir and S. Sankar, Analytical wheel models for ride dynamic simulation of off-road tracked vehicles, *Vehicle System Dynamics*, vol. 27, pp. 37-63 (1997)
- G Genta, *Motor Vehicle Dynamics: Modeling and Simulation*, ISBN 9810229119, World Scientific Publishing Co., Singapore (2006)
- St. Germann, M. Wurtenberger and A. Daib, Monitoring of the friction coefficient between tyre and road surface, *IEEE WE*, vol. 4(1), pp. 613-618 (1994)
- O Gietelink, . Ploeg, B De Schutter and M Verhaegen, Development of advanced driver assistance systems with vehicle hardware-in-the-loop simulations, *Vehicle System Dynamics*, Vol. 44, No. 7, p569-590 (2006)
- T D Gillespie, *Fundamentals of Vehicle Dynamics*, ISBN 1-56091-199-9, Society of Automotive Engineers, Inc (1992)
- K Guo, Y Chuang, D Lu, S Chen, and W Lin, A study on speed-dependent tyre-road friction and its effect on the force and the moment, *Vehicle System Dynamics*, Vol. 43, Supplement, p329-340 (2005)
- W. Hirschberg, G. Rill and H. Weinfurter, User-appropriate tyre-modelling for vehicle dynamics in standard and limit situations, *Vehicle System Dynamics*, vol. 38, no. 2, pp. 103-125 (2002)

- H Imine, Y Delanne and N K M Sirdi, Road profile input estimation in vehicle dynamics simulation, *Vehicle System Dynamics*, Vol. 44, No. 4, p285-303 (2006)
- K Kim, J Kim, K S Huh, K Yi and D Cho, A real-time multi-vehicle simulator for longitudinal controller design, *Vehicle System Dynamics*, Vol. 44, No. 5, p369-386, (2006)
- W Kortum and O Vaculin, Is multibody simulation software suitable for mechatronic systems? *Vehicle System Dynamics Supplement 40*, p1-16 (2003)
- J. Lacombe, Tire model for simulations of vehicle motion on high and low friction road surfaces, *Proc. 2000 Winter Simulation Conf.*, pp. 1025-1034
- L. Li, F.Y. Wang and Q. Zhou, Integrated longitudinal and lateral tire/road friction modeling and monitoring for vehicle motion control, *IEEE Trans. Intelligent Transportation Sys.*, vol. 7, no. 1 (2006)
- G. Mastinu, S. Gaiazzi, F. Montanaro and D.Pirola, A semi-analytical tyre model for steady- and transient-state simulations, *Vehicle System Dynamics Supp.*, vol. 27, pp. 2-21 (1997)
- N Miyashita and K Kabe, A study of the cornering force by use of the analytical tyre model, *Vehicle System Dynamics*, Vol. 43, Supplement, 2005, pp123-134
- C. Oertel, On modeling contact and friction calculation of tyre response on uneven roads, *Vehicle System Dynamics Supp.*, vol. 27, pp. 289-302 (1997)
- W Pan and Y E Papelis, Real-time dynamic simulation of vehicles with electronic stability control: modeling and validation, *Int. J Vehicle System Modelling and Testing*, Vol. 1, p143-167 (2005)
- E Pennestri, PP Valentini and L Vita, Comfort analysis of car occupants: comparison between multibody and finite element models, *Int. J. Vehicle Systems Modelling and Teasting*, Vol. 1, No. 1, p 68-78 (2005)
- R Rajamani, *Vehicle Dynamics and Control*, ISBN 0-387-26396-9, Springer, (2006)
- W Pasillas-Lepine, Hybrid modeling and limit cycle analysis for a class of five-phase anti-lock brake algorithms, *Vehicle System Dynamics*, Vol. 44, No. 2, p173-188 (2006)
- W.R. Pasterkamp and H.B. Pacejka, The tyre as a sensor to estimate friction, *Vehicle System Dynamics*, vol. 27, pp. 409-422 (1997)
- R Russo, M Terzo and F Timpone, Software-in-the-loop development and validation of a cornering brake control logic, *Vehicle System Dynamics – Int. Journal of Vehicle Mechanics and Mobility*, Vol. 45, No.2, pp149-163 (2007)

T Shim and C Ghike, Understanding the limitations of different vehicle models for roll dynamics studies, *Vehicle System Dynamics*, Vol. 45, No. 3, p191-216 (2007)

J Svendenius, M Gafvert, A semi-empirical dynamic tire model for combined-slip forces, *Vehicle System Dynamics*, Vol 44, No.2, pp189-208 (2006)

T Shim and D Margolis, Model-based road friction estimation, *Vehicle System Dynamics*, Vol. 41, No. 4, p249-276 (2004)

M J Steenbergen, Modeling of wheels and rail discontinuities in dynamic wheel-rail contact analysis, *Vehicle System Dynamics*, Vol. 44, No. 10, p763-787, (2006)

SAE, *Vehicle Dynamics Terminology*, SAE J670e, Society of Automotive Engineers, Warrendale, PA.

S Shen, J Wang, P Shi, and G Premier, Nonlinear dynamics and stability analysis of vehicle plane motions, *Vehicle System Dynamics*, Vol. 45, No. 1, p15-35 (2007)

E. Velenis, P. Tsiotras, C.C. Wit and M. Sorine, Dynamic tyre friction models for combined longitudinal and lateral vehicle motion, *Vehicle System Dynamics*, vol. 43, no. 1, pp. 3-29 (2005)

C.C. Wit and R. Horowitz, Observers for tire/road contact friction using only wheel angular velocity information, *IEEE Proc. 38th Conf. Decision & Control Phoenix*, pp. 3932-3937, USA, Dec. 1999

K. Yi, K. Hedrick and S. Lee, Estimation of tire-road friction using observer based identifiers, *Vehicle System Dynamics*, vol. 31, pp. 233-261 (1999)